# Proceedings of the I·R·E

SEPTEMBER 1941

VOLUME 29 NUMBER 9

Three New U-H-F Triodes

Operating Data and Ratings of Vacuum-Tube Rectifiers

Coupling Networks

Antennas of Arbitrary Size and Shape

High-Frequency Transmission

Institute of Radio Engineers

**More than 100 types of tubes for use in Commercial Broadcasting, Point to Point Communication, Ultra High Frequency Transmission, Electro Medical Apparatus, High Voltage Rectification and many Industrial Applications.**

# We're in the Army* now

* U. S. Army, Navy, Civil, and Aeronautical Departments, etc.

. . . and faced with a continuous step-up in the demand for AMPEREX Transmitting and Rectifying Tubes for the armed services.

Despite the fact that your valued commercial orders for certain tube types must be subordinated to problems arising from the national emergency, the priorities situation, restrictions on certain rare refractory metals and materials, etc. . . . we <u>are</u> still able to fill all your orders.

*However, in this period of unusual stress, we ask your consideration and cooperation in anticipating your requirements so that we may maintain our customary rapid delivery schedules.*

## AMPEREX ELECTRONIC PRODUCTS

79 WASHINGTON STREET • BROOKLYN, NEW YORK

BOARD OF DIRECTORS

Frederick E. Terman, *President*
Adolfo T. Cosentino, *Vice President*
Alfred N. Goldsmith, *Editor*
Haraden Pratt, *Treasurer*
Harold P. Westman, *Secretary*
Austin Bailey
Adolph B. Chamberlain
Ivan S. Coggeshall
Melville Eastham
Harold T. Friis
Virgil M. Graham
O. B. Hanson
Raymond A. Heising
Lawrence C. F. Horle
C. M. Jansky, Jr.
Frederick B. Llewellyn
Browder J. Thompson
Hubert M. Turner
Arthur F. Van Dyck
Harold A. Wheeler
Lynde P. Wheeler

•

Harold R. Zeamans, *General Counsel*

•

BOARD OF EDITORS

Alfred N. Goldsmith, *Editor*
Ralph R. Batcher
Lloyd V. Berkner
Philip S. Carter
Lewis M. Clement
Elmer W. Engstrom
William L. Everitt
Peter C. Goldmark
Frederick W. Grover
C. M. Jansky, Jr.
John D. Kraus
Frederick B. Llewellyn
Samuel S. Mackeown
Edward L. Nelson
Harry F. Olson
Greenleaf W. Pickard
Haraden Pratt
Conan A. Priest
Leon J. Sivian
Lynne C. Smeby
Browder J. Thompson
Harold A. Wheeler
Lynde P. Wheeler
Laurens E. Whittemore
Gerald W. Willard
William Wilson
Charles J. Young

•

Helen M. Stote, *Assistant Editor*

John D. Crawford, *Advertising Manager*

# Proceedings of the I·R·E

*Published Monthly by*
The Institute of Radio Engineers, Inc.

VOLUME 29 — *September, 1941* — NUMBER 9

Three New Ultra-High-Frequency Triodes ..... K. C. DeWalt 475

The Determination of Operating Data and Allowable Ratings of Vacuum-Tube Rectifiers ..... J. C. Frommer 481

Reactance Networks for Coupling Between Unbalanced and Balanced Circuits ..... S. Frankel 486

Theory of Antennas of Arbitrary Size and Shape ..... S. A. Schelkunoff 493

High-Frequency Radio Transmission Conditions, August, 1941, with Predictions for November, 1941 ..... 521

Discussion on "Radiation from Rhombic Antennas," by Donald Foster ..... Leonard Lewin and Donald Foster 523

Institute News and Radio Notes ..... 524

Board of Directors ..... 524

Executive Committee ..... 524

Sections ..... 524

Membership ..... 526

Contributors ..... 528

Entered as second-class matter October 26, 1927, at the post office at Menasha, Wisconsin, under the Act of February 28, 1925, embodied in Paragraph 4, Section 538 of the Postal Laws and Regulations. Publication office, 450 Ahnaip Street, Menasha, Wisconsin. Editorial and advertising offices, 330 West 42nd St., New York, N. Y. Subscription, $10.00 per year; foreign, $11.00.

*Copyright, 1941, by The Institute of Radio Engineers, Inc.*

# THE INSTITUTE OF RADIO ENGINEERS

INCORPORATED

## New York Meeting—October 1, 1941

## Rochester Fall Meeting, November 10, 11, and 12, 1941

### SECTION MEETINGS

| | | |
|---|---|---|
| ATLANTA<br>October 17 | DETROIT<br>October 17 | PHILADELPHIA<br>October 2 |
| CHICAGO<br>October 17 | LOS ANGELES<br>October 21 | PITTSBURGH<br>October 13 |
| CLEVELAND<br>October 23 | | WASHINGTON<br>October 13 |

### SECTIONS

**ATLANTA**—Chairman, A. W. Shropshire, Secretary, G. M. Howard, 856 St. Charles Ave., N. E., Atlanta, Ga.

**BALTIMORE**—Chairman, V. D. Hauck, Jr.; Secretary, G. J. Gross, Pennsylvania Water and Power Co., 1611 Lexington Bldg., Baltimore, Md.

**BOSTON**—Chairman, J. M. Henry; Secretary, R. O. Oberg, Northeastern University, Boston, Mass.

**BUENOS AIRES**—Chairman, P. J. Noizeux; Secretary, L. C. Simpson, RCA Victor Argentina, Bartolome Mitre, 1961, Buenos Aires, Argentina.

**BUFFALO-NIAGARA**—Chairman, E. H. Roy; Secretary, Leroy Fiedler, 53 Rosedale Ave., Hamburg, N. Y.

**CHICAGO**—Chairman, G. I. Martin; Secretary, R. A. Kay, RCA Institutes, Inc., 1154 Merchandise Mart, Chicago, Ill.

**CINCINNATI**—Chairman, J. M. McDonald; Secretary, W. L. Schwesinger, Crosley Corp., Cincinnati, Ohio.

**CLEVELAND**—Chairman, Carl E. Smith; Secretary, W. G. Hutton, 7314 Dorothy Ave., Parma, Ohio.

**CONNECTICUT VALLEY**—Chairman, F. G. Webber; Secretary, C. I. Bradford, 187 Glenarden Dr., Fairfield, Conn.

**DALLAS-FORT WORTH**—Chairman, D. A. Peterson; Secretary, P. C. Barnes, WFAA-WBAP, Grapevine, Tex.

**DETROIT**—Chairman, M. Cottrell; Secretary, Paul Frincke, WJBK, 6559 Hamilton Ave., Detroit, Mich.

**EMPORIUM**—Chairman, R. K. Gessford; Secretary, C. W. Reash, Hygrade Sylvania Corp., Emporium, Pa.

**INDIANAPOLIS**—Chairman, A. N. Curtiss; Secretary, T. N. Rosser, P. R. Mallory & Co., 3029 E. Washington St., Indianapolis, Ind.

**KANSAS CITY**—Chairman, Harner Selvidge; Secretary, G. L. Taylor, Midland Radio School, Power and Light Bldg., Kansas City, Mo.

**LOS ANGELES**—Chairman, W. W. Lindsay, Jr.; Secretary, C. F. Wolcott, 1609 S. Western Ave., Los Angeles, Calif.

**MONTREAL**—Chairman, E. A. Laport; Secretary, W. A. Nichols, Canadian Broadcasting Corp., 1012 Keefer Bldg., Montreal, Que.

**NEW ORLEANS**—Chairman, G. H. Peirce; Secretary, D. W. Bowman, 8327 Sycamore St., New Orleans, La.

**PHILADELPHIA**—Chairman, C. C. Chambers; Secretary, R. L. Snyder, 103 Franklin Rd., Glassboro, N. J.

**PITTSBURGH**—Chairman, P. N. Bossart; Secretary, Ralph Overholt, Jr., 7211 Thomas Blvd., Pittsburgh, Pa.

**PORTLAND**—Chairman, E. R. Meissner; Secretary, L. M. Belleville, 361 N. E. 75th Ave., Portland, Ore.

**ROCHESTER**—Chairman, H. J. Klumb; Secretary, O. L. Angevine, Jr., Stromberg-Carlson Telephone Manufacturing Co., Rochester, N. Y.

**SAN FRANCISCO**—Chairman, L. J. Black; Secretary, Karl Spangenberg, Electrical Engineering Dept., Stanford University, Calif.

**SEATTLE**—Chairman, K. H. Ellerbeck; Secretary, R. J. Gleason, Pacific Alaska Airways, Inc., 3314 White Bldg., Seattle, Wash.

**TORONTO**—Chairman, R. H. Klingelhoeffer; Secretary, L. C. Simmonds, 301 King St., E., Toronto, Ont.

**TWIN CITIES**—Chairman, C. A. Culver; Secretary, N. B. Coil, 1664 Thomas St., St. Paul, Minn.

**WASHINGTON**—Chairman, M. H. Biser; Secretary, C. M. Hunt, WJSV, 817 Earle Bldg., Washington, D. C.

# Three New Ultra-High-Frequency Triodes*

K. C. DEWALT†, ASSOCIATE, I.R.E.

***Summary***—*The design requirements affecting power tubes at high frequencies are discussed and their application in the development of three new water- and forced-air-cooled triodes are outlined.*

*For water-cooled operation these three types have the following ratings:*

| | *Maximum Frequency for Full Ratings* megacycles | *Approximate Output per Tube—Class C* kilowatts |
|---|---|---|
| GL-880 | 25 | 25 |
| GL-889 | 50 | 10 |
| GL-8002 | 150 | 1.8 |

*Characteristics and constructional details of the new tubes are described. The use of a re-entrant anode in the largest type is of particular interest. By this design, in which the anode is folded back on itself twice, the length of internal leads to the grid and filament structures is reduced to approximately one quarter the length required in conventional designs.*

*Fin-type coolers for forced-air cooling of the anode are described.*

THE requirements of television and frequency modulation necessitated the development of new types of amplifier tubes to deliver high power at high frequencies. These special requirements compose several main items of opposing nature as follows: 1. minimum inductance to electrodes, 2. minimum capacitance between electrodes, 3. minimum transit-time effects, 4. maximum frequency for stable amplifier operation, 5. maximum output, and 6. low impedance to operate in broad-band circuits.

The maximum frequency rating determines, to a large extent, many of the design details. The maximum frequency determines the size by dictating the capacitance and inductance values and therefore the power capabilities. The electrode spacings must be small to reduce transit-time effects and conversely the spacings must be large to reduce capacitance. Electrode areas must be chosen to be consistent with power ratings and yet must be as small as possible to reduce capacitance and inductance. The tube must be designed to operate properly into the required circuit impedance, which for most of these applications means low impedance with low plate voltage and high plate current, necessitating large electrode areas and close spacings.

All of these considerations require compromising and proper balancing to obtain the best design consistent with the limitations of our existing knowledge. Thus, we see that from the practical standpoint, there is a limiting boundary, set up by a power-versus-frequency chart beyond which we have thus far been unable to penetrate. To delve into this unknown region requires new ideas and different modes of attack which undoubtedly will come to the surface as development progresses.

* Decimal classification: R330. Original manuscript received by the Institute, February 21, 1941. Presented, Sixteenth Annual Convention, New York, N. Y., January 10, 1941.

† Vacuum Tube Engineering Department, General Electric Company, Schenectady, N. Y.

It has been shown[1,2] that grid loading caused by the transit time of electrons moving from the cathode to the anode is a function of the grid-plate transconductance, frequency squared, cathode-grid transit time squared, and grid-anode transit time. This last factor usually can be ignored in transmitting tubes because the operating voltages can be chosen so that this effect is minimized.

Considering transit time from the practical standpoint in any specific case where the design is established by frequency and power considerations, the grid-loading effects can be reduced by making the electrode spacings and driving voltage as small as possible. In other words, the grid-plate transconductance should be as high as is consistent with capacitance values. In electrode structures utilizing cage-type filaments, there should be sufficient strands to result in maximum utilization of the anode surface. That is, the effective cathode area should at least equal the anode area so as to obtain the maximum transconductance. Since the capacitance of two coaxial cylinders is inversely proportional to the logarithm of the diameter ratio and transconductance is inversely proportional to distance to the four-thirds power, we can effect a greater increase in transconductance by reducing spacings than is obtained in capacitance. Thus it is seen that reducing electrode spacings is proper up to the limitations imposed by mechanical-design considerations. This procedure is consistent with high-current design so that efficient operation in low-impedance circuits can be realized.

Electrode areas must be kept as small as possible to reduce electrode capacitance and inductance. Therefore, the dissipation per unit area will be high and water- or forced-air cooling becomes a necessity even in small-sized tubes. Grid designs must be used such that grid temperatures are well below values which would result in primary grid emission.[3] Primary grid emission causes unstable operation or reduced efficiency.

Grid materials having low emission efficiency combined with treated surfaces to obtain the maximum heat radiation are required. Methods of providing heat conduction from the grid structure to external conductors also assist in reducing the grid temperature to a safe value. In some cases it may be necessary to

[1] F. B. Llewellyn, "Phase angle of vacuum tube transconductance at very high frequencies," PROC. I.R.E., vol. 22, pp. 947–956; August, 1934.

[2] W. R. Ferris, "Input resistance of vacuum tubes as ultra-high-frequency amplifiers," PROC. I.R.E., vol. 24, pp. 82–107; January, 1936.

[3] I. E. Mouromtseff and H. N. Kozanowski, "Grid temperature as a limiting factor in vacuum tube operation," PROC. I.R.E., vol. 24, pp. 447–454; March, 1936.

resort to water-cooling of the grid electrodes. Such grids have been developed and tested and perform very satisfactorily even with high-emission-efficiency filaments where the grid becomes coated with active materials.

Lead inductance remains as one of the final factors which must be overcome. Several articles[4,5] have described the effects of lead inductance as producing similar grid-loading effects as does transit time. In considering external-anode tubes, the main effects are in grid and cathode circuit inductances. Inductance in the grid circuit increases the difficulties of neutralization and limits the frequency for stable amplifier performance. Inductance in the cathode circuit causes degeneration and increases grid loading. Methods have been described[6] whereby the cathode inductance can be split between the grid and anode circuits so as to neutralize the effects of grid loading. In practice, these methods are difficult to realize so that the only recourse is to reduce the lead inductance to the lowest value possible. This is accomplished by shortening the leads as much as possible and by providing multiple leads of large area.

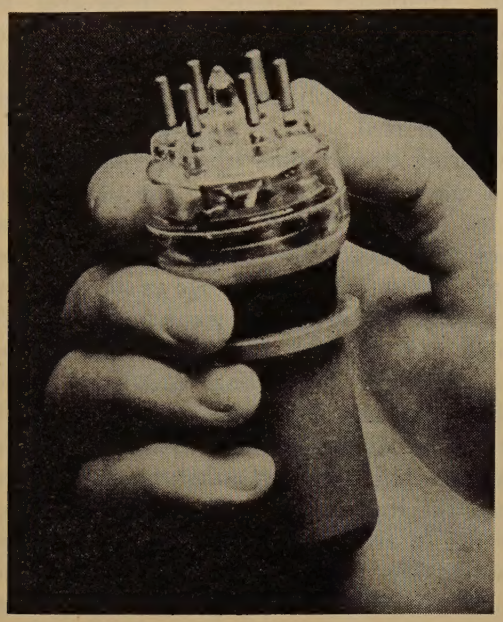

Fig. 1—GL-8002—transmitting tube.

Since sufficient glass length must be provided to correspond to the insulation required a further compromise must be made between glass length and lead length. One method of circumventing this problem is to introvert the anode so that short leads can be maintained while still obtaining sufficient insulation. This method will be discussed later as applied to the GL-880 design.

Forced-air cooling for transmitting tubes has become of general interest and has been applied to several high-power types within the past few years. As this interest spread to the high-frequency field it became increasingly important to design optimum-efficiency coolers in small sizes. Little was known about the theoretical design of fin coolers for vacuum tubes and much of the information had to be developed. These theoretical design data are now so complete and accurate that all details of cooler designs can be worked out in advance and the optimum design for any particular case can be set without even building a sample. In the design of forced-air coolers the main limitation for broadcast stations is the noise level. No definite data have been correlated to show the relation between air volume, air velocity, blower type, etc., with regard to noise. However, for operation as required in the usual broadcast station, the air velocity through the cooler should not exceed about 3000 feet per minute.

Three new high-frequency transmitting tubes have been designed around these fundamental considerations. In each power class a compromise between capacitance, efficiency, transit time, insulation, and lead inductance was arrived at so as to result in as near optimum performance as possible.

## GL-8002

The GL-8002 is the smallest size and is illustrated in Fig. 1. This tube was developed for a plate dissipation of 1200 watts and a power input of 3000 watts in class C telegraph service.

It utilizes a double-helix pure-tungsten filament with three leads brought out to terminals so that the filament sections can be paralleled to reduce inductance. The filament itself is a large-diameter helix so that small spacings and relatively high perveance is obtained. The grid is wound on six stay rods mounted from a supporting collar which is held rigidly in position from the three grid leads. These grid leads are sealed with the filament leads in a molded terminal flare so that the grid-filament structure can be assembled accurately and later sealed in the anode. Particular attention was devoted to the grid design and spacing arrangements to obtain low driving power and high-efficiency operation.

As a result of the compromise between capacitance, transit time, and characteristics, the grid-filament clearance is only 0.060 inch and the grid-anode clearance only 0.084 inch. These close spacings require the utmost care in assembly and seal-in as a displacement of a few mils would either cause short circuits or adversely affect the operating characteristics. These factors are important in most tube manufacture but as greater refinement and precision are approached, special technique is required and exceedingly accurate aligning fixtures become necessary.

[4] B. J. Thompson, "Review of ultra-high-frequency vacuum tube problems." *RCA Rev.*, vol. 3, pp. 146–155; October, 1938.

[5] M. J. O. Strutt and A. van der Ziel, "The causes for the increase of the admittances of modern high-frequency amplifier tubes on short waves," PROC. I.R.E., vol. 26, pp. 1011–1032; August, 1938.

[6] F. Preisach and I. Zakarias, "Input conductance," *Wireless Eng.*, vol. 17, p. 147; April, 1940.

The anode of the 8002 has an active length of $1\frac{1}{4}$ inches and a diameter of $1\frac{1}{8}$ inches. The outside diameter of the anode is determined by the dissipation and cooling requirements whereas the inside diameter must conform to the spacings necessary from the capacitance and transit-time standpoints. Because of the relation of these dimensions, the anode wall becomes three times as thick as has been used previously, which brought out new problems, especially since anodes for high-vacuum tubes must be drawn from sheet material.

TABLE I

GL-8002

Technical Information

| | |
|---|---|
| General Design | |
| Number of electrodes | 3 |
| Filament voltage | 16 volts |
| Filament current | 39 amperes |
| Direct interelectrode capacitances, approximate | |
| Plate-to-grid | 9 micromicrofarads |
| Grid-to-filament | 8 micromicrofarads |
| Plate-to-filament | 0.5 micromicrofarad |
| Over-all dimensions | |
| Maximum length | $4\frac{1}{16}$ inches |
| Maximum diameter | $1\frac{7}{8}$ inches |
| Type of cooling—water and forced air | |

Class C Radio-Frequency Power Amplifier and Oscillator, Telegraphy. (Key-down conditions per tube without modulation. Essentially negative modulation may be used if the positive peak of the audio-frequency envelope does not exceed 115 per cent of the carrier conditions.)

| | |
|---|---|
| Direct plate voltage | 3500 volts |
| Direct grid voltage | −500 volts |
| Direct plate current | 1.0 ampere |
| Direct grid current | 0.1 ampere |
| Plate input | 3000 watts |
| Plate dissipation | 1200 watts |

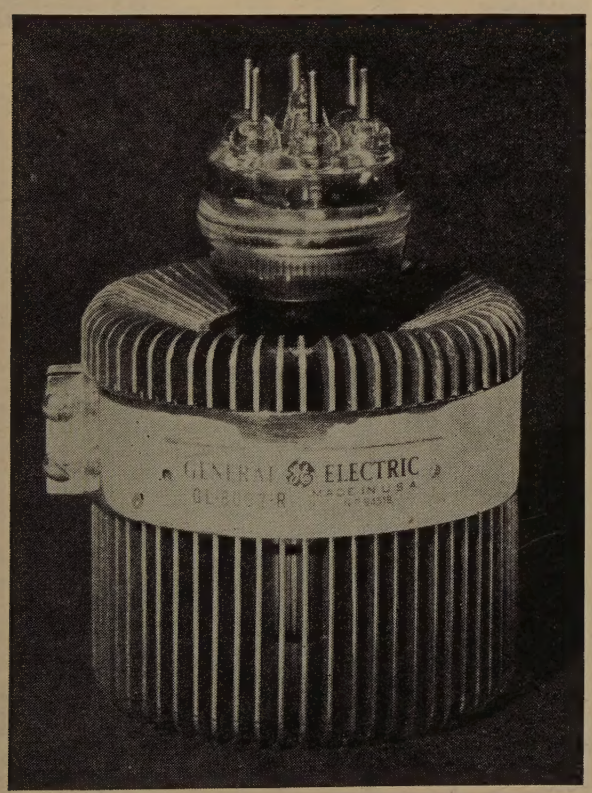


Fig. 2—GL-8002-R—transmitting tube.

The complete tube is only $4\frac{1}{16}$ inches long and $1\frac{7}{8}$ inches in diameter and with its water jacket can be mounted directly into transmission-line circuits. Because of short lead lengths and compact neutralizing circuits a pair of these tubes can be operated stably at frequencies as high as 250 megacycles.

The technical data for the 8002 are summarized in Table I. Full ratings apply up to a frequency of 150 megacycles. The 8002 may be used either in television or frequency-modulation transmitters. It forms an ideal driver stage for higher-power transmitters of either type.

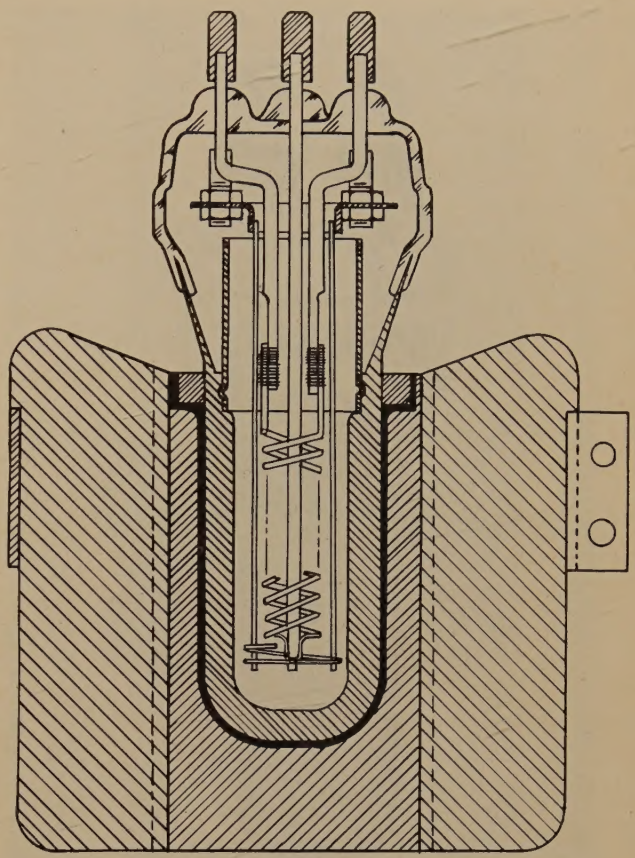

Fig. 3—GL-8002-R—transmitting tube, cross-sectional view, full scale.

## GL-8002-R

The 8002-R is simply the 8002 soldered into a fin cooler as illustrated in Fig. 2. A cross-sectional view is shown in Fig. 3. The fin cooler is designed for full water-cooled ratings but because of its increased diameter the corresponding maximum frequency rating is limited to 120 megacycles. The 8002 is particularly well adapted to air cooling because the thick anode section distributes the heating uniformly and precludes power limitation caused by "hot-spotting."

The fin cooler for the 8002-R is designed for optimum cooling performance in order to result in the smallest possible size consistent with air-velocity and air-volume limitations. The cooler itself consists of 60 copper fins silver soldered to a slotted copper hub. A retainer band encloses a portion of the fin length and facilitates mounting in the air duct.

Technical information on the 8002-R is shown in Table II. Two tubes are used to develop 3 kilowatts in frequency-modulation transmitters.

## GL-889

The 889 represents the next larger size and is illustrated in Fig. 4. It was developed primarily for the

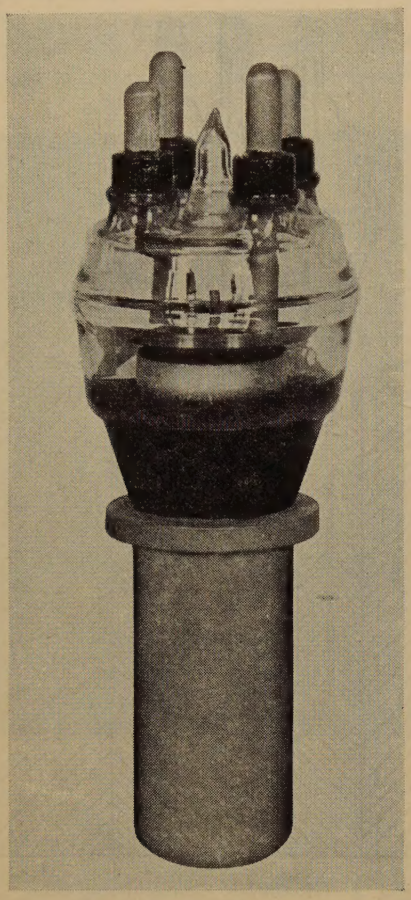

Fig. 4—GL-889—transmitting tube.

output stage of medium-powered television transmitters but has found wide application in many other services. The 889 has a plate dissipation rating of 5 kilowatts and a power-input rating of 16 kilowatts for class C telegraph service. Full ratings apply up to a frequency of 50 megacycles and reduced ratings up to 150 megacycles.

TABLE II
GL-8002-R
Technical Information

| | |
|---|---|
| General Design | |
| Number of electrodes | 3 |
| Filament voltage | 16 volts |
| Filament current | 39 amperes |
| Direct interelectrode capacitances, approximate | |
| Plate-to-grid | 9 micromicrofarads |
| Grid-to-filament | 8 micromicrofarads |
| Plate-to-filament | 0.5 micromicrofarad |
| Over-all dimensions | |
| Maximum length | 5⅞ inches |
| Maximum diameter | 3 11/16 inches |
| Type of cooling—forced air | |

Class C Radio-Frequency Power Amplifier and Oscillator, Telegraphy.
(Key-down conditions per tube without modulation. Essentially negative modulation may be used if the positive peak of the audio-frequency envelope does not exceed 115 per cent of the carrier conditions.)

| | |
|---|---|
| Direct plate voltage | 3500 volts |
| Direct grid voltage | −500 volts |
| Direct plate current | 1.0 ampere |
| Direct grid current | 0.1 ampere |
| Plate input | 3000 watts |
| Plate dissipation | 1200 watts |

The air flow should be 100 cubic feet per minute and the temperature of the incoming air should not exceed 45 degrees centigrade. The glass temperature must not be allowed to exceed 150 degrees centigrade. Ordinarily, deflecting vanes diverting the outgoing air toward the terminal seals provide sufficient cooling.

The filament of the 889 is a cage-type structure consisting of 6 strands of pure-tungsten wire. The filament spring is mounted in 2 cup containers away from the heat zone so that proper spring tension is maintained throughout the life of the tube. Each filament terminates in a molybdenum lead and these leads are connected to plates so that alternate strands are in parallel. The grid and filament terminals are copper thimbles sealed to a four-post, molded pyrex dish so that the assembly can be completed before the final anode seal is made. Copper rods, ⅜ inch in diameter, form the connecting leads between the copper thimbles and the grid and filament structures. In this manner, lead inductance is reduced and, by providing two grid leads, common coupling between excitation and neutralizing circuits is eliminated.

The technical data and characteristics for the 889 are shown in Table III and Fig. 5. Two 889's may be

TABLE III
GL-889
Technical Information

| | | | | |
|---|---|---|---|---|
| General Characteristics | | | | |
| Electrical | | | | |
| Filament voltage | | | | 11 volts |
| Filament current | | | | 125 amperes |
| Amplification factor, $E_b$ = 5 kv, $I_b$ = 1.0 amp. $E_c$ = −75 v, $E_f$ = 11 v a.c. | | | | 21 |
| Grid-plate transconductance | | | | 9000 micromhos |
| Direct interelectrode capacitances | | | | |
| Grid-plate | | | | 17.8 micromicrofarads |
| Grid-filament | | | | 19.5 micromicrofarads |
| Plate-filament | | | | 2.5 micromicrofarads |
| Class C Radio-Frequency Power Amplifier and Oscillator (Key-down conditions per tube without modulation.) | | | | |
| Direct plate voltage | 5000 | 6000 | 7500 | 8500 volts |
| Direct grid voltage | −500 | −600 | −800 | −1000 volts |
| Direct plate current | 1.5 | 1.8 | 2.0 | 2.0 amperes |
| Direct grid current, approximate | 0.19 | 0.21 | 0.24 | 0.25 ampere |
| Plate input | | | | 16 kilowatts |
| Plate dissipation | | | | 5 kilowatts |
| Peak radio-frequency grid input voltage, approximate | 1200 | 1460 | 1830 | volts |
| Driving power, approximate | 220 | 290 | 400 | watts |
| Plate power output | 5 | 7 | 10 | kilowatts |

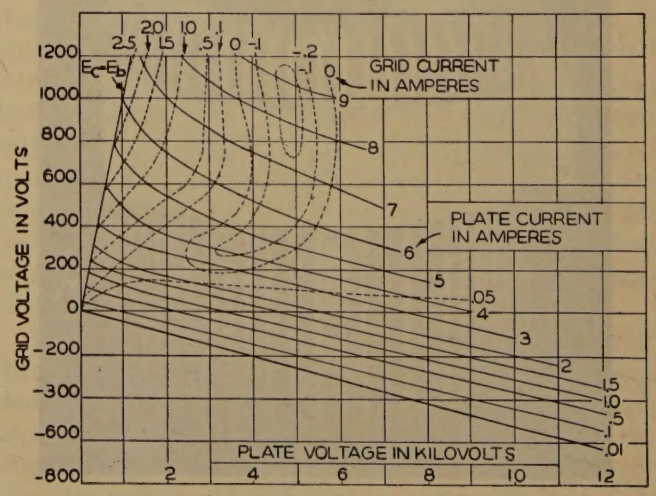


Fig. 5—GL-889—characteristics.

used for the output stage of a 1-kilowatt television transmitter for all bands up to 108 megacycles. For frequency modulation two tubes develop 10 kilowatts output with operation well within their ratings.

## GL-889-R

A fin cooler designed for 5 kilowatts plate dissipation is applied to the 889 and is illustrated in Fig. 6. Due to the increased size of the anode structure, the maximum frequency of the 889-R is limited to 25 megacycles at full ratings although it can be used at reduced ratings up to 100 megacycles. The cooler consists of 90 radial fins brazed to a slotted copper hub. The anode of the 889 is soldered in the hub with high-melting-point solder so that failures due to solder softening are eliminated.

TABLE IV

GL-889-R

Technical Information

| | | | | |
|---|---|---|---|---|
| General Characteristics | | | | |
| Electrical | | | | |
| Filament voltage | | | | 11 volts |
| Filament current | | | | 125 amperes |
| Amplification factor, $E_b$=5 kv, $I_b$=1.0 amp. $E_c$=−75 v, $E_f$=11 v a.c. | | | | 21 |
| Grid-plate transconductance | | | | 9000 micromhos |
| Direct interelectrode capacitances | | | | |
| Grid-plate | | | | 20.7 micromicrofarads |
| Grid-filament | | | | 19.5 micromicrofarads |
| Plate-filament | | | | 2.5 micromicrofarads |
| Class C Radio-Frequency Power Amplifier and Oscillator. (Key-down conditions per tube without modulation.) | | | | |
| Direct plate voltage | 5000 | 6000 | 7500 | 8500 volts |
| Direct grid voltage | −500 | −600 | −800 | −1000 volts |
| Direct plate current | 1.5 | 1.8 | 2.0 | 2.0 amperes |
| Direct grid current, approximate | 0.19 | 0.21 | 0.24 | 0.25 ampere |
| Plate input | | | | 16 kilowatts |
| Plate dissipation | | | | 5 kilowatts |
| Radiator temperature | | | | 180 degrees centigrade |
| Peak radio-frequency grid input voltage, approximate | 1200 | 1460 | 1830 | volts |
| Driving power, approximate | 220 | 290 | 400 | watts |
| Plate power output | 5 | 7 | 10 | kilowatts |

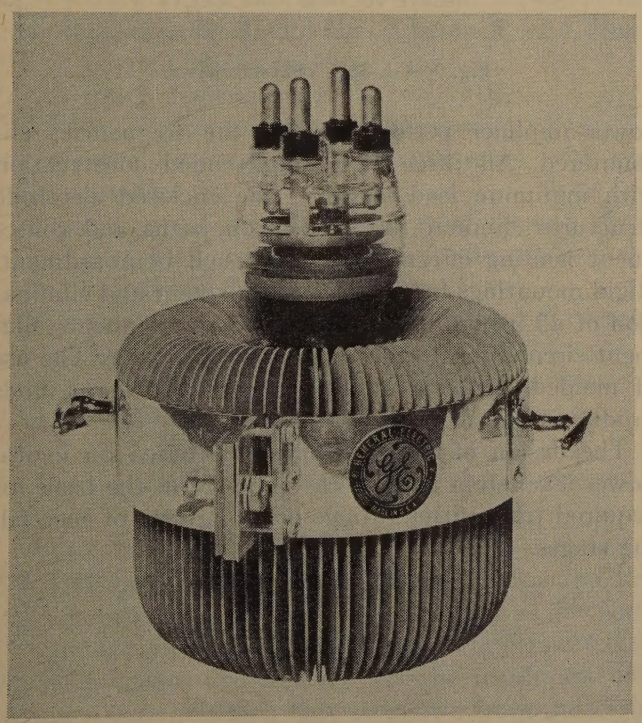

Fig. 6—GL-889-R—transmitting tube.

Technical data on the GL-889-R are shown in Table IV. Two tubes are used in frequency-modulation transmitters to deliver 10 kilowatts output up to 50 megacycles.

## GL-880

The 880 is designed for 20 kilowatts plate dissipation and is of particular interest because of the unique

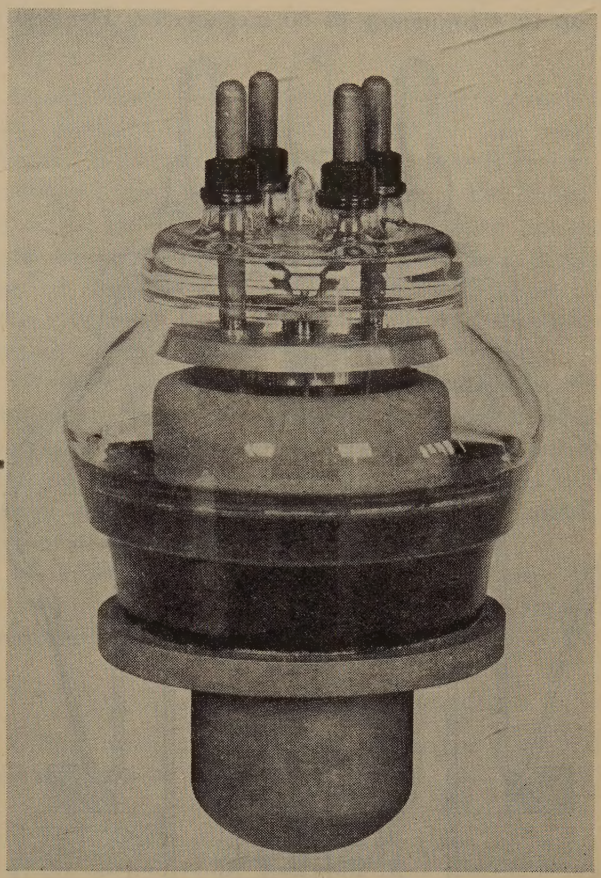

Fig. 7—GL-880—transmitting tube.

anode design. As tube size is increased it becomes more and more difficult to keep the lead inductance to reasonable values consistent with the frequency requirements. This is especially true as the plate voltage usually is higher and greater insulation lengths must be provided. These difficulties were overcome, in part, by introverting the anode. In other words, by folding the anode back on itself twice the lead length was reduced approximately 10 inches below that required in previous designs. This construction is illustrated in the photograph (Fig. 7) and in the cross-sectional view of Fig. 8. As can be seen from the cutaway view, the lead length to the active portion of the electrodes is approximately 4 inches. Isolating over 4 kilowatts of filament power plus other heating effects only 4 inches from the glass terminal mount becomes quite a problem and further reduction of lead lengths is exceedingly difficult. The filament consists of 12 strands of pure tungsten mounted in a cage construction and operates on 12.6 volts and 320 amperes. The 880 as well as the 889 utilizes copper thimble seals mounted on a molded pyrex dish.

The technical data and characteristics for the 880 are shown in Table V and Fig. 9. For frequencies up

to 25 megacycles, full ratings are allowed and two tubes develop 50 kilowatts carrier power in plate-modulated broadcast transmitters. For frequency modulation two tubes are used for the 50-kilowatt amplifier up to a frequency of 50 megacycles. The 880 is

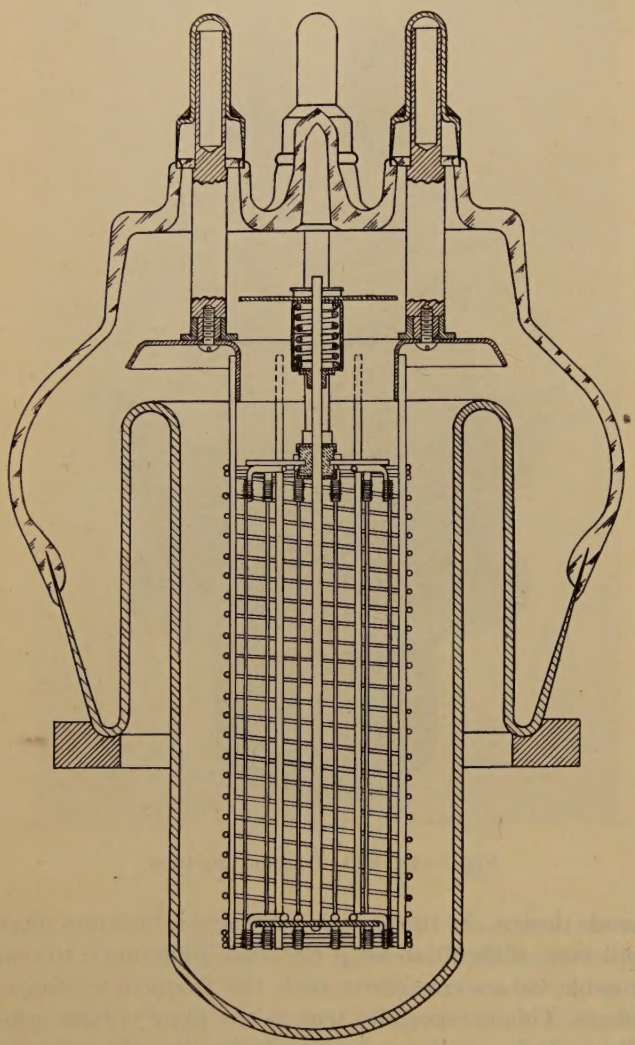

Fig. 8—GL-880—transmitting tube, cross-sectional view, full scale.

ideally suited to broad-band television amplifiers because the plate impedance necessary for the tube is even lower than that required from the band-width standpoint.

The development of these tubes combines several common design features to obtain stable and efficient

TABLE V

GL-880

Technical Information

| | | | | |
|---|---|---|---|---|
| General Characteristics | | | | |
| Electrical | | | | |
| Filament voltage | | | | 12.6 volts |
| Filament current | | | | 320 amperes |
| Amplification factor | | | | 20 |
| Grid-plate transconductance, $I_b$ = 2.0 | | | | 21,000 micromhos |
| Direct interelectrode capacitances | | | | |
| Grid-plate | | | | 26 micromicrofarads |
| Grid-filament | | | | 29 micromicrofarads |
| Plate-filament | | | | 2.6 micromicrofarads |
| Class C Radio-Frequency Power Amplifier and Oscillator. (Key-down conditions per tube without modulation.) | | | | |
| Direct plate voltage | 7500 | 10,000 | 10,000 | 10,500 volts |
| Direct grid voltage | −600 | −800 | −800 | −1200 volts |
| Direct plate current | 5 | 4.5 | 6 | 6 amperes |
| Direct grid current, approximate | 0.45 | 0.4 | 0.5 | 0.6 ampere |
| Plate input | | | | 60 kilowatts |
| Plate dissipation | | | | 20 kilowatts |
| Peak radio-frequency grid input voltage, approximate | 1250 | 1400 | 1500 | volts |
| Driving power, approximate | 560 | 550 | 750 | watts |
| Plate power output | 27 | 34 | 45 | kilowatts |

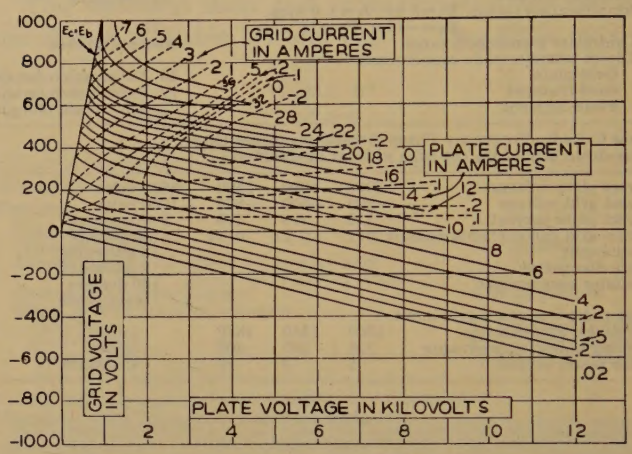


Fig. 9—GL-880—characteristics.

power-amplifier performance at the frequencies encountered. All three have single-ended construction with minimum lead lengths. The enclosed electrode structures eliminate stray electron paths and consequent heating effects caused by such bombardment. Rigid mountings for the grid and filament and elimination of all insulators except in the low-frequency filament circuits result in improved performance. The use of molded glass parts and accurate sealing methods produce uniform characteristics.

The design of the three types is based on logical power-level steps so that the tubes form the basis for required transmitter ratings or for drivers of succeeding stages.

# The Determination of Operating Data and Allowable Ratings of Vacuum-Tube Rectifiers*

J. C. FROMMER†, NONMEMBER, I.R.E.

***Summary***—*Among the operating data of thermionic rectifiers only transformer voltage, output voltage, and output current are readily accessible. In determining the permissible limits of operation however, peak current, inverse voltage, and plate dissipation must be considered. This paper gives formulas and a graph to determine these latter values from the former, to rate limits of operation, and to draw the dynamic characteristics for any valve.*

## I. Symbols

$E$ = the instantaneous voltage between an anode and the cathode of the tube.
$E_{eff}$ = the root-mean-square value of the transformer voltage between either plate and the center tap.
$E_0$ = the output voltage.
$E_l$ = unity of voltage in Fig. 2 $= (cI_l)^{2/3}$.
$I$ = the instantaneous cathode current.
$I_p$ = the peak value of cathode current.
$I_{pm}$ = the permissible limit of peak cathode current.
$I_0$ = the output current.
$I_c$ = symbol for the expression $c^{-2/5}W^{3/5}$ ("equivalent constant current," the continuous cathode current at which some dissipation $W$ is reached).
$I_{cm}$ = the continuous cathode current at which the permissible dissipation is reached with direct current on the valve.
$I_l$ = unity of current in Fig. 2 $= (1/c)E_l^{3/2}$.
$W$ = energy loss on one plate (dissipation).
$R$ = ohmic resistance effective in series with one anode.
$x$ = the angle of the alternating-current cycle measured from an origin at the crest of the transformer voltage.
$\phi$ = the value of this angle $x$ at the end of current flow.
$c$ = the constant in the space-charge equation.
$F(\phi)_k$ = symbol for the integral $(1/2)\int_{-\phi}^{+\phi}(\cos x - \cos\phi)^k dx$.
$n$ = the number of phases in polyphase systems.

## II. Introduction

THE limiting factors which must be considered in determining the operating conditions for vacuum-tube rectifiers are (1) the heat generated at the plate (plate dissipation), (2) the maximum momentary current which may be drawn from the cathode (peak cathode current), and (3) the voltage between the cathode and plates of the tube (peak inverse voltage, sometimes root-mean-square voltage).

* Decimal classification: R337. Original manuscript received by the Institute, November 13, 1940; revised manuscript received, June 10, 1941.

† 3155 Pine Grove Ave., Chicago, Ill.

Further care must be taken that surge voltages and surge currents may not damage the tube: this question however is outside the scope of the present paper.

The mathematical relations between the values referred to under (1), (2), and (3) and the operating data have been established theoretically. A graph plotted from these formulas gives the dynamic characteristics and the values necessary to establish operating ratings of any rectifier tube.

In the following treatment ideal conditions are assumed; i.e., that the transformer voltage is sinusoidal, the choke is of infinite inductance in choke-input service, and the transformer is of infinite capacity in condenser-input service. These assumptions cause no serious deviations from actual operation.

All calculations refer to full-wave systems. Half-wave condenser input and polyphase choke input are dealt with in section VI.

## III. The Fundamental Equations

Ohmic resistance in the transformer is neglected in this section.

### *1. Choke Input*

If the dotted condenser on Fig. 1a is disconnected, it represents a full-wave choke-input rectifier.

The output current is maintained constant by the choke. As this circuit contains no condenser to store the difference between valve current and output current,

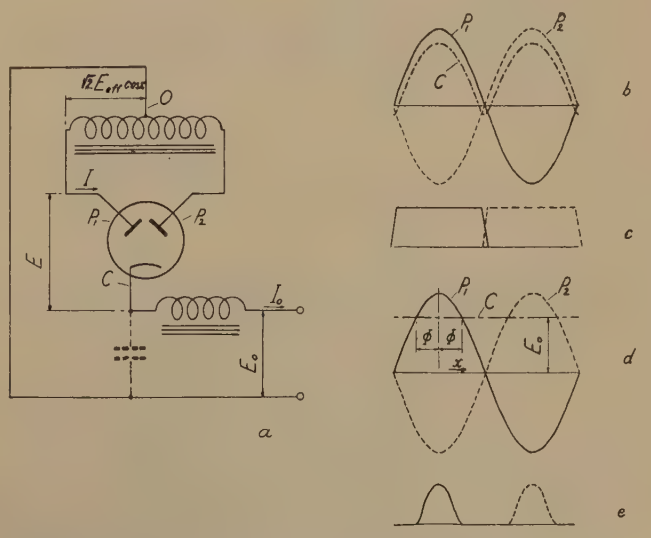


Fig. 1—Fundamentals. a. Schematic of double-wave rectifier (in choke input the dotted condenser is disconnected). b. Time curves of voltage in choke-input service. c. Time curves of valve currents in choke-input service. d. Time curves of voltages in condenser-input service. e. Time curves of valve currents in condenser-input service.

the valve current must always equal the output current. This in turn is only possible if the cathode assumes a voltage curve which secures a constant cathode current throughout the cycle. Constant current is maintained by constant voltage; thus, in choke-input rectifiers, the cathode floats at a voltage below the voltage of the more positive anode by the value necessary to draw the output current.[1] The time curve of cathode voltage is represented on Fig. 1b (curve *C*). The individual currents to the two plates are represented on Fig. 1c. As is seen on this figure, the peak cathode current is equal to the output current:

$$I_p = I_0. \tag{1}$$

The plate dissipation is

$$W = \frac{1}{2\pi}\int_{-\pi}^{+\pi} EI dx. \tag{2}$$

The relation between $E$ and $I$ is given by the space-charge law

$$I = \frac{1}{c} E^{3/2}. \tag{3}$$

The current to one plate is equal to the output current but it flows only during half a cycle; the curves of Fig. 1c can be approximated fairly by rectangular lines enclosing the same area. Therefore, after substituting $E$ from (3)

$$W = \tfrac{1}{2}(cI_0)^{2/3}I_0 = \tfrac{1}{2}c^{2/3}I_0^{5/3}. \tag{4}$$

As a simple measure of plate dissipation a value $I_c$, the "equivalent constant current" will be determined. This is a direct current which, drawn from one plate, would produce the same dissipation as that occurring on one plate of the tube under investigation. This measure permits direct reference to investigations at which the plate is heated by direct current.

If direct current is applied between the cathode and the anode of the valve, the dissipation is

$$W = EI. \tag{5}$$

With (3),

$$W = (cI_c)^{2/3}I_c = c^{2/3}I_c^{5/3} \tag{6}$$

whence

$$I_c = c^{-2/5}W^{3/5}. \tag{7}$$

Equating (4) and (6) the equivalent constant current is found to be

$$\boxed{I_c = (\tfrac{1}{2})^{3/5}I_0}. \tag{8}$$

The output voltage is the mean value of voltage between the cathode and the center tap (curve *C* of Fig. 1b). With fair approximation the mean value of this curve is the mean value of the positive parts of the voltage curves of both the anodes (curves $P_1$ and $P_2$) reduced by the voltage drop of the valve:

$$E_0 = \frac{2}{\pi}\sqrt{2}\,E_{\text{eff}} - (cI_0)^{2/3}. \tag{9}$$

The peak inverse voltage is found at the maximal distance between curves *P* and *C*:

$$2\sqrt{2}\,E_{\text{eff}} - (cI_0)^{2/3}. \tag{10}$$

The integration yields for the root-mean-square voltage across the valve[2]

$$\sqrt{2}\,E_{\text{eff}} - \frac{2}{\pi}(cI_0)^{2/3}. \tag{11}$$

*2. Condenser Input*

Fig. 1a, with the dotted condenser in action, represents a full-wave condenser-input rectifier. The time curves of voltage and current through the valve are given in Figs. 1d and 1e. The voltage between an anode and the middle tap of the transformer is

$$\sqrt{2}\,E_{\text{eff}} \cos x. \tag{12}$$

The voltage between the cathode and the middle tap is held constant by the condenser. It is equal to the output voltage $E_0$. The voltage across the valve is the difference of these:

$$E = \sqrt{2}\,E_{\text{eff}} \cos x - E_0. \tag{13}$$

Current flow begins when the angle $x$ reaches $-\phi$ and ceases at $+\phi$. At these points the voltage across the valve is zero. Whence

$$E_0 = \sqrt{2}\,E_{\text{eff}} \cos \phi. \tag{14}$$

Substituting (14) into (13)

$$E = \sqrt{2}\,E_{\text{eff}}(\cos x - \cos \phi). \tag{15}$$

Substituting this into (3)

$$I = \frac{1}{c}\left[\sqrt{2}\,E_{\text{eff}}(\cos x - \cos \phi)\right]^{3/2}. \tag{16}$$

The output current drawn from the tube is the time integral of the current for both plates simultaneously:

$$I_0 = 2\,\frac{1}{2\pi}\int_{-\phi}^{+\phi}\frac{1}{c}\left[\sqrt{2}\,E_{\text{eff}}(\cos x - \cos \phi)\right]^{3/2}dx. \tag{17}$$

The following abbreviation will be used:

$$F(\phi)_k = \frac{1}{2}\int_{-\phi}^{+\phi}(\cos x - \cos \phi)^k dx. \tag{18}$$

(For numerical values of this integral see the Appendix.)

With (18), equation (17) assumes the form

$$I_0 = \frac{2}{\pi c}(\sqrt{2}\,E_{\text{eff}})^{3/2}F(\phi)_{3/2}. \tag{19}$$

[1] At the change of phase the cathode will assume a voltage at which the two plates together give the output current.

[2] Root-mean-square voltage is of interest when high frequency is rectified. Equation (11) is obtained by neglecting a portion smaller than the square of the second term divided by the first term.

The peak value of cathode current (equation (16)) is

$$I_p = \frac{1}{c}\left[\sqrt{2}\,E_{\text{eff}}(1 - \cos\phi)\right]^{3/2}. \tag{20}$$

By division of (19) by (20)

$$\boxed{\frac{I_0}{I_p} = \frac{2}{\pi}\left(\frac{1}{1 - \cos\phi}\right)^{3/2} F(\phi)_{3/2}}. \tag{21}$$

The dissipation on one plate is

$$W = \frac{1}{2\pi}\int_{-\phi}^{+\phi} EI\,dx \tag{22}$$

and on substituting (15), (16), and (18)

$$W = \frac{1}{\pi c}\left(\sqrt{2}\,E_{\text{eff}}\right)^{5/2} F(\phi)_{5/2}. \tag{23}$$

The equivalent constant current $I_c$ is found by insertion of (23) into (7):

$$I_c = \frac{1}{c}\,\pi^{-3/5}\left(\sqrt{2}\,E_{\text{eff}}\right)^{3/2}\left[F(\phi)_{5/2}\right]^{3/5} \tag{24}$$

and by division of (19) by (24)

$$\boxed{\frac{I_0}{I_c} = \frac{2}{\pi^{2/5}}\,\frac{F(\phi)_{3/2}}{\left[F(\phi)_{5/2}\right]^{3/5}}}. \tag{25}$$

The peak inverse voltage is (as seen on Fig. 1d)

$$(1 + \cos\phi)\sqrt{2}\,E_{\text{eff}}. \tag{26}$$

The root-mean-square voltage across the valve is

$$\sqrt{2(\cos\phi)^2 + 1}\,E_{\text{eff}}. \tag{27}$$

## IV. Construction of the Dynamic Characteristics of Rectifiers

### 1. *Choke Input*

Equation (9) gives this curve for an ideal transformer without voltage drop. With a resistance $R$ in the circuit of the valve

$$E_0 = \frac{2}{\pi}\sqrt{2}\,E_{\text{eff}} - (cI_0)^{2/3} - I_0R. \tag{28}$$

### 2. *Condenser Input*

This curve can be constructed (if the ohmic resistance of the transformer is neglected) from (14) and (19) with $\phi$ as the parameter.

With the resistance $R$ in the circuit of the valve we can write from (15)

$$\sqrt{2}\,E_{\text{eff}}(\cos x - \cos\phi) = (cI)^{2/3} + IR. \tag{29}$$

Hence

$$\sqrt{2}\,E_{\text{eff}}(1 - \cos\phi) = (cI_p)^{2/3} + I_pR. \tag{30}$$

For given conditions we can work out $\phi$ as a function of $I_p$ from (30); with $\phi$ we get $E_0$ from (14). $I_0$ could be obtained from (21) if the voltage across the valve were sinusoidal. The resistance in the circuit, however, will distort this relation. For very high ohmic resistances it is the current through the valve which is sinusoidal and we obtain

$$\frac{I_0}{I_p} = \frac{2}{\pi}\left(\frac{1}{1 - \cos\phi}\right)F(\phi)_1. \tag{31}$$

Numerical values of this other extreme deviate from those of (21) by a small fraction only (see (48)) so that interpolation will always give reliable results.

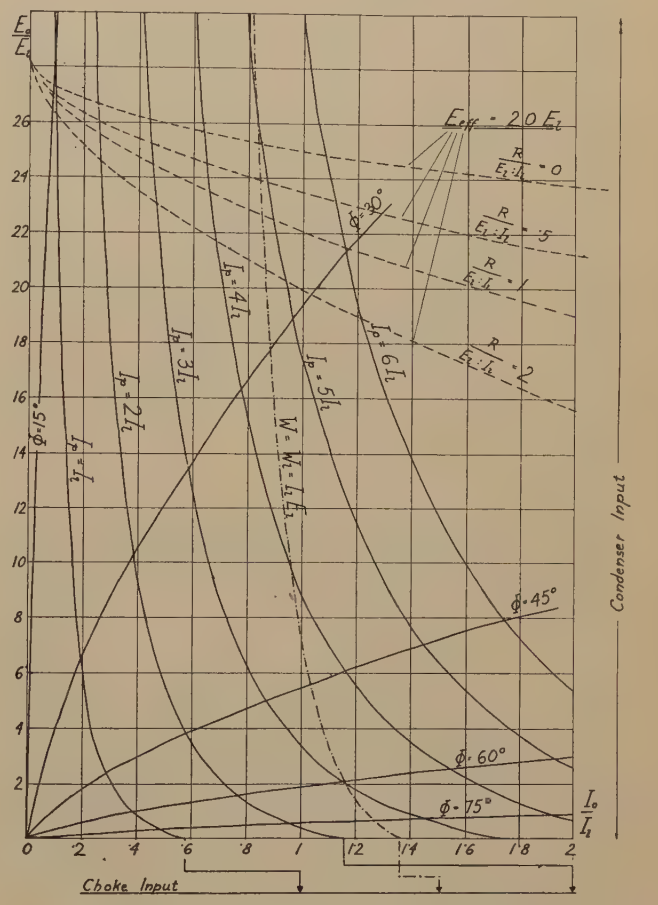


Fig. 2—Universal diagram showing the dynamic characteristics and permissible limits of output for full-wave condenser-input rectifiers.

The co-ordinates are output currents and output voltages expressed in terms of any current $I_l$ and the voltage $E_l = (cI_l)^{2/3}$.

The dash-dotted line joins the points at which (for a transformer without voltage drop) dissipation is $W = E_l\,I_l$. The lines marked $I_p = I_l$, $I_p = 2\,I_l$, etc., join points at which the peak current through the valve reaches 1 times, 2 times, etc. $I_l$ (for a transformer without voltage drop).[1]

The lines $E_{\text{eff}} = 20\,E_l$ give dynamic characteristics with and without voltage drop in the transformer.

The whole plane relates to condenser input. On the bottom are indicated the output current values at which (independently of the output voltage) the same dissipation and peak current are reached in choke-input service.

[1] Voltage drop in the transformer will only diminish both peak current and dissipation.

These characteristic curves have been drawn in a quite universal form on Fig. 2. The unity of current and voltage are here any freely choosen values $I_l$ and

$E_l$ between which the relation

$$I_l = \frac{1}{c} E_l^{3/2} \tag{32}$$

exists. Actually the dynamic characteristics are drawn for the transformer voltage $E_{eff} = 20\ E_l$. Thus if we want the dynamic characteristics of any tube for any fixed value of $E_{eff}$, we must choose the unity $E_l$ to be one twentieth of this $E_{eff}$ and reckon $I_l$ from (32) with the constant $c$ of the valve under investigation. With these units the curves give the dynamic characteristics of the individual type of rectifier tube for the transformer voltage selected. The resistance of the transformer $R$ must be expressed in terms of the quotient $E_l : I_l$ and, generally, we must interpolate the curve for the desired value between those drawn. For the equations of these universal characteristics see Appendix.

## V. Safe Ratings of Rectifiers

Set first the permissible limits of peak cathode current ($I_{pm}$), plate dissipation, and inverse voltage theoretically or experimentally. $I_{cm}$, the equivalent constant current pertaining to the permissible dissipation, can be reckoned from (7). If the permissible dissipation is established by application of direct current then $I_{cm}$ is obtained directly.

### *1. Choke Input*

According to (1) the output current should be held below the permissible peak cathode current. According to (8) $(1/2)^{3/5} I_0$ should be held below $I_{cm}$:

$$I_0 \leqq I_{pm} \tag{33}$$

$$I_0 \leqq 2^{3/5} I_{cm} = 1.516 I_{cm}. \tag{34}$$

The permissible output voltage could be worked out with (9), (10), and (11); this however could be only of theoretical interest, the usual way of specifying maximal permissible transformer voltage being quite satisfactory.

### *2. Condenser Input*

For condenser input, peak current and dissipation vary according to the angle of current flow. This angle is determined[3] by $E_0$ and $I_0$. Thus for every point of the field of the dynamic characteristics the peak current and dissipation can be worked out. These values are shown on Fig. 2. Curves $I_p = I_l$, $I_p = 2I_l$, etc., give the permissible limits of output for peak current for tubes with a permissible cathode current of $I_l$, $2I_l$, etc. Curve $W = I_l E_l$ gives the permissible limit of output for dissipation for a tube with $I_{cm} = I_l$.

If we want to find the safe limits of operation of any rectifier tube we make $I_l$ equal to $I_{cm}$ of the individual tube type and determine $E_l$ from (32). Now we express the permissible peak cathode current of the tube as a multiple of $I_l$ and find (or interpolate) the curve pertaining to the corresponding value of $I_p/I_l$. The tube should not be used for an output the co-ordinates of which lie to the right of either the line $W = E_l I_l$ or the line traced for $I_p/I_l$.

Another family of curves connects the points at which (again for a transformer without drop) $\phi$, the angle of current flow equals 15 degrees, 30 degrees, etc. For the equations of all these curves see the Appendix.

## VI. Half-Wave Condenser Input and Polyphase Choke Input

The foregoing paragraphs dealt only with full-wave operation. The results can be extended as follows.

### *1. Half-Wave Condenser Input*

For equal transformer voltage and output voltage and peak current through the valve, the peak cathode current and the dissipation on the working plate are the same, while the output current is exactly half that obtained with full-wave operation. Thus all equations and graphs established for full-wave operation are valid for half-wave operation if $I_0$ is replaced[4] by $2\ I_0$ (half wave).

### *2. Polyphase Choke Input*

If the arguments of section III are applied to three-phase, or generally to $n$-phase choke input the following results are obtained.

The peak cathode current equals the output current independently of the number of phases. Each plate draws the total output current during $1/n$th time of the total cycle. The cathode potential floats under the voltage of the most positive (the working) plate by $(cI_0)^{2/3}$.

Hence

$$I_p = I_0 \tag{35}$$

$$W = \frac{1}{n} I_0 (cI_0)^{2/3} \tag{36}$$

or, analogous to (8),

$$I_c = \left(\frac{1}{n}\right)^{3/5} I_0. \tag{37}$$

Further, analogous to (9),

$$E_0 = \sqrt{2}\, E_{eff} \frac{n}{\pi} \sin \frac{\pi}{n} - (cI_0)^{2/3}. \tag{38}$$

## VII. Appendix

For numerical calculations we need the numerical values of the integrals

$$F(\phi)_k = \frac{1}{2} \int_{-\phi}^{+\phi} (\cos x - \cos \phi)^k dx \tag{18}$$

[3] This is for a given value of $c$ and for a transformer without ohmic voltage drop by substituting (14) into (19). If the ohmic resistance is not negligible, both dissipation in the tube and peak current will be less, for in this case the current is drawn for a longer period through the valve than without ohmic voltage drop. Therefore, when limiting the output of the tube it is safe to suppose the absence of ohmic voltage drop.

[4] The condenser is supposed to be of infinite capacitance. To remain close to this assumption actual rectifiers in half-wave connection require considerably higher input capacitance than those in a full-wave connection.

with the exponents $k=1$, 3/2, 2, 5/2 for the different values of $\phi$ between 0 and $\pi/2$. These integrals can be expressed in finite form only if the exponent $k$ is an integer. Numerical calculations however show that these finite expressions give, especially for low values of $\phi$, a very small difference of two large quantities. Therefore, it is preferable to use the approximation

$$\cos x - \cos\phi = (1-\cos\phi)\left(1-\frac{x^2}{\phi^2}\right). \tag{39}$$

With this approximation, which gives very small errors within the limits of our investigations, we have

$$F(\phi)_1 = \frac{2}{3}(1-\cos\phi)\phi \tag{40}$$

$$F(\phi)_2 = \frac{8}{15}(1-\cos\phi)^2\phi \tag{41}$$

$$F(\phi)_3 = \frac{16}{35}(1-\cos\phi)^3\phi. \tag{42}$$

From these values by interpolation

$$F(\phi)_{3/2} = 0.58(1-\cos\phi)^{3/2}\phi \tag{43}$$

$$F(\phi)_{5/2} = 0.48(1-\cos\phi)^{5/2}\phi. \tag{44}$$

The universal dynamic characteristics of Fig. 2 are obtained in the following way.

Bring (30) to the form

$$\sqrt{2}(1-\cos\phi) = \left(\frac{I_p}{I_l}\right)^{2/3}\frac{(cI_l)^{2/3}}{E_{eff}} + \frac{I_p}{I_l}\frac{I_lR}{E_{eff}} \tag{45}$$

with (32)

$$\sqrt{2}(1-\cos\phi) = \left(\frac{I_p}{I_l}\right)^{2/3}\frac{E_l}{E_{eff}} + \frac{I_p}{I_l}\frac{R}{E_l:I_l}\frac{E_l}{E_{eff}}. \tag{46}$$

Bring (14) to the form

$$\frac{E_0}{E_l} = \frac{E_{eff}}{E_l}\sqrt{2}\cos\phi. \tag{47}$$

By substituting (43) and (40) into (21) and (31) and multiplying by $I_p/I_l$

$$\frac{I_0}{I_l} = \frac{I_p}{I_l}\frac{2}{\pi}\frac{2}{3}\phi \cdots \frac{I_p}{I_l}\frac{2}{\pi}0.58\phi. \tag{48}$$

The following interpolation has been used:

$$\frac{I_0}{I_l} = \frac{I_p}{I_l}\frac{2}{\pi}\frac{0.667\dfrac{I_p}{I_l}\dfrac{R}{E_l:I_l} + 0.58\left(\dfrac{I_p}{I_l}\right)^{2/3}}{\dfrac{I_p}{I_l}\dfrac{R}{E_l:I_l} + \left(\dfrac{I_p}{I_l}\right)^{2/3}}\phi. \tag{49}$$

With $I_p/I_l$ as the parameter first find $\phi$ from (46), then $E_0/E_l$ from (47), and $I_0/I_l$ from (49).[5]

The points of the curve $W=I_l\,E_l$ (i.e. $I_c=I_l$) are obtained as follows: Multiply (25) by $I_c/I_l=1$.

$$\frac{I_0}{I_l} = \frac{2}{\pi^{2/5}}\frac{F(\phi)_{3/2}}{[F(\phi)_{5/2}]^{3/5}}. \tag{50}$$

Now substitute (14) into (24), whence with (32) and $I_c=I_l$

$$\frac{E_0}{E_l} = \left(\frac{\pi}{F(\phi)_{5/2}}\right)^{2/5}\cos\phi. \tag{51}$$

These two equations give, with $\phi$ as parameter, the points of the curve $W=I_l\,E_l$.

To obtain the points of equal peak current multiply (21) by $I_c/I_l$

$$\frac{I_0}{I_l} = \frac{2}{\pi}\left(\frac{1}{1-\cos\phi}\right)^{3/2}F(\phi)_{3/2}\frac{I_p}{I_l}. \tag{52}$$

Now substitute (14) into (20) and with (32) bring it to the form

$$\frac{E_0}{E_l} = \frac{\cos\phi}{1-\cos\phi}\left(\frac{I_p}{I_l}\right)^{2/3}. \tag{53}$$

These two equations give, with $\phi$ as parameter, the co-ordinates of the curves along which peak current is equal.

The lines for $\phi=$ 15 degrees, 30 degrees, etc., are obtained by connecting the points obtained with the same value of $\phi$ in the above family of curves.

## VIII. Conclusion

Formulas have been given connecting output voltage and output current with peak current and plate dissipation for full-wave rectifiers. Fig. 2 gives the theoretical dynamic characteristics for condenser-input rectifiers, the points of the field of the dynamic characteristics at which some predetermined plate dissipation is reached, and those at which some prefixed peak current is reached. This graph has ratios as co-ordinates, so that it can be applied to any type of rectifier tubes. The results are extended to half-wave condenser input and polyphase choke input.

[5] The co-ordinates of the points of the dynamic characteristics.

# Reactance Networks for Coupling Between Unbalanced and Balanced Circuits*

S. FRANKEL†, ASSOCIATE, I.R.E.

***Summary***—*The problem of transferring electrical energy from unbalanced sources to balanced loads is usually handled by interposing an isolation transformer between the source and the load. In situations where the isolation transformer proves unsatisfactory, resort must be had to other means. Alford has described certain 2-mesh reactance networks which often serve as satisfactory substitutes for the isolation transformer.*

*In this paper a general theorem is derived for the arbitrary 4-terminal linear passive network, demonstrating necessary and sufficient conditions for satisfactory matching of unbalanced sources and balanced loads. The design of networks satisfying these conditions is independent of the impedances of the source and load; a network satisfying the conditions of this theorem will match an unbalanced source of any arbitrary internal impedance to a balanced load of any arbitrary impedance. In general, any particular reactance network satisfies these conditions at only a few isolated frequencies, at most. In the particular case of the isolation transformer they are satisfied at all frequencies. Certain previously known networks are shown to be special cases of this general class; lattice networks satisfying the conditions of the theorem are described in some detail.*

*The paper concludes with a brief discussion of a well-known network often used to match partly unbalanced sources to balanced loads.*

## I. Introduction

IN DEALING with so-called "4-terminal" transducers in communication network theory, we are usually required to distinguish between two types of sources and sinks of power. These types are commonly referred to as "unbalanced" or "single-ended"

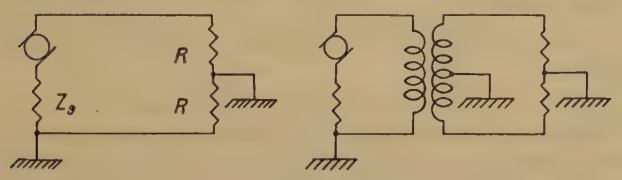


a Fig. 1 b

(a) Incorrect method of connecting a single-ended generator to a balanced load. (b) Correct method.

and "balanced" or "double-ended," respectively, the terms referring to the electrical condition of source or sink with respect to ground. Thus a 2-terminal generator or a 2-terminal load that has one terminal connected to ground through an impedanceless path is called "single-ended." On the other hand, if the generator is so related to ground that the open-circuit voltages measured from each terminal to ground are equal in magnitude but opposite in phase, or if the load is so related to ground that the impedance measured from each terminal to ground are equal in magnitude and phase angle, the generator or the load is called "balanced." Occasionally we need also to deal with sources or sinks that are neither single-ended nor balanced as defined above, but whose electrical condition is intermediate between these extremes.

* Decimal classification: R142. Original manuscript received by the Institute, November 26, 1940; revised manuscript received, July 21, 1941.

† Federal Telegraph Company, Newark, N. J.

The necessity for distinguishing between these types is common knowledge in the communications art and is exemplified by the condition shown in Fig. 1a. Here we show a single-ended generator with internal impedance $Z_g$ connected directly to a balanced load $2R$; it is immediately evident that one half of the load is short-circuited through ground.

It thus becomes necessary to interpose a transducer between the generator and the load to remove the difficulty indicated in Fig. 1a. We have no *a priori* reason for supposing that such a transducer exists; but to settle this question we need only point out that at least one such network has been in use for many years, namely the "isolation transformer." By means of this transformer satisfactory connections can be made between the different types of sources and sinks as shown in Fig. 1b. Furthermore these connections are satisfactory for all values of load and generator impedance. The secondary of the transformer is grounded at its electrical mid-point.

The isolation-transformer method is satisfactory over a continuous band of frequencies, regardless of load or generator impedance, so long as transformers realized in practice approximate the conditions shown in Fig. 1b. Actually such transformers possess distributed electrostatic capacitance between the primary and the secondary which, at sufficiently high frequencies, permits a charging current to flow from the high-voltage side of the primary into the secondary, thus setting up an appreciable unbalance component in the secondary. At such frequencies an electrostatic shield may be interposed between the primary and the secondary, the shield being returned to ground. If the ground return of the shield is an impedanceless path, the electrostatic coupling between primary and secondary becomes negligible.

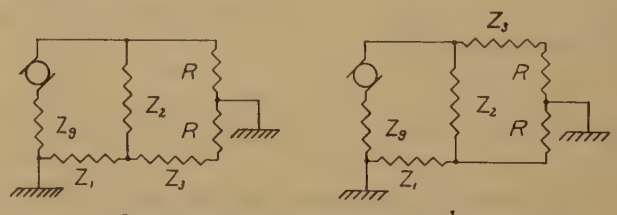


a b

Fig. 2—Alford networks for matching a single-ended generator to a balanced load.

As the frequency is increased still further, the problem of returning the shield to ground becomes extremely serious because of the inductance of the lead, and the effectiveness of the shield is correspondingly diminished. Another objection to the shield at high frequencies is the fact that it introduces capacitance to

ground in the load as seen by the generator. If the generator is, for example, a class C amplifier, this capacitance will limit the amplifier plate efficiency at high frequencies by diminishing the maximum obtainable $L$-$C$ ratio for the amplifier load.

For these reasons it sometimes becomes desirable to find substitutes for the isolation transformer. A minimum requirement of any such substitute is that it perform the matching function independently of the magnitude of generator or load impedance. A group of such networks has been described by Alford.[1] Two types of reactance networks as shown in Fig. 2 are involved. When proper values are assigned to $Z_1, Z_2$, and $Z_3$, balanced voltages will appear across the load regardless of the value of $Z_g$ and $R$. In the case of Fig. 2a, the proper relations are, as shown by Alford,

$$\left.\begin{aligned} Z_2 &= -2Z_1 \\ Z_3 &= -2Z_1 \end{aligned}\right\}. \tag{1}$$

In the case of Fig. 2b, the proper relations are

$$\begin{aligned} Z_2 &= -2Z_1 \\ Z_3 &= 2Z_1. \end{aligned} \tag{2}$$

It is clear that, as the problem has been stated so far, one impedance (say, $Z_1$) may be selected arbitrarily, and then the rest are determined by (1) or (2), whichever is applicable. Alford has shown how to calculate the impedances in certain cases so that, in addition to matching single-ended and balanced sources

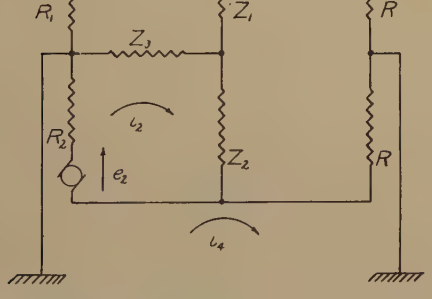


Fig. 3—Method of obtaining balanced voltages across a balanced load where the generator is partly unbalanced.

and sinks, the networks may be made to dissipate a minimum of energy when the inductances are assumed to have a definite ratio of reactance to resistance, or $Q$.

When a generator is neither balanced nor single-ended, but has an electrical condition intermediate between these two, a network similar to that of Fig. 3 is often used to obtain balanced voltages across the load. A rough explanation of the method of operation of this circuit is as follows: Suppose we assume the existence of two voltages $E_1$ and $E_2$, such that

$$E_1 + E_2 = e_1$$
$$E_1 - E_2 = e_2.$$

The solution of this pair of equations is

$$E_1 = \tfrac{1}{2}(e_1 + e_2)$$
$$E_2 = \tfrac{1}{2}(e_1 - e_2).$$

Now it is clear that if the voltages across the load are balanced, $e_1+e_2=0$, so that $E_1=0$. Thus $E_1$ is a measure of the amount of unbalance and in fact, from these simple expressions, it is clear that $E_1$ sends current down the impedances labeled $Z_1$ and $Z_2$ in the same direction. Thus, as far as $E_1$ is concerned, these impedances are in parallel, and if $Z_2=Z_1$ their net impedance is $Z_1/2$. These impedances in series with $Z_3$ offer a resonant path to ground for current caused by

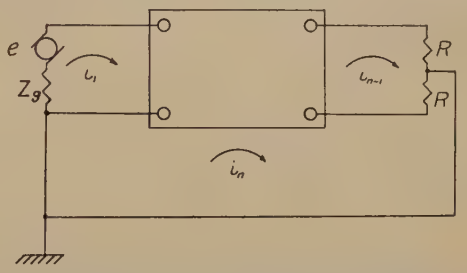


Fig. 4—General 4-terminal network for obtaining balanced voltages across a balanced load when the generator is single-ended; the network must satisfy the requirement that $i_n=0$.

$E_1$, provided $Z_3=-Z_1/2$, thus reducing $E_1$ to zero. This contradiction shows that $E_1$ cannot be different from zero in the idealized circuit shown, provided the generator impedances are different from zero.

A more rigorous proof of the performance of this network is given at the conclusion of this paper. The similarity of the network to those of Alford should be noticed. In fact, if we open-cricuit $e_2$ we obtain substantially the configuration of Fig. 2a. We might well also notice in passing that if, in Fig. 2a, we change $R$ to $R-Z_3$, we get the configuration of Fig. 2b since, by (1) and (2), the $Z_3$ of Fig. 2b has the opposite sign to that of Fig. 2a if the $Z_2$'s are the same in both cases.

## II. The General Problem

Having proceeded thus far in the search for balancing networks, we inquire whether a rational procedure can be set up for finding all reactance networks which will match, say, a single-ended generator to a balanced load, independently of the magnitude of the load and generator impedances. To this end consider Fig. 4, which shows a linear passive network joining a single-ended generator to a balanced load. The total network, including input, output, and ground-return loops, consists of $n$ meshes. For balanced voltages across the load, a necessary and sufficient condition is that $i_n=0$. The condition is necessary, for if the voltages are balanced, the electrical mid-point of the load is at zero potential above ground. The condition is also sufficient; for if $i_n=0$, the current through each half of

[1] Andrew Alford, "Matching Network," U. S. Patent No. 2,165,086, July 4, 1939.

the load is $i_{n-1}$ and the voltage drops across the load are therefore equal in magnitude and opposite in sign with respect to ground. We thus accept for our criterion of balance

$$i_n = 0. \tag{3}$$

We write next for the equations of the network[2]

$$\left.\begin{aligned}
(Z_g + Z'_{11})i_1 + Z_{12}i_2 + \cdots + Z_{1n}i_n &= e \\
Z_{21}i_1 + Z_{22}i_2 + \cdots + Z_{2n}i_n &= 0 \\
\cdots\cdots\cdots\cdots\cdots\cdots\cdots\cdots & \\
Z_{n-1,1}i_1 + Z_{n-1,2}i_2 + \cdots + (2R + Z'_{n-1,n-1})i_{n-1} & \\
\quad + (-R + Z'_{n-1,n})i_n &= 0 \\
Z_{n1}i_1 + Z_{n2}i_2 + \cdots + (-R + Z'_{n,n-1})i_{n-1} & \\
\quad + (R + Z'_{nn})i_n &= 0
\end{aligned}\right\} \tag{4}$$

where $Z_{jk}$ = mutual impedance between the $j$th and $k$th meshes $= Z_{kj}$

$Z_{jj}$ = self-impedance, $j$th mesh

$$\begin{aligned}
Z_g + Z'_{11} &= Z_{11} \\
2R + Z'_{n-1,n-1} &= Z_{n-1,n-1} \\
-R + Z'_{n-1,n} &= Z_{n-1,n} = Z_{n,n-1} = -R + Z'_{n,n-1} \\
R + Z'_{nn} &= Z_{nn}.
\end{aligned}$$

Calling $D$ the determinant of the network and $A_{1n}$ the cofactor of $Z_{1n}$, we have

$$i_n = A_{1n}e/D.$$

Thus, to satisfy (3), we have $A_{1n} = 0$ as a necessary condition unless $D = \infty$, and $A_{1n} = 0$ as also a sufficient condition provided $D = 0$. Thus, unless[3] $D = 0$ or $\infty$, a necessary and sufficient condition that load voltages be balanced is

$$A_{1n} = 0$$

that is,

$$\begin{vmatrix}
Z_{21}, & Z_{22}, & \cdots, & Z_{2,n-2}, & Z_{2,n-1} \\
Z_{31}, & Z_{32}, & \cdots, & Z_{3,n-2}, & Z_{3,n-1} \\
\cdots & \cdots & \cdots & \cdots & \cdots \\
Z_{n-1,1}, & Z_{n-1,2}, & \cdots, & Z_{n-1,n-2}, & (2R+Z'_{n-1,n-1}) \\
Z_{n1}, & Z_{n2}, & \cdots, & Z_{n,n-2}, & (-R+Z'_{n,n-1})
\end{vmatrix} = 0. \tag{5}$$

The first point to notice is that (5) does not contain $Z_g$; thus the condition for balance is automatically independent of $Z_g$. As a corollary we may say that the self-impedance of the first mesh is of no importance unless it makes $D = 0$. The second point to notice is that the expression is linear in $R$, i.e., of the form[4]

$$A + BR = 0 \tag{5a}$$

where $A$ and $B$ are functions of the $Z$'s. Now (5a) is true for all values of $R$ if, and only if, $A = 0$ and $B = 0$.

[2] See, for example, E. A. Guillemin, "Communication Networks," vol. I, John Wiley and Sons, New York, N. Y., 1931, pp. 125 ff.

[3] In general we need not worry about the value of $D$ since it is a function of $Z_g$ and $R$ as well as the constants of the transducer. Thus only under peculiar conditions of $Z_g$ and $R$ would $D$ accidentally become zero.

[4] See, for example, M. Bocher, "Introduction to Higher Algebra," Macmillan Company, New York, N. Y., 1938, chapter II.

Thus the condition for voltage balance is that two equations in the $Z$'s be satisfied simultaneously. Otherwise the $Z$'s are quite arbitrary. Notice in this connection the Alford conditions (1) and (2). It is now apparent that only two equations need be satisfied regardless of the number of meshes.

The equation $A = 0$ is readily obtained by setting $R = 0$ in (5) and (5a). We obtain, therefore, for the first condition

$$\begin{vmatrix}
Z_{21}, & Z_{22}, & \cdots, & Z_{2,n-2}, & Z_{2,n-1} \\
Z_{31}, & Z_{32}, & \cdots, & Z_{3,n-2}, & Z_{3,n-1} \\
\cdots & \cdots & \cdots & \cdots & \cdots \\
Z_{n-1,1}, & Z_{n-1,2}, & \cdots, & Z_{n-1,n-2}, & Z'_{n-1,n-1} \\
Z_{n1}, & Z_{n2}, & \cdots, & Z_{n,n-2}, & Z'_{n,n-1}
\end{vmatrix} = 0. \tag{6a}$$

To obtain the second equation ($B = 0$) we merely differentiate[5] (5a) (or (5)) with respect to $R$. Thus we get for the second condition:

$$\begin{vmatrix}
Z_{21}, & Z_{22}, & \cdots, & Z_{2,n-2}, & 0 \\
Z_{31}, & Z_{32}, & \cdots, & Z_{3,n-2}, & 0 \\
\cdots & \cdots & \cdots & \cdots & \cdots \\
Z_{n-1,1}, & Z_{n-1,2}, & \cdots, & Z_{n-1,n-2}, & 2 \\
Z_{n1}, & Z_{n2}, & \cdots, & Z_{n,n-2}, & -1
\end{vmatrix} = 0. \tag{6b}$$

Any network satisfying (6a) and (6b) will match an unbalanced source of any internal impedance to a balanced load of any impedance.

Furthermore it is apparent that the design of the network is independent of the source or load impedance.

It should be emphasized at this point that since the various impedances appearing in (6a) and (6b) are in general rational algebraic functions of frequency, the equations themselves are in general algebraic functions of frequency, and therefore satisfied for a finite number of frequencies, at most. In the usual design they are satisfied exactly for one frequency only, and satisfied approximately in a band containing this frequency, the error in the approximation tending to zero with the band width. In the particular case of the isolation transformer it turns out that the conditions are satisfied independently of frequency.

## III. Alford Networks

Let us apply these results to the network of Fig. 2a where, including the ground loop, we have three meshes, or $n = 3$. Thus (6a) and (6b) become, respectively

$$\begin{vmatrix} Z_{21} & Z'_{22} \\ Z_{31} & Z'_{32} \end{vmatrix} = 0, \quad \text{and} \quad \begin{vmatrix} Z_{21} & 2 \\ Z_{31} & -1 \end{vmatrix} = 0.$$

Taking proper precautions with regard to signs[2] we notice from Fig. 2a that

[5] See, for example, Metzler and Muir, "Theory of Determinants," Longmans, Green and Company, New York, N. Y., 1933, p. 70.

$$Z_{21} = -Z_2$$
$$Z_{31} = -Z_1$$
$$Z'_{22} = Z_2 + Z_3$$
$$Z'_{32} = -Z_3$$

so that the equations of condition become

$$\begin{vmatrix} -Z_2 & Z_2+Z_3 \\ -Z_1 & -Z_3 \end{vmatrix} = 0, \quad \text{and} \quad \begin{vmatrix} -Z_2 & 2 \\ -Z_1 & -1 \end{vmatrix} = 0.$$

When expanded these become

$$Z_2Z_3 + Z_1Z_2 + Z_1Z_3 = 0$$
$$Z_2 + 2Z_1 = 0.$$

Substituting the second of these in the first, we get

$$-2Z_1Z_3 - 2Z_1^2 + Z_1Z_3 = 0$$

so that for $Z_1 \neq 0$,

$$-2Z_3 - 2Z_1 + Z_3 = 0.$$

Hence we can take for our final result

$$\left.\begin{aligned} Z_2 + 2Z_1 &= 0 \\ Z_3 + 2Z_1 &= 0 \end{aligned}\right\} \tag{7}$$

which are obviously equivalent to (1). Similar results are readily deduced for Fig. 2b.

## IV. Three-Mesh Networks—The Lattice Structure

When we come to the case where $n=4$, we have, by (6a) and (6b),

$$\begin{vmatrix} Z_{21} & Z_{22} & Z_{23} \\ Z_{31} & Z_{32} & Z'_{33} \\ Z_{41} & Z_{42} & Z'_{43} \end{vmatrix} = 0 \tag{8a}$$

and

$$\begin{vmatrix} Z_{21} & Z_{22} & 0 \\ Z_{31} & Z_{32} & 2 \\ Z_{41} & Z_{42} & -1 \end{vmatrix} = 0. \tag{8b}$$

Expansion of (8b) according to the elements of the last column gives

$$2A_{23} + A_{33} = 0 \tag{9a}$$

where

$$A_{23} = \begin{vmatrix} Z_{21} & Z_{22} \\ Z_{41} & Z_{42} \end{vmatrix}, \qquad A_{33} = \begin{vmatrix} Z_{21} & Z_{22} \\ Z_{31} & Z_{32} \end{vmatrix}. \tag{10}$$

Expansion of (8a) gives similarly

$$Z_{23}A_{13} - Z'_{33}A_{23} + Z'_{43}A_{33} = 0 \tag{9b}$$

where

$$A_{13} = \begin{vmatrix} Z_{31} & Z_{32} \\ Z_{41} & Z_{42} \end{vmatrix}. \tag{11}$$

Substitution of (9a) in (9b) for $A_{33}$ gives

$$Z_{23}A_{13} - (Z'_{33} + 2Z'_{43})A_{23} = 0. \tag{9c}$$

Equations (9a) and (9c) must be satisfied for this type of network. As an example consider the bridge circuit of Fig. 5. Here we have

$$Z_{21} = -(Z_1 + Z_3)$$
$$Z_{22} = Z_1 + Z_2 + Z_3 + Z_4$$
$$Z_{23} = -(Z_3 + Z_4)$$
$$Z_{31} = Z_3$$
$$Z'_{33} = Z_3 + Z_4$$
$$Z_{41} = -Z_3$$
$$Z_{42} = Z_3$$
$$Z'_{43} = -Z_3.$$

Hence by (10) and (11),

$$A_{13} = \begin{vmatrix} Z_3 & -(Z_3+Z_4) \\ -Z_3 & Z_3 \end{vmatrix} = -Z_3Z_4$$

$$A_{23} = \begin{vmatrix} -(Z_1+Z_3) & (Z_1+Z_2+Z_3+Z_4) \\ -Z_3 & Z_3 \end{vmatrix} = Z_3(Z_2+Z_4)$$

$$A_{33} = \begin{vmatrix} -(Z_1+Z_3) & (Z_1+Z_2+Z_3+Z_4) \\ Z_3 & -(Z_3+Z_4) \end{vmatrix} = Z_1Z_4 - Z_2Z_3.$$

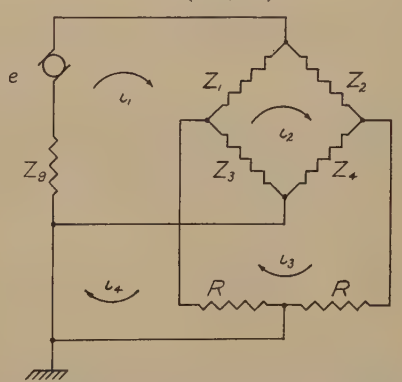


Fig. 5—The bridge or lattice type of balancing network.

Hence (9a) and (9c) become

$$\left.\begin{aligned} Z_2Z_3 + Z_1Z_4 + 2Z_3Z_4 &= 0 \\ Z_2Z_3 - Z_2Z_4 + 2Z_3Z_4 &= 0 \end{aligned}\right\}. \tag{12}$$

By inspection, we get

$$Z_2 = -Z_1. \tag{13a}$$

Substituting this in the first part of (12), we get, solving for $Z_4$,

$$Z_4 = \frac{Z_3}{1 + 2\dfrac{Z_3}{Z_1}}. \tag{13b}$$

Equations (13a) and (13b) are the conditions of balance. Note that we may now specify any two impedances as long as they are consistent with these conditions. The remaining two impedances may then be determined from the conditions for balance (13a) and (13b).

Equation (13b) is of sufficient interest to warrant further comment. Although an infinite number of variations are possible, a few are of special interest. We consider first the case where $Z_3 = -Z_1$. In that case we

get $Z_4 = -Z_3$. One network satisfying these conditions is shown in Fig. 6, where the bridge has been redrawn in the form of a lattice. R. C. Curtis of Wired Radio, Inc., has called the author's attention to the apparent fact that this network will deliver balanced output regardless of the condition of the generator with respect to ground. This additional property exists by virtue of the fact that the network is electrically symmetrical with respect to its input terminals.

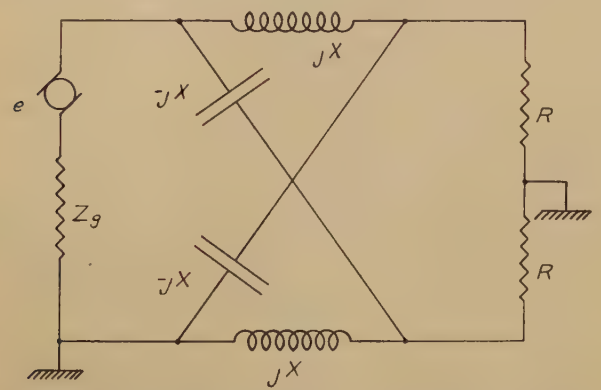


Fig. 6—The symmetrical lattice type of balancing network. The output from this network is balanced for any degree of generator unbalance.

Another case of interest is that for which $Z_1 = -2Z_3$. In that case $Z_4$ becomes infinite by (13b). A little study shows that this case gives the network of Fig. (2b). Similarly, if we make $Z_3$ infinite, we get

$$\lim_{Z_3=\infty} Z_4 = \lim_{Z_3=\infty} \left[ \frac{Z_3}{1 + 2\dfrac{Z_3}{Z_1}} \right] = Z_1/2.$$

This network is exactly the same as that of the preceding case.

## V. Further Considerations Pertaining To Lattice Structures

Returning now to Fig. 5, we assume temporarily that the impedances of the network are simple reactance arms (single inductances or single capacitances), so that we may write $Z_1 = jX_1$, $Z_2 = jX_2$ etc.,

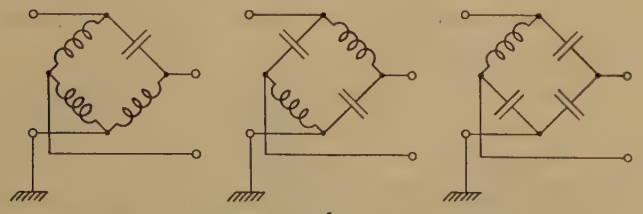


Fig. 7—Various lattice types of balancing networks.

where $X_1, \cdots, X_4$ are restricted only to be real positive or negative quantities. Various relations between the $X$'s lead to networks involving three inductances and one capacitance, two inductances and two capacitances, or one inductance and three capacitances. These relations we proceed now to investigate, using (13a) and (13b).

I. Take $X_3 > 0$.

(a) Take $X_1 > 0$. Hence $X_4 > 0$ by (13b) and $X_2 < 0$ by (13a). The configuration is of the type shown in Fig. 7a.

(b) Take $X_1 < 0$. Hence $(Z_3/Z_1) < 0$. If $(Z_3/Z_1) < -\frac{1}{2}$, then $X_4 < 0$ while if $(Z_3/Z_1) > -\frac{1}{2}$, then $X_4 > 0$. In either case $X_2 > 0$. The first of these corresponds to Fig. 7b, while the second is of the type of Fig. 7a.

II. Take $X_3 < 0$.

(a) Take $X_1 > 0$. Hence $(Z_3/Z_1) < 0$. If $(Z_3/Z_1) < -\frac{1}{2}$, then $X_4 > 0$ while if $(Z_3/Z_1) > -\frac{1}{2}$, then $X_4 > 0$. In either case $X_2 < 0$. The first of these corresponds to Fig. 7b, the second to Fig. 7c.

(b) Take $X_1 < 0$. Hence $X_4 < 0$, while $X_2 > 0$. This again corresponds to Fig. 7c.

These conditions exhaust the possibilities of this configuration except that, obviously, any of the simple

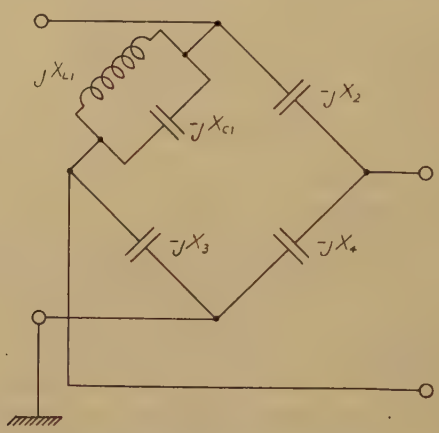


Fig. 8—Lattice type of balancing network adapted for use in the plate circuits of class C amplifiers.

impedance arms may be replaced by more complex arms whose net 2-terminal reactance is the same at the frequency under consideration.

Before discussing a specific application, we write the expression for the input impedance of the network of Fig. 5, subject to the balance conditions (13a) and (13b). This is easily shown[2] to be

$$Z = -\frac{Z_1^2}{R} - \frac{Z_1}{2}\left(1 + \frac{Z_1}{Z_3}\right) = -\frac{Z_2^2}{R} + \frac{Z_2}{2}\left(1 - \frac{Z_2}{Z_3}\right). \qquad (14a)$$

If we substitute pure reactances for the $Z$'s, (14a) takes the form

$$Z = \frac{X_1^2}{R} - j\frac{X_1}{2}\left(1 + \frac{X_1}{X_3}\right) = \frac{X_2^2}{R} + j\frac{X_2}{2}\left(1 - \frac{X_2}{X_3}\right). \qquad (14b)$$

The first thing to notice in (14b) is that the resistive component inverts the load. The balancing network thus has this property in common with the tank circuit of radio-frequency amplifiers and with "quarter-wave" $\pi$ networks. The second thing to notice is that, unless the load has a reactive component (and except in the trivial case $X_1 = 0$, $X_2 = 0$), the input impedance

is a pure resistance if, and only if, $X_1 = -X_3$, or $X_2 = X_3$. This last requirement is satisfied by the network of Fig. 6. Thus this network presents a pure resistance load to the generator.

We consider now, in some detail, the special arrangement of Fig. 8, in which to begin with we stipulate only that $X_{L1} < X_{C1}$ so that the configuration is of the type of Fig. 7c. Of the three types shown in Fig. 7, this type is the only one that offers a capacitive return to ground at the input side for frequencies which increase without limit. This is a desirable condition for the load circuit of radio-frequency amplifiers, if high-frequency parasitic oscillations are to be avoided. The network of Fig. 8 is shown in Fig. 9, incorporated in a radio-frequency amplifier. The coupler $M$ serves two purposes. One of these is to vary the load coupled to the balancing network; the other will be brought out in the subsequent discussion. Referring now to Fig. 8, we have, in order to satisfy (13a)

$$\frac{X_{L1}X_{C1}}{X_{C1} - X_{L1}} = X_2 \tag{15a}$$

and in order to satisfy (13b),

$$X_4 = \frac{X_3}{1 - 2\dfrac{X_3(X_{C1} - X_{L1})}{X_{L1}X_{C1}}}. \tag{15b}$$

For the type of configuration of Fig. 7c we must also meet the requirement that

$$X_3 < \frac{1}{2}\,\frac{X_{L1}X_{C1}}{X_{C1} - X_{L1}}. \tag{15c}$$

We shall stipulate now that the network is to be designed to constitute a balanced bridge at some harmonic of the working frequency, say the $n$th. The voltage across the output terminals at the harmonic frequency is then zero. The voltage from each terminal to ground, however, is generally different from zero. This brings out the second purpose of the coupler $M$, which is to isolate these voltages so that the net effect on the secondary is zero. If capacitive effects raise the harmonic level to an undesirable level, the coupler may be provided with a shield. In this instance the effect of the shield on the performance of the amplifier is negligible. The condition required to balance out the $n$th harmonic is

$$\frac{Z_1^{(n)}}{Z_2^{(n)}} = \frac{Z_3^{(n)}}{Z_4^{(n)}} \tag{16a}$$

where the various $Z$'s represent the impedances of the network at the $n$th harmonic. Applied to Fig. 8 specifically, this condition is

$$\frac{X_{L1}X_{C1}}{i\left(nX_{L1} - \dfrac{X_{C1}}{n}\right)} \cdot \frac{n}{-jX_2} = \frac{X_3}{X_4}. \tag{16b}$$

To be specific we shall consider only the case for the second harmonic. This is generally of most interest anyway. Putting $n = 2$ in (16b), and removing the $j$'s

$$\frac{X_{L1}X_{C1}}{2X_{L1} - \dfrac{X_{C1}}{2}} \cdot \frac{2}{X_2} = \frac{X_3}{X_4}. \tag{15d}$$

Finally, we specify the input impedance to the network which should usually be a pure resistance for proper amplifier operation. Clearly, from (14b), this is possible only if $R$ has a reactive component. Let the load looking into the coupler $M$ be $2(R_m + jX_m)$. Then (14b) becomes, after some reduction and with due cognizance of algebraic signs,

$$Z = \frac{R_m X_2^2}{R_m^2 + X_m^2} - j\left[\frac{X_2}{2}\left(1 - \frac{X_2}{X_3}\right) + \frac{X_2^2 X_m}{R_m^2 + X_m^2}\right]. \tag{17}$$

If this is to be a pure resistance,

$$\frac{1}{2}\left(1 - \frac{X_2}{X_3}\right) + \frac{X_2 X_m}{R_m^2 + X_m^2} = 0. \tag{18}$$

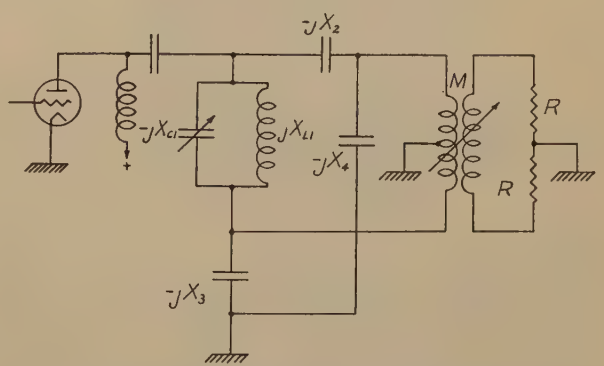


Fig. 9—The balancing network of Fig. 8 incorporated in the plate circuit of a class C amplifier.

On the other hand, designating the input resistance by $R_p$,

$$R_p = \frac{R_m X_2^2}{R_m^2 + X_m^2}. \tag{19}$$

We only point out here that when $X_m > 0$, (18) can only be satisfied if $X_2 > X_3$, while if $X_m < 0$, it is necessary that $X_2 < X_3$. Equation (19) is satisfied by varying the coupling on $M$.

Disregarding for the present the question of input impedance, we have to satisfy (15a), (15b), and (15d), subject to the restriction (15c). After some manipulation we get

$$\left.\begin{aligned} X_2 &= \frac{X_{L1}X_{C1}}{X_{C1} - X_{L1}} \\ X_3 &= \frac{1}{2}\,\frac{X_{L1}X_{C1}}{X_{C1} - X_{L1}} \cdot \frac{5X_{C1} - 8X_{L1}}{X_{C1} - 4X_{L1}} \\ X_4 &= \frac{1}{8}\,\frac{X_{L1}X_{C1}}{X_{C1} - X_{L1}} \cdot \frac{5X_{C1} - 8X_{L1}}{X_{L1} - X_{C1}} \end{aligned}\right\}. \tag{20}$$

Dividing by $X_{L1}$ and putting $\alpha = X_{L1}/X_{C1}$ (see Fig. 10)

$$\left.\begin{aligned} \frac{X_2}{X_{L1}} &= \frac{1}{1-\alpha} && \text{A} \\ \frac{X_3}{X_{L1}} &= \frac{1}{2}\,\frac{1}{1-\alpha}\cdot\frac{5-8\alpha}{1-4\alpha} && \text{B} \\ \frac{X_4}{X_{L1}} &= \frac{1}{8}\,\frac{8\alpha-5}{(1-\alpha)^2} && \text{C} \end{aligned}\right\} \quad (21)$$

subject to the restriction from (15c)

$$\frac{X_3}{X_{L1}} < \frac{1}{2}\,\frac{1}{1-\alpha}. \quad (22)$$

It is readily verified from these equations that we must have

$$5/8 < \alpha < 1.$$

Fig. 10 shows the various ratios of (21) plotted as functions of $\alpha$.

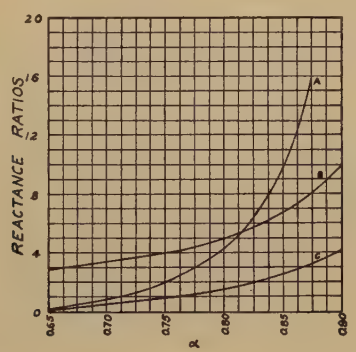


Fig. 10—Reactance ratios for the networks of Figs. 8 and 9 plotted as a function of $\alpha = X_{L1}/X_{C1}$; $A$ is a plot of $X_4/X_{L1}$; $B$ is a plot of $X_2/X_{L1}$; and $C$ is a plot of $X_3/X_{L1}$.

If Fig. 9 represents a typical class C amplifier stage, tuning of the plate circuit is accomplished by short-circuiting temporarily across $M$ and varying $X_{C1}$ until the direct plate current is a minimum. Suppose then that the conditions for balance are satisfied at frequency $f_1$. If we change to frequency $f_2$, such that $f_2 = kf_1$, we get new reactances (designated by primes) as follows:

$$\left.\begin{aligned} X_{L1}' &= kX_{L1} \\ X_2' &= \frac{1}{k}X_2 \\ X_3' &= \frac{1}{k}X_3 \\ X_4' &= \frac{1}{k}X_4 \end{aligned}\right\}. \quad (23a)$$

We then retune $X_{C1}$ by the method described above. This procedure automatically satisfies (15a) at the new frequency, Hence we can write

$$X_{C1}' = \frac{X_{L1}'X_2'}{X_2' - X_{L1}'} = \frac{kX_{L1}X_2}{X_2 - k^2X_{L1}} \quad (23b)$$

Using (23a) and (23b) it is readily demonstrated that (15b) holds at the new frequency. Hence, if tuning is accomplished by the method described above, balanced output is maintained at all frequencies. It is not true, however, that attenuation to the second harmonic remains perfect when operation is transferred to another frequency; the bridge balance is destroyed. Over a limited range on either side of $f_1$, the attenuation remains large, and can be made as large as desired by suitably restricting the tuning band. Calculation of design data for this purpose is beyond the scope of this paper.

## VI. Correction of Partial Unbalance

We conclude with a more rigorous discussion of the network of Fig. 3 used for correcting partial unbalances in generator voltage. For that purpose consider Fig. 3. The determinant of the network is

$$D = \begin{vmatrix} R_1+Z_1+Z_3 & -Z_3 & -Z_1 & 0 \\ -Z_3 & R_2+Z_2+Z_3 & -Z_2 & -R_2 \\ -Z_1 & -Z_2 & Z_1+Z_2+2R & -R \\ 0 & -R_2 & -R & R_2+R \end{vmatrix}$$

while the voltage matrix is

$$\begin{Vmatrix} e_1 \\ e_2 \\ 0 \\ -e_2 \end{Vmatrix}.$$

Necessary and sufficient conditions for balance are then

$$Ae_1 - (B-C)e_2 = 0, \qquad D \neq 0$$

where

$$A = \begin{vmatrix} -Z_3 & R_2+Z_2+Z_3 & -Z_2 \\ -Z_1 & -Z_2 & Z_1+Z_2+2R \\ 0 & -R_2 & -R \end{vmatrix}$$

$$B = \begin{vmatrix} R_1+Z_1+Z_3 & -Z_3 & -Z_1 \\ -Z_1 & -Z_2 & Z_1+Z_2+2R \\ 0 & -R_2 & -R \end{vmatrix}$$

$$C = \begin{vmatrix} R_1+Z_1+Z_3 & -Z_3 & -Z_1 \\ -Z_3 & R_2+Z_2+Z_3 & -Z_2 \\ -Z_1 & -Z_2 & Z_1+Z_2+2R \end{vmatrix}. \quad (24)$$

If (24) is to be true for all values of $e_1$ and $e_2$, we must have

$$A = 0, \qquad B = C. \quad (25)$$

When expanded, $A$ may be written in the form

$$A = a_1R + a_2R_2 + a_3RR_2 = 0 \quad (26)$$

where the $a$'s do not contain $R_1$, $R_2$, or $R$.

If this is to be true for all values of $R$ and $R_2$,

$$a_1 = a_2 = a_3 = 0;$$

i.e.,

$$\left[\frac{\partial A}{\partial R}\right]_{R_2=0} = \left[\frac{\partial A}{\partial R_2}\right]_{R=0} = \frac{\partial^2 A}{\partial R \partial R_2} = 0.$$

Performing these operations on the determinant $A$ we get

$$\left[\frac{\partial A}{\partial R}\right]_{R_2=0} \equiv \left[\frac{\partial A}{\partial R_2}\right]_{R=0}$$

and

$$\left.\begin{aligned} Z_1Z_2 + Z_1Z_3 + Z_2Z_3 &= 0 \\ Z_1 + 2Z_3 &= 0 \end{aligned}\right\} \tag{27}$$

from which we obtain, immediately,

$$Z_3 = -\tfrac{1}{2}Z_1, \qquad Z_1 = Z_2. \tag{28}$$

It remains to show that under (28), $B \equiv C$. To see this, substitute (28) in the expressions for $B$ and $C$, getting

$$B = \begin{vmatrix} R_1 + \tfrac{1}{2}Z_1 & \tfrac{1}{2}Z_1 & -Z_1 \\ -Z_1 & -Z_1 & 2Z_1 + 2R \\ 0 & -R_2 & -R \end{vmatrix}$$

$$C = \begin{vmatrix} R_1 + \tfrac{1}{2}Z_1 & \tfrac{1}{2}Z_1 & -Z_1 \\ \tfrac{1}{2}Z_1 & R_2 + \tfrac{1}{2}Z_1 & -Z_1 \\ -Z_1 & -Z_1 & 2Z_1 + 2R \end{vmatrix}.$$

In the expression for $C$, interchange the second and third rows, getting

$$C = -\begin{vmatrix} R_1 + \tfrac{1}{2}Z_1 & \tfrac{1}{2}Z_1 & -Z_1 \\ -Z_1 & -Z_1 & 2Z_1 + 2R \\ \tfrac{1}{2}Z_1 & R_2 + \tfrac{1}{2}Z_1 & -Z_1 \end{vmatrix}.$$

Next multiply the elements of the second row by $\frac{1}{2}$ and add the results respectively to the elements of the third row, getting

$$C = -\begin{vmatrix} R_1 + \tfrac{1}{2}Z_1 & \tfrac{1}{2}Z_1 & -Z_1 \\ -Z_1 & -Z_1 & 2Z_1 + 2R \\ 0 & R_2 & R \end{vmatrix}.$$

Finally, change the signs of the elements of the last row, to get

$$C = \begin{vmatrix} R_1 + \tfrac{1}{2}Z_1 & \tfrac{1}{2}Z_1 & -Z \\ -Z_1 & -Z_1 & 2Z_1 + R \\ 0 & -R_2 & -R \end{vmatrix} \equiv B$$

which was to be proved.

# Theory of Antennas of Arbitrary Size and Shape*

S. A. SCHELKUNOFF†, ASSOCIATE, I.R.E.

***Summary***—*In this paper there are presented (1) a quite general method of antenna analysis; (2) a physical picture of transmission phenomena in antennas, based on this method; and (3) an expression for the input impedance of antennas of any shape, whose transverse dimensions are small compared with the wavelength. In a brief historical sketch of the antenna problem the factors which must be taken into consideration in solving the problem are discussed.*

*While in ordinary transmission lines the voltage is proportional to the charge, this is not the case in antennas. The explanation lies in the fact that antennas are* multiple *transmission lines (like wave guides) and not* simple, *that is, single-mode transmission lines. Our present theory is based on the voltage-current equations since these appear to be considerably simpler than charge-current equations. The latter are considered only briefly.*

*In the absence of dissipation and in so far as the total voltage wave and the "principal" current wave are concerned, radiation is strictly an end effect. In so far as the total current and the total charge waves are concerned, radiation effects are distributed (nonuniformly) along the entire antenna.*

*In the first approximation, regardless of the shape of the wire the charge is proportional to the voltage and waves are sinusoidal, the current wave having nodes while the voltage wave and the charge wave antinodes at the ends of the antenna. The second approximation depends on the* shape *of the longitudinal cross section of the antenna as well as on the* size *of the transverse cross section.*

*Our analysis is based on Maxwell's equations but the final results are quite simple and the physical picture growing out of this mathematics is attractive to an engineer. It is permissible to think that a wave emerging from a generator in the center of an antenna is guided by an antenna until it reaches its "boundary sphere" passing through the ends of the antenna and separating the antenna region from the external space; at the boundary sphere some energy passes into the external space and some is reflected back—a situation existing at the juncture between two transmission lines with different characteristic impedances. We may also think of the antenna as the wall of an electric horn with an aperture so wide that one can hardly see the horn itself—just like a Cheshire Cat: only the grin can be seen. In fact, the mathematics that we use is that appropriate to wave guides and electric horns.*

* Decimal classification: R120. Original manuscript received by the Institute, April 25, 1941.

† Bell Telephone Laboratories, Inc. New York, N. Y.

*The antenna problem is stated in Section I and its history is briefly discussed in Section II; Section III contains a summary and a discussion of the results for antennas with uniformly distributed capacitance (conical antennas); Section IV is devoted to antennas with nonuniformly distributed capacitance; Section V presents a derivation of the formulas contained in Section III; Section VI reviews the induced-electromotive-force method of computing radiation and its use in the present problem; Section VII is devoted to the current-charge equations; Section VIII is devoted to wave propagation along parallel wires; in Section IX an expression is given for the impedance of an infinitely long cylindrical wire; and Section X deals with an approximation needed in our discussion of the problem.*

## I. Introduction

### *Two Problems*

IT IS beyond the scope of this paper to discuss adequately prior work on radiation from conductors of finite length and only a few representative papers will be cited. Two problems have presented themselves. In Problem A the current distribution in an antenna is given and it is required to find the field and, hence, the external electromotive forces needed to produce the given current distribution. Problem B is the inverse of A: The distribution of applied or external forces in an antenna is given and it is required to obtain the field and, hence, the current produced by the applied forces.

Problem A has been solved rigorously and completely with the aid of retarded potentials. On the other hand, Problem B presents many difficulties and it is the engineer's hard luck that he happens to be interested in just this problem.

*Solution of Problem A Is Useful within Limits*

The solution of Problem A is not altogether useless to the engineer. Theory is not the only source of information concerning the current distribution produced by given forces. For example, the current distribution can be determined experimentally, thus, it has been known long ago that on a thin wire the current is distributed almost sinusoidally (Fig. 1) and this fact has been employed to obtain approximately the radiated power, the input impedance, and the field. If the length of the wire is in the neighborhood of one half of the wavelength (or one quarter of $\lambda$ if the ground takes the place of the other half), the results are fairly satisfactory from the practical point of view.[1] But when the length becomes equal to 1 wavelength, then a more accurate solution becomes necessary. The theoretical radiation pattern may be still good enough (except in the former "null directions") but the input

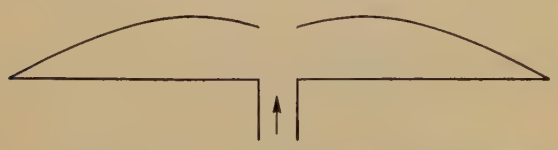

Fig. 1—Current distribution in an infinitely thin perfectly conducting antenna of any shape is sinusoidal with current nodes at the ends of the antenna. This distribution may be taken as the first approximation for thin antennas.

impedance is computed to be infinite. While infinity may be regarded as a legitimate first approximation to a large quantity, it is a useless approximation. For free-space antennas of length $n\lambda$, practical applications require a second approximation and this, in so far as theory is concerned, leads us back to Problem B.

## II. History of Problem B and General Comments on Methods for Its Solution

*Two Methods of Approach and an Unproved "Proposition $\alpha$"*

Broadly speaking, we may distinguish between two methods of approach to the solution of Problems B. Some writers[2-6] have based their work on Maxwell's equations, that is, on the electromagnetic laws that are considered well established; while, other writers[7-12] repulsed by the complexity of such methods, ventured to start from a new and unproved premise. This new Proposition $\alpha$ may be formulated as follows: power losses due to radiation produce the same effect on transmission of electric waves along conducting wires as losses due to dissipation. This premise is inconsistent with Maxwell's equations (see Section VIII); and yet, with its aid some approximate results have been obtained. We shall return to this point later.

*Spheroidal Antennas*

Those writers who prefer "safe" premises as a point of departure have to look for some particular shape of conductors which would lend itself more readily to mathematical treatment. Spheroids have been the first to attract attention. Abraham[2] treated *free* oscillations on a perfectly conducting thin prolate spheroid and obtained an expression for the resonant frequencies or wavelengths. Recently, Page and Adams[5] and, then, Ryder in his as yet unpublished thesis, have dealt with *forced* oscillations on spheroids.

*Slow Convergence off Resonance*

There is a weakness inherent in the method used by Page and Adams. This method employs spheroidal harmonics and off resonance leads to complicated and slowly converging series. In their numerical computations, the authors limited themselves to spheroids about one-half wavelength long.[13]

*The Importance of Shape*

An important point, however, is that while in the first approximation the current distribution is independent of the size of the transverse cross section of the antenna and of the shape of the longitudinal cross section and is sinusoidal for all conductors, in the second approximation the current distribution depends on both factors. It was Rayleigh[14] who, in discussing Abraham's[2] and Pollock's[15] papers, was the first to point out that resonant frequencies of finite wires are independent of the shape of the wires in the first approximation but not in the second. Rayleigh's

[1] There may be occasions, of course, when a more accurate solution would be desirable and, certainly, no one is likely to object to having one, provided it is simple enough.

[2] M. Abraham, "Die electrischen Schwingungen um einen stabförmigen Leiter, behandelt nach der Maxwell'schen Theorie," *Ann. der Phys.*, vol. 66, pp. 435–472, 1898.

[3] L. V. King, "On the radiation field of a perfectly conducting base insulated cylindrical antenna over a perfectly conducting plane earth, and the calculation of radiation resistance and reactance," *Phil. Trans.*, ser. A, pp. 381–422; November 2, 1937.

[4] G. Mie, "Elektrische Wellen an Zwei Parallelen Drahten," *Ann. der. Phys.*, p. 248, 1900.

[5] Leigh Page and Norman I. Adams, Jr., "The electrical oscillations of a prolate spheroid, Paper I," *Phys. Rev.*, pp. 819–831; May 15, 1938.

[6] John R. Carson, "Propagation of periodic currents over non-uniform lines," *Electrician*, pp. 272–273; March 4, 1921.

[7] C. P. Steinmetz, "The general equations of the electric circuit —III," *Proc. A.I.E.E.*, p. 255, 1919.

[8] Ronold King, "Telegraphist's equations at ultra-high frequencies," *Physics*, pp. 121–125; April, 1935.

[9] P. O. Pedersen, "Radiation from a vertical antenna over flat perfectly conducting earth, *Ingenirvidenskabelige Skrifter*, ser. A, Nr. 38, 1935.

[10] E. Siegel und J. Labus, "Scheinwiderstand von Antennen," *Hochfrequenz. und Elektroakustik*, Bd. 43, pp. 166–172, 1934.

[11] J. Labus, "Rechnerische Ermittlung des Impedanz von Antennen," *Hochfrequenz. und Elektroakustik*, Bd. 41, pp. 17–23, 1933.

[12] L. J. Chu and J. A. Stratton, "Forced oscillations of a prolate spheroid," *Jour. Appl. Phys.*, pp. 241–248; March, 1941.

[13] Since completion of this paper, L. J. Chu and J. A. Stratton[12] have published a comprehensive discussion of forced oscillations on prolate spheroids and dealt with the conditions off resonance as well as near resonance.

[14] Lord Rayleigh, "On the electrical vibrations associated with thin terminated conducting rods," *Phil. Mag.*, pp. 104–107; July, 1904.

[15] J. A. Pollock, "A comparison of the periods of the electrical vibrations associated with simple circuits," *Phil. Mag.*, pp. 635–652; June, 1904.

conclusion is borne out by Englund's experiments[16] and by our calculations. In fact, not only the resonant frequencies but other quantities as well are affected, in the second approximation, by the size of the transverse cross section of the antenna and the shape of the longitudinal cross section; consequently, a way must be found to take these factors into consideration.

*Cylindrical Antennas*

A different method was chosen by King.[3] Starting from an integral equation, he obtained the second approximation to the solution of Problem B for a thin cylindrical wire and his work could be extended to wires of other shapes. If anything, this method is more complicated than the one employed in the case of spheroidal antennas and it does not lend itself to any simple physical interpretation; one just has to take the final quantitative results. On the other hand, the calculations are carried out for cylindrical antennas which are of greater practical interest than spheroidal antennas.

*Our Method and Its Advantages*

We also start with Maxwell's equations but choose *conical* conductors. There are several advantages to this choice. In the first place, the functions to which one is naturally led represent *waves* on the wire rather than *free oscillations*. Consequently, the conditions existing off resonance can be studied just as readily as those near resonance. Furthermore, this means that no complications will arise if we break the wire at some point and insert a resistance, or any impedance, for that matter.

The difference between our method of treating the conical wire and the conventional method of treating the spheroid is precisely the difference existing between two possible methods of dealing with a finite section of an ordinary transmission line. On one hand, the voltage and the current in such a section can always be represented as the result of interference of progressive waves traveling in opposite directions; and, on the other hand, the same quantities can be represented in terms of "harmonics" corresponding to natural oscillations in the section of the line. The first method is so much simpler than the second, which gives the results as infinite series of partial fractions, that probably only few are even aware that the solution could have been found by the second method in the first place.

*The Shape of Conductors May Be Taken into Account*

Another advantage in our choice of conical shape is that in the second approximation the effects of the shape of the conductor become separated from the "end effect" or radiation.[17] Consequently, the equations developed for conical wires can be amended to take care of the "shape effect."

[16] C. R. Englund, "The natural period of linear conductors," *Bell Sys. Tech. Jour.*, pp. 404–419; July, 1928.

*Antenna as a Transmission Line*

Finally, our method turns out to be consistent with a physical picture which is rather attractive to the engineer. Let us suppose that a wire is energized at the center. A spherical wave emerging from the generator is guided by the antenna until it reaches the limit of the "antenna region," that is, the sphere passing through the ends of the antenna; there, some of the energy passes into the outer space and some is reflected back, a situation existing when one transmission line is joined to another.

*Antenna as an Electric Horn*

We may also think of the wire as the wall of an electric horn with an aperture so wide that one can hardly see the horn itself. In fact, the mathematical analysis

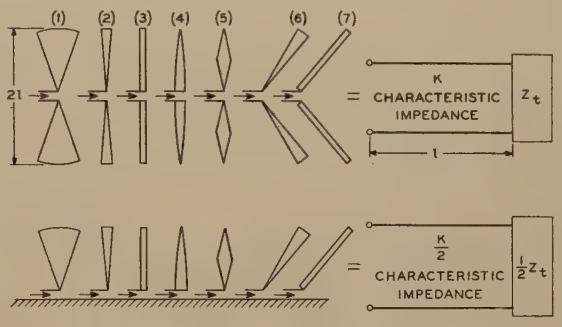


Fig. 2—The input impedance of a conical antenna of any size is equal to the input impedance of a uniform transmission line with a certain "output" impedance $Z_t$. The input impedance of a thin antenna of any shape may be similarly represented, except that the characteristic impedance will be variable.

used by us is precisely the analysis appropriate to wave guides and electric horns. We end up with a picture of the antenna as a transmission line (Fig. 2) whose output impedance $Z_t$ represents the end effect. The real part $R_t$ of $Z_t$ represents radiation and should properly be called the "radiation resistance"; it is the resistance of the outer space as seen from the ends of the antenna. Unfortunately, this name has been generally given to a quantity which turns out to be equal to $K^2/R_t$.

*Methods Based upon an Unproved Hypothesis*

The idea that the ordinary transmission-line theory could be amended to take care of radiation effects had occurred to Steinmetz[7] as long ago as 1919, in connection with his studies of electric waves on parallel wires. He failed to obtain correct results because twice he was deceived by physical intuition. In the first place, he believed that radiation losses and dissipation losses produce the same effect on transmission of waves. In effect this was a new proposition, which we have called Proposition $\alpha$, that could be inconsistent with established laws and thus he was taking chances. It is perfectly true that each element of current-carrying wire

[17] From the point of view developed in this paper there is no difference between the "end effect" and radiation.

radiates power; but at the same time it receives equal power from the surrounding medium due to the action of other elements plus power that is dissipated in that element.[18] In such circumstances, it is impossible to decide in advance just how radiation affects the current and voltage distribution on the wire.

### *The Hypothesis Is Wrong*

In Section VIII there is given a simple and straightforward proof that the *voltage across a pair of parallel perfectly conducting wires is not attenuated.* This proves that Proposition $\alpha$ is not true as it stands. Nevertheless, we shall have an occasion to point out that there is some truth in this proposition.

### *Effect of Phase Velocity on Radiation*

This brings us to another point. Proposition $\alpha$ has nothing to do (at least directly) with the very large value that Steinmetz obtained for the total radiation from a parallel pair. He used the same method which had been used before and which has been used since for approximate solutions of similar problems; but he apparently thought that since the phase velocity of waves along the line was very high he could make it infinite, and assume, in making calculations of radiation, that the currents along the entire line were in phase. Thus, he found that the radiated power was proportional to the length of the line while in reality the power radiated by a long line is independent of its length.[4,19] This discrepancy is due entirely to the effect of phase velocity of the current waves along the line and has nothing to do with the manner in which radiation affects the current distribution itself. For a discussion of other aspects of the problem of radiation from parallel wires the reader is referred to Carson.[20]

### *Single Wires*

Pedersen[9] and also Siegel and Labus[10,11] made use of Proposition $\alpha$ in their equations for a single wire but they based their computations on more nearly the actual current distribution in the wire. Thus they computed an approximately correct total radiated power and only then they postulated the character of its distribution.

Pederson has tried two different hypotheses. First he assumed that radiation loss is concentrated at the current antinode and then he assumed it to be distributed uniformly along the antenna. The current distributions calculated on either of these two assumptions turned out to be nearly the same and checked fairly satisfactorily with a measured current distribution.

Naturally, the calculated expression for voltage distribution must necessarily be wrong (Section VIII); but no voltage measurements have ever been made. Furthermore, for comparatively short antennas the current distribution does not markedly depend on just where the power is lost (see Section X).

Whatever may be said about the method, Pedersen succeeded in obtaining better approximations to the solution of the antenna problem than the ones available at that time.

## III. Antennas with Uniform Characteristic Impedances—General Discussion and Summary

### *Perfect Conductivity*

Unless otherwise specified all conductors are assumed to be perfect. This assumption simplifies the mathematics and separates the effect of radiation on transmission of waves along an antenna from the effect of dissipation. In the first approximation it is reasonable to suppose that the two effects are independent and can be superimposed.

### *Transmission Modes*

Until recently whenever one thought of electric waves guided by a pair of parallel wires or by coaxial cylindrical conductors, one was apt to visualize a picture of electric lines of force extending from one conductor to the other and lying in planes perpendicular to them, that is, in equiphase surfaces. One was conscious that near the ends of the conductors the field was somewhat warped; but one felt that the end effect was small and could be ignored. Thus one was concerned with one configuration of lines of force, with one propagation constant, with one phase velocity, with one characteristic impedance, and with one pair of transmission equations, that is, with one *transmission mode.* A transmission line with a single transmission mode will be called a *simple* transmission line.

But physical transmission lines are multiple. They are capable of guiding many types of waves, with different configurations of lines of force, with different propagation constants and with different characteristic impedances. Recently, this fact has burst into prominence in connection with the waves in hollow metal tubes; but the conventional lines are also multiple lines. The only reason why in the past they were regarded as simple lines is due to the fact that their transverse dimensions were so small compared with the wavelengths in which engineers happened to be interested that only the first transmission mode was quantitatively significant.

This situation may be made clearer by an analogy with an electric circuit comprised of a physical resistor, a physical inductor, and a physical capacitor in series. Such a circuit is usually regarded as a *simple* electric circuit, with one natural frequency or, taking the

[18] If the wire is perfectly conducting, the tangential electric intensity must vanish at the surface of the wire and the flow of power from the wire or to the wire is 0. If the wire is imperfectly conducting the flow of power is into the wire and not out of it.

[19] John R. Carson, "Radiation from transmission lines," *Jour. A.I.E.E.*, p. 789; October, 1921.

[20] John R. Carson, "The guided and radiated energy in wire transmission," *Jour. A.I.E.E.*, pp. 906–913; October, 1924.

decrement into account, with one "natural oscillation constant." In reality the circuit can oscillate in infinitely many modes; it is only because the first natural frequency is very much lower than the rest that in ordinary applications the circuit behaves as if it were a simple circuit.

The most prominent transmission mode of a given line will be called the "principal" or the "dominant" mode.

*Principal Waves Guided by Two Coaxial Cones*

Let two coaxial conical conductors, having a common axis (Fig. 3), be energized at the common apex. Intuitively one feels that if the cones were of infinite length, the wave would be such that the lines of elec-

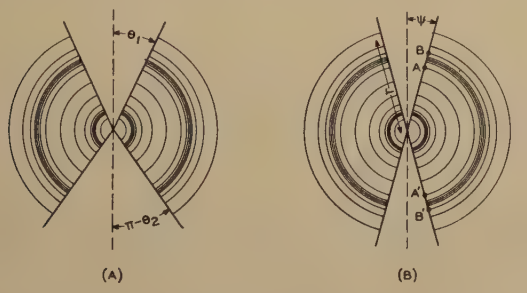


Fig. 3—Cross sections of infinitely long conical conductors and electric lines of force for principal waves.

tric force would follow the meridians of spheres concentric with the apex of the cones. There is indeed a wave, namely, the transverse electromagnetic spherical wave (TEM) for which this is true[21]; this wave turns out to be the most prominent and we shall call it the principal wave.

If we imagine a homogeneous spherical conductor coinciding with some equiphase surface, then the outward-bound progressive wave will be reflected from it. Electric lines, however, will still follow the meridians.

*Equations for Principal Waves*

Even from elementary considerations it is obvious that in so far as principal waves are concerned, the double cone is a *uniform* transmission line. Consider, for example, the capacitance per unit length $AB$ (Fig. 3 (B)). The length of the lines of electric force and the circumference of the conductor are both proportional to the distance $r$ from the apex; hence, the capacitance remains unchanged.[22]

Principal waves are just as easily treated rigorously.[21] The series inductance $L$ and the shunt capacitance $C$ per unit length and the characteristic impedance $K$ are found to be (for the double cone in Fig. 3(B))

$$L = \frac{\mu}{\pi} \log \cot \frac{\psi}{2}, \qquad C = \frac{\pi\epsilon}{\log \cot \frac{\psi}{2}},$$

$$K = \frac{\eta}{\pi} \log \cot \frac{\psi}{2} = 120 \log \cot \frac{\psi}{2}, \tag{1}$$

where $\psi$ is the angle of the cone.[25] The phase velocity of these waves is equal to that of light.

The principal voltage and the principal current can then be expressed in the following general form

$$V_0(r) = V_0^+ e^{-i\beta r} + V_0^- e^{i\beta r}, \qquad \beta = \frac{\omega}{v} = \frac{2\pi}{\lambda},$$

$$I_0(r) = I_0^+ e^{-i\beta r} + I_0^- e^{i\beta r},$$

$$V_0^+ = KI_0^+, \qquad V_0^- = -KI_0^-. \tag{2}$$

The voltage between the corresponding points $A$ and $A'$ is defined here as the line integral of the electric intensity along any curve joining $A$ and $A'$ and lying completely in the equiphase surface passing through $A$ and $A'$. This definition is in keeping with the usual definition of the voltage across a pair of parallel wires. This voltage is difficult to measure except near the origin and may be regarded as an auxiliary variable that helps us to find measurable quantities such as the input impedance, current distribution, etc.

Fig. 4 is a graph of $K$ as a function of the reciprocal angle. For cones of small angle, $1/\psi$ is approximately

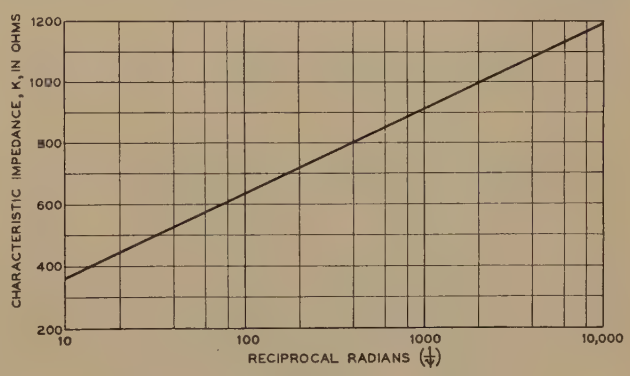


Fig. 4—The characteristic impedance of conical antennas of types shown in Fig. 3(B) as a function of the reciprocal cone angle $\psi = a/l$, where $l$ is the length of the cone and $a$ is its maximum radius.

equal to $r/\rho$, where $\rho$ is the radius of the cone at distance $r$ from the apex, and

$$K = 120 \log \frac{2}{\psi} = 120 \log \frac{2r}{\rho}. \tag{3}$$

When this ratio $r/\rho$ is 100, then $K = 635$ ohms; and for $r/\rho = 1000$, $K = 913$ ohms. It is hardly necessary

[21] S. A. Schelkunoff, "Transmission theory of spherical waves," *Trans. A.I.E.E.*, pp. 744–750, 1938.

[22] Excellent elementary discussions of principal waves on a double cone may be found in a paper by Howe[23] and on page 183 of a paper by Carter.[24]

[23] G. W. O. Howe, "The nature of the electromagnetic waves employed in radio telegraphy and the mode of their propagation," *Elec. Rev.*, pp. 486–489; September 26, 1913.

[24] P. S. Carter, "Simple television antennas," *RCA Rev.*, pp. 168–185; October, 1939.

[25] The quantity $\eta$ is the intrinsic impedance of the medium between the cones; for air $\eta$ is approximately equal to 120 $\pi$ or 377 ohms.

to point out that $K$ varies much slower than the ratio $r/\rho$.

*Standing Principal Waves*

If at $r=l$ we assume a reflecting sphere, then the amplitudes of progressive waves in (2) will be equal and standing waves will result. For a perfectly conducting sphere at $r=l$, we shall have

$$I_0(r) = I_0 \cos \beta(l - r),$$
$$V_0(r) = V_0 \sin \beta(l - r), \qquad V_0 = iKI_0. \tag{4}$$

These are the equations for a spherical cavity resonator and are of no direct interest in our present problem.

If the sphere were a perfect "magnetic" conductor, then the current $I_0(l)$ would have to vanish instead of the voltage and the voltage-current equations would be

$$I_0(r) = I_0 \sin \beta(l - r),$$
$$V_0(r) = V_0 \cos \beta(l - r), \qquad V_0 = - iKI_0. \tag{5}$$

We know from experience that the current distribution in a thin wire is approximately that given by (5). This suggests that the impedance of free space as seen from the "output" ends of the antenna is so high compared with $K$ that an almost complete reflection takes place. Later in this paper we shall actually prove that as $K$ tends to infinity, the current and voltage distributions on a conical wire, on any wire for that matter, approach (5).

If the spherical sheet at $r=l$ had some finite impedance, we should have

$$I_0(r) = I_0 \sin \beta(l - r) + I^0 \cos \beta(l - r),$$
$$V_0(r) = V_0 \cos \beta(l - r) + V^0 \sin \beta(l - r),$$
$$V_0 = - iKI_0, \qquad V^0 = iKI^0. \tag{6}$$

The input and the output impedances would then be

$$Z_i = \frac{V_0(0)}{I_0(0)} = K \frac{- iI_0 \cos \beta l + iI^0 \sin \beta l}{I_0 \sin \beta l + I^0 \cos \beta l},$$
$$Z_t = \frac{V_0(l)}{I_0(l)} = \frac{V_0}{I^0} = - iK \frac{I_0}{I^0}. \tag{7}$$

*Sphere of Discontinuity*

Equations (6) would have represented the actual conditions in a conical antenna (Fig. 5), were it not for the fact that the space outside the boundary sphere $S$ is a multiple transmission line with a set of transmission modes different from that in the antenna region. In particular, in free space there is no transmission mode which is even similar to the principal mode just discussed by us. For the latter, the field concentration near the conductors (if they are thin) is exceedingly high, because the conductors can support high currents quite readily. On the other hand, all radial currents in dielectrics are comparatively feeble and the magnetic intensity near the $A-B$ axis outside $S$ must be very small.

Hence the energy carried by the principal wave from 0 to the boundary sphere $S$ must travel thenceforward in different transmission modes and besides an ordinary reflection of the principal wave, secondary waves in

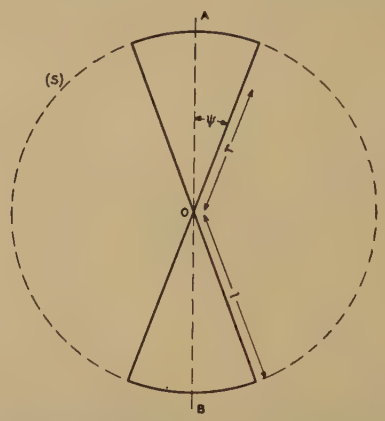


Fig. 5—The cross section of a conical antenna of length $l$ and of the "boundary sphere" $S$.

the antenna region will be generated to match the field outside $S$. This is our picture of how the "end effect" comes into being. "Radiation" is one part of this end effect; the reactive field associated with the secondary waves is the other part. The "sphere of discontinuity" is the "aperture" of the antenna regarded as an electric horn.

*Free-Space Transmission Modes*

Before considering secondary transmission modes in the antenna region, we shall review briefly the modes of transmission in free space. The principal mode in free space is characterized by electric lines of force whose shape is suggested in Fig. 6(A). The energy emitted by a very small doublet travels outward in this mode. The electric field has two components, the radial component $E_r$ and the meridian component $E_\theta$. The

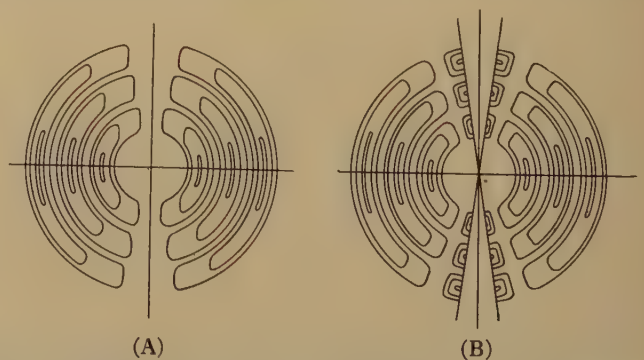

(A) (B)

Fig. 6—Electric lines for the first-order transverse magnetic spherical waves: (A) lines in free space; (B) lines in the presence of two coaxial conical conductors.

former is proportional to $\cos \theta$ and the latter to $\sin \theta$, where $\theta$ is the angle with the axis of the wave. The radial displacement current flows in one direction in the "northern" hemisphere and in the opposite direction in the southern. The two hemispheres play parts

of the two conductors in a transmission line. Of course, the radial displacement current is not distributed uniformly within each hemisphere; the current density is maximum along the axis of the wave. We should note, perhaps, that while $E_r$ varies ultimately as $r^{-2}$, where $r$ is the distance from the doublet, the radial current density per unit solid angle and hence the total radial current in each hemisphere are independent of the distance, except for the phase factor $e^{-i\beta r}$.

The lines of electric force corresponding to the second transmission mode are shown in Fig. 7(A). Higher transmission modes will have still more sets of closed loops. Mathematically all these modes are represented by zonal harmonics; the radial electric intensity is proportional to $P_n(\cos\theta)$ and the meridian intensity to $(d/d\theta)P_n(\cos\theta)$.

(A) (B)

Fig. 7—Electric lines for the second-order transverse magnetic spherical waves: (A) lines in free space; (B) lines in the presence of two coaxial conical conductors.

Any field outside the antenna region, having circular symmetry, can be represented as the resultant of a number of waves traveling in the above-discussed transmission modes.

*Secondary Transmission Modes in the Antenna Region*

Suppose we have a free-space wave like that shown in Fig. 6(A) and suppose we insert a thin conical conductor coaxial with the axis of the wave (Fig. 6(B)). Electric lines of force must be perpendicular to the conductor; but since the meridian intensity near the axis is small, we do not expect a very radical change in the configuration of the lines of force and we expect that this configuration will resemble the one shown in Fig. 6(B). This is indeed the case. The major difference is that in the presence of the conical conductor the radial electric intensity (and hence the radial current density) is highest not at the surface of the conductor but at some distance from it. Right at the surface of the cone, the radial intensity vanishes. As the angle of the cone gets smaller, the field distribution becomes more nearly like free-space field distribution except in the ever-diminishing region adjacent to the cone.

Fig. 7(B) shows how the second[26] mode in the antenna region is related to the second mode in free space. Incidentally, if the antenna is energized at its center, this mode and all other even modes do not appear. This is because the conduction currents associated with them flow in opposite directions in the two halves of the antenna, while the currents produced by the generator must flow in the same direction.

*The Total Voltage Associated with Any Secondary Wave in the Antenna Region Is Zero*

As in the case of the principal wave we define the voltage between two points on the upper and lower cones as the line integral of the electric intensity along any path joining the point of the upper cone to the point of the lower cone, provided the path is situated in the equiphase circuit passing through the two points.[27] It is shown in Section V that for all secondary waves in the antenna region this voltage is equal to zero

$$V_m(r) = 0. \tag{8}$$

*Conduction Currents Accompanying Secondary Waves Vanish at the Origin*

It is shown in Section V that the conduction current accompanying any secondary wave vanishes at the origin

$$I_m(0) = 0. \tag{9}$$

Near the origin $I_m(r)$ varies as $r^{m+1+\Delta}$, where, approximately, $\Delta = 120/K$. Thus the effect of the secondary current waves on the total current is rather unimportant near the origin, but becomes more pronounced near the output terminals of the antenna.

*Voltage-Current Equations*

We can now write the complete voltage-current equations for a perfectly conducting transmitting antenna energized at its center in the following form:

$$V(r) = V_0(r), \quad I(r) = I_0(r) + \bar{I}(r), \tag{10}$$

where the principal voltage-current waves are given by (6) and the total secondary current $\bar{I}(r)$ is the sum of odd secondary current waves

$$\bar{I}(r) = I_1(r) + I_3(r) + I_5(r) + \cdots, \quad \bar{I}(0) = 0. \tag{11}$$

The total voltage wave consists of just two principal waves, of which the second represents the effect of incomplete reflection at the boundary sphere $S$. As the result of this incomplete reflection, the voltage maximum does not occur at $r = l$. This is the only effect of radiation on the voltage wave; no "attenuation" is introduced into the voltage wave.

The total current wave, on the other hand, is affected more radically.

*Imperfectly Conducting Antennas*

It will be seen that $\bar{I}(r)$ is rather small compared with $I_0(r)$ and it is natural then to assume that the

[26] It is really the third if we count the principal; but it is more convenient to designate the principal mode in the antenna region as the 0th mode.

[27] If the points are not situated in the same equiphase surface, then the voltage between them is not defined.

imperfect conductivity of an antenna will manifest itself largely through the principal wave which will become

$$I_0(r) = -iI_0 \sinh \Gamma(l-r) + I^0 \cosh \Gamma(l-r),$$
$$V_0(r) = -iKI_0 \cosh \Gamma(l-r) + KI^0 \sinh \Gamma(l-r). \quad (12)$$

The propagation constant $\Gamma$ is given by

$$\Gamma = \frac{R}{2K} + i\beta, \quad (13)$$

where $R$ is the resistance (of both cones) per unit length.

*The Charge Is not Generally Proportional to the Voltage*

It is evident that for principal waves, the electric charge $q_0(r)$ per unit length is proportional to the voltage $V_0(r) = V(r)$. The charge $q_m(r)$ associated with a secondary wave, being proportional to the derivative of the current, does not vanish while the corresponding voltage does; this means that the total charge is not proportional to the total voltage.

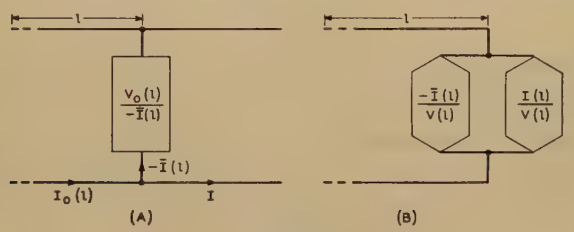


Fig. 8—The relation between principal, secondary, and total currents at the ends of an antenna.

In a simple uniform transmission line the charge is proportional to the voltage and it does not matter whether we write the transmission equations in the voltage-current form or in the charge-current form; but these two possible forms are quite different in the case of multiple transmission lines unless one mode predominates over all others. The charge-current equations are more complicated than the voltage-current equations and are here considered (see Section VII) only because of their bearing on the idea that radiation takes place continuously along the antenna. In that section we shall show that the effect of radiation on the distribution of the total charge (but not the total voltage) and the total current in an antenna may be represented by a continuously distributed series resistance and a continuously distributed series inductance in addition to the normal inductance of the antenna regarded as a simple transmission line. This coupled with the fact that for comparatively short antennas the precise distribution of this resistance has but little effect on the current distribution, explains why equations obtained by Pedersen, Siegel, Labus and others turn out to be fairly satisfactory approximations to the antenna solution, provided we replace in their equations $V$ by a quantity proportional to $q$. On the whole, however, we find the voltage-current equations much simpler; and in these equations, radiation may be represented as a terminal impedance.

*Secondary Waves in an Antenna Affect the Amplitudes of the Principal Waves in a Way an Output Impedance Would*

Consider the principal waves in the antenna as given by (6). Substituting from (10) into the expression for the output impedance $Z_t$ and taking its reciprocal, we have

$$Y_t = \frac{1}{Z_t} = \frac{I_0(l)}{V_0(l)} = \frac{I(l)}{V(l)} + \frac{-\bar{I}(l)}{V(l)}. \quad (14)$$

Thus the output admittance consists of two admittances in parallel.

Transmission-line diagrams (Fig. 8) represent the above relationship graphically. The current $-\bar{I}(l)$ is that part of the principal current which is diverted into a shunt admittance. Whenever a capacitor (or any impedor) is shunted across a pair of wires, we can look upon this capacitor as a practical means for producing a local field superimposed upon the normal field surrounding the pair of wires. Broadly speaking the capacitor is an irregularity in the transmission line. Sudden termination of the wires in the antenna case is also an irregularity producing a field which is superimposed upon the normal field of the principal waves guided by the antenna.

The total current $I(l)$ may be different from zero. For instance, if the tops of the conical conductors are large, appreciable current may flow over the edge; or, if the antenna itself is thin, end capacitances may be provided by a number of wires spreading fanwise from the ends of the antenna wires. However, if the cross section of the ends of the antenna is small and no loading is provided, then the total current is zero and

$$I_0(l) = -\bar{I}(l), \qquad Y_t = \frac{-\bar{I}(l)}{V(l)}. \quad (15)$$

This is the case with which we are specifically concerned in this paper.

*The Output Impedance of a Transmitting Antenna*

In Section V we shall prove that if the characteristic impedance of the antenna is large and if the total current at the ends of the antenna is zero, then we have approximately

$$\frac{I^0}{I_0} = \frac{F(L) - iG(L)}{K}, \quad (16)$$

where the "phase length" of each cone is[28]

$$L = \frac{2\pi l}{\lambda}. \quad (17)$$

[28] It is hoped that our use of $L$ to designate the phase length and the inductance will not lead to confusion. This use of $L$ in the second sense is only occasional and it will be obvious from the context when it is meant to designate the inductance.

The functions $G(L)$ and $F(L)$ are given by the series

$$G(L)=30\pi L\sum_{m=0}^{\infty}\frac{4m+3}{(m+1)(2m+1)}J^2_{2m+3/2}(L),$$
$$F(L)=-30\pi L\sum_{m=0}^{\infty}\frac{4m+3}{(m+1)(2m+1)}J_{2m+3/2}(L)N_{2m+3/2}(L). \quad (18)$$

Presently we shall give much simpler expressions for these functions.

Substituting in (7), we have for the output impedance

$$Z_t=\frac{K^2}{G(L)+iF(L)}. \quad (19)$$

It is worth noting that at a distance of $\frac{1}{4}$ wavelength from the terminals, this impedance appears as

$$\frac{K^2}{Z_t}=G(L)+iF(L). \quad (20)$$

The graphs of the real and imaginary parts of this transformed impedance are shown in Fig. 9.

*The Input Impedance*

The input impedance of the antenna is obtained from the usual transmission-line equations or directly from (7); thus we have

$$Z_i=K\frac{(G+iF)\cos\left(L-\frac{\pi}{2}\right)+iK\sin\left(L-\frac{\pi}{2}\right)}{K\cos\left(L-\frac{\pi}{2}\right)+i(G+iF)\sin\left(L-\frac{\pi}{2}\right)}$$
$$=K\frac{G\sin L+i(F\sin L-K\cos L)}{(K\sin L+F\cos L)-iG\cos L}. \quad (21)$$

Separating the real and the imaginary parts, we obtain

$$Z_i=\frac{G-i\left[\frac{1}{2}K\sin 2L+F\cos 2L-\frac{F^2+G^2}{2K}\sin 2L\right]}{\sin^2 L+\frac{F}{K}\sin 2L+\frac{F^2+G^2}{K^2}\cos^2 L}. \quad (22)$$

*The Case of an Infinitely Large K*

If $K$ is infinitely large, then $I^0=0$ and the current distribution in the antenna becomes

$$V(r)=V_0\cos\beta(l-r),$$
$$I(r)=I_0\sin\beta(l-r). \quad (23)$$

From (22) we find that the input impedance tends asymptotically to

$$Z_i\to\frac{G(L)+iF(L)}{\sin^2 L}-iK\cot L. \quad (24)$$

Since the input current tends to $I_0\sin L$, the complex flow of power is

$$\Psi=\tfrac{1}{2}[G(L)+iF(L)-\tfrac{1}{2}iK\sin 2L]I_0^2. \quad (25)$$

The preceding expressions are the first approximations to the antenna equations.

*Formulas for G(L) and F(L)*

The above asymptotic formulas provide a very convenient method for obtaining $G$ and $F$ functions. Since (25) represents the power flow *when the current is sinusoidal* with a node at the end of the antenna, $G(L)$ must be the so-called "radiation resistance" as referred to the maximum current. This resistance is independent of the shape of the antenna and hence is equal to that of a cylindrical wire. The latter can and has been computed either by the Poynting flux method

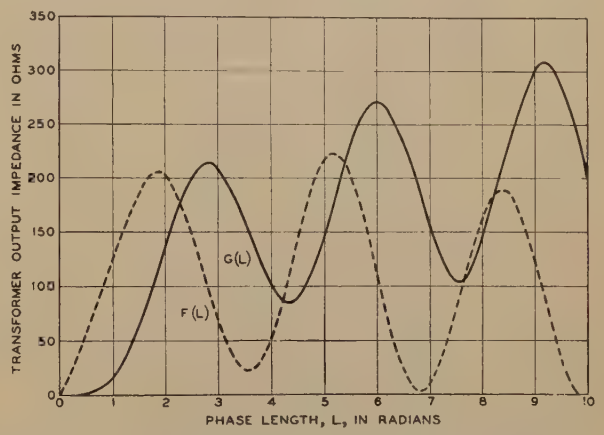


FIG. 9—The real and the imaginary parts of the "transformed" output impedance $K^2/Z_t=G(L)+iF(L)$, where $L=2\pi l/\lambda$.

or by the induced-electromotive-force method (see Section VI). The latter method can also be used for computing $F(L)$, except that this time it is necessary to make calculations for *conical* antennas. As will be seen in Section IV, antennas of other shapes than conical will have an extra reactive component which must be attributed to the nonuniformity of the line rather than to the end effect.

Thus we have obtained the following expressions

$$G(L)=60(C+\log 2L-\mathrm{Ci}\,2L)+30(C+\log L-2\,\mathrm{Ci}\,2L+\mathrm{Ci}\,4L)\cos 2L+30(\mathrm{Si}\,4L-2\,\mathrm{Si}\,2L)\sin 2L,$$
$$F(L)=60\,\mathrm{Si}\,2L+30(\mathrm{Ci}\,4L-\log L-C)\sin 2L-30\,\mathrm{Si}\,4L\cos 2L, \quad (26)$$

where $C=0.577\cdots$ is Euler's constant.

The method just outlined can be used successfully for obtaining second approximations to antenna problems when terminal conditions are other than those considered in this paper.

*Resonance*

From (22) we observe that the input reactance will vanish when

$$\tan 2L=-\frac{2KF}{K^2-G^2-F^2}. \quad (27)$$

Inasmuch as we are concerned here with approximations as far as the first powers of the characteristic admittance $1/K$, we approximate (27) by

$$\tan 2L = -\frac{2F}{K}. \tag{28}$$

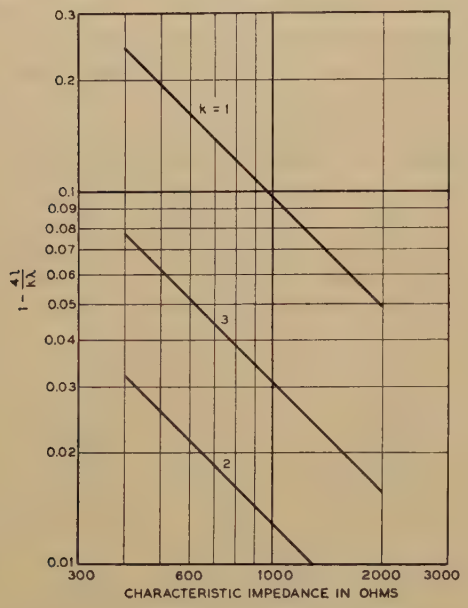


Fig. 10—Deviation of the resonant length of conical antennas from $2l=k\lambda/2$.

The solution of the above equation is

$$2L = k\pi - \frac{2F\left(\frac{k\pi}{2}\right)}{K}, \quad k = 1, 2, \cdots. \tag{29}$$

Hence, the input reactance of a conical antenna vanishes when

$$\frac{4l}{k\lambda} = 1 - \frac{2F\left(\frac{k\pi}{2}\right)}{\pi k K} = 1 - \frac{120\,\mathrm{Si}\,k\pi + 60(-)^{k+1}\,\mathrm{Si}\,2k\pi}{\pi k K}. \tag{30}$$

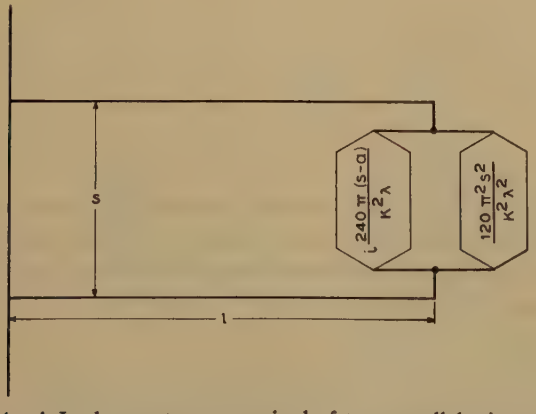


Fig. 11—A Lecher system comprised of two parallel wires, short-circuited at the left end with a metal disk. A parallel combination of two admittance boxes on the right represents the end effect; the conductance box represents radiation and the second box the end capacitance. It is assumed that $s$ is substantially smaller than $l$.

If it were not for the end effect, the resonant lengths of antennas would be given by $2l=k\lambda/2$. The end effect makes antennas resonate when they are somewhat shorter than $k\lambda/2$. For the first three resonances the shortening effect is shown in Fig. 10. For higher resonances the shortening is substantially equal to $45\lambda/K$, when $k$ is odd, and $15\lambda/K$ when $k$ is even.

In antennas of other shapes than conical, another factor affects resonant lengths. This factor will be considered in Section IV.

*Resonance in Lecher Systems*

The shortening effect just discussed exists also in Lecher systems and for the same reason. A sudden discontinuity introduces a terminal capacitance. Consider a Lecher system "short-circuited" with a metal disk at one end and open at the other (Fig. 11). The "open end" is not electrically open and the impedance across it represents the power loss by radiation and the end capacitance. If $s$ is the interaxial separation between the wires and $a$ is their radius, then in the neighborhood of the principal resonance we have approximately

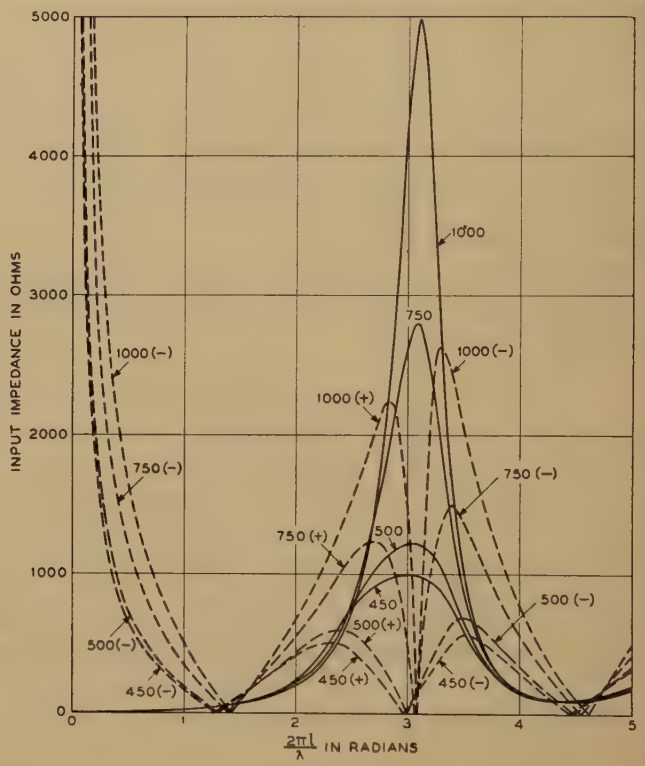


Fig. 12—The input impedance of conical antennas as a function of $2\pi l/\lambda$ and $K$. Solid curves represent the real component and the dotted curves the imaginary.

$$C = \frac{120(s-a)}{K^2 v}, \quad G = \frac{120\pi^2 s^2}{K^2\lambda^2}, \quad K = 120\log\frac{s}{a}, \tag{31}$$

where $v$ is the velocity of light. These values have been computed by the method of the induced electromotive force from the sinusoidal current distribution, taken as the first approximation to the true distribution.

In this case it is easy to show that for the principal resonance

$$\lambda = 4l + 4vCK. \tag{32}$$

Substituting from (31), we have

$$\lambda = 4l + \frac{480(s - a)}{K}. \tag{33}$$

For this case, Englund[16] has obtained the following relation experimentally

$$\lambda = 4l + 12.4, \tag{34}$$

for wavelengths from 400 to 750 centimeters. In his setup $s = 10.1$ centimeters, $a = 0.635$ centimeter, and

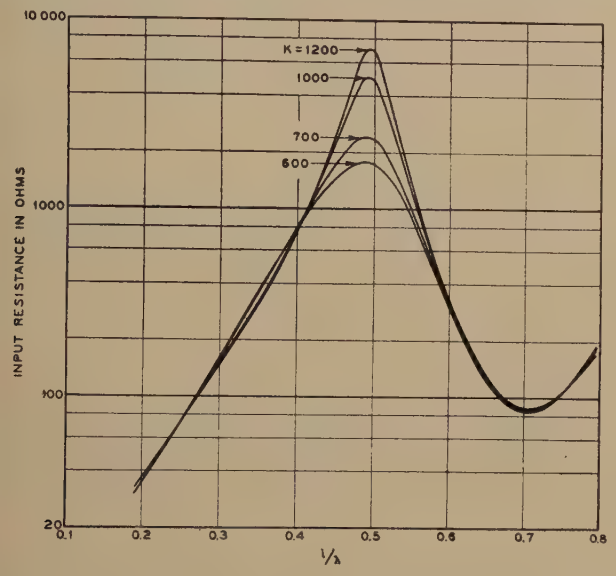


Fig. 13—The input resistance of conical antennas.

$K = 332$ ohms. Substituting these values in (33) we obtain

$$\lambda = 4l + 13.7. \tag{35}$$

Some of the discrepancy between the measured and the calculated values is probably due to the fact that the diameter of the short-circuiting disk was only 15.5 centimeters whereas in computing $C$ we have assumed the disk to be large enough for the current in it to produce the same effect on the Lecher system as the "image" of the system in the disk. Some of the discrepancy (to the extent of a few millimeters) must be ascribed to the second-order errors in the computed value and in measurements. The more precise value of $C$ contains small terms depending on the length $l$ of the Lecher system; but Englund's formula does not include such a term.

*Input Resistance and Reactance Curves*

The input impedance of conical antennas may be computed from (22). This impedance depends on the characteristic impedance and on the length of the antenna. In Fig. 12 the resistance and the reactance are plotted as functions of $2\pi l/\lambda$, where $2l$ is the length of the antenna in free space. The characteristic impedance $K$ is the parameter; it is defined by (1) and plotted in Fig. 4. For a vertical antenna of length $l$

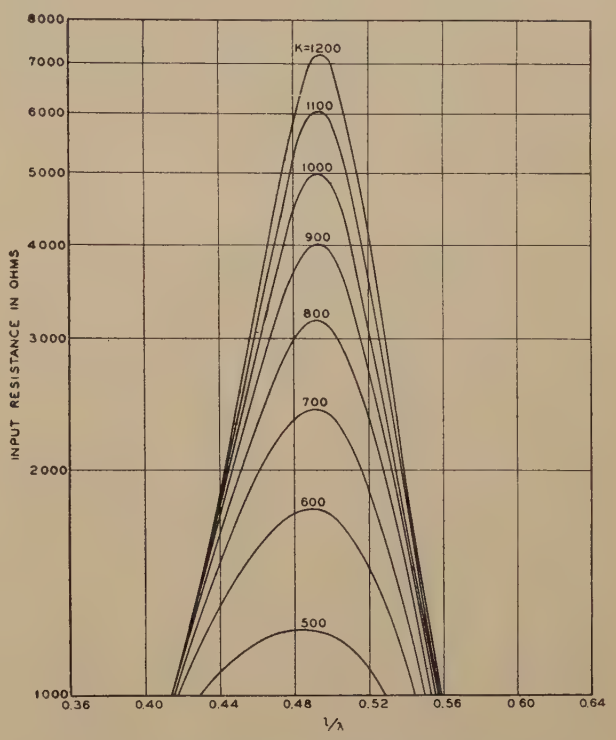


Fig. 14—The input resistance of conical antennas in the neighborhood of the second resonance.

above a perfectly conducting ground we can use the same set of curves and only divide by two the ordinates and the characteristic impedance. For example, the maximum resistance of an antenna in free space, with $K = 1000$, is about 5000; for a vertical antenna of the same size, $K = 500$, and the maximum resistance is 2500.

In Fig. 13 the input resistance alone is shown. It will be observed that the input resistance depends very markedly on $K$ in the region (shown on a larger scale

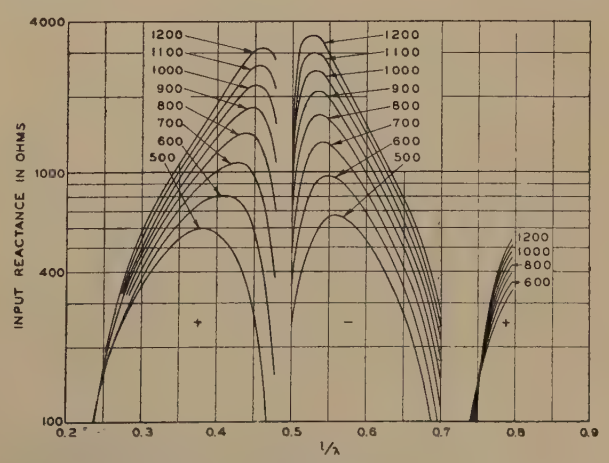


Fig. 15—The input reactance of conical antennas.

in Fig. 14) around the second resonance, or more generally in regions around even resonances. The reactance curves are shown separately in Fig. 15.

*Current Distribution*

In practice, precise knowledge of current distribution is of lesser importance than knowledge of the input impedance. This is because the directive gain of antennas and their radiation patterns are not very sensitive to the changes in the current distribution. Radiation patterns will be affected seriously only in those directions in which radiation is small.

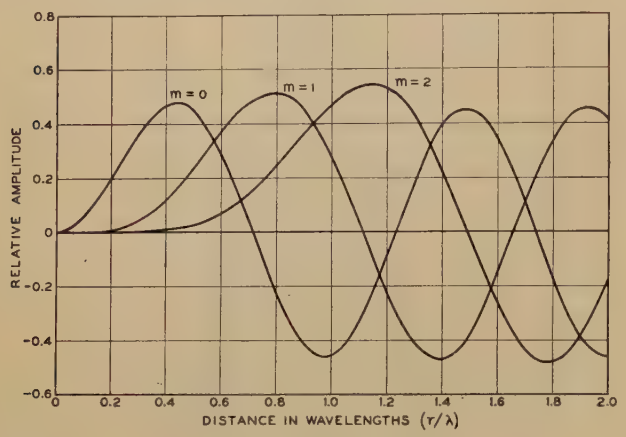


Fig. 16—The amplitudes of the first, third, and fifth ($m=0$, 1, 2) secondary waves as functions of the distance from the center of the antenna.

The current distribution is given by (10) and (11). In Section V we obtain the following approximate expression for a typical secondary wave:

$$I_{2m+1}(r) = I_0 \frac{30\pi(4m+3)L}{(m+1)(2m+1)K} \left[N_{2m+3/2}(L) + iJ_{2m+3/2}(L)\right] \cdot \sqrt{\frac{r}{l}} J_{2m+3/2}\left(\frac{Lr}{l}\right). \quad (36)$$

First of all let us consider individual secondary waves. Near $r=0$, the amplitude of the $(2m+1)$st current wave varies nearly[29] as $r^{2m+1}$. Fig. 16 illustrates the way in which the amplitudes of the 1st, 3rd, and 5th ($m=0$, 1, 2) vary with the distance from the origin. If this distance is less than $\frac{1}{4}$ wavelength, only the 1st wave is important; at distances smaller than $\frac{1}{2}$ wavelength only the 1st and the 3rd[30] are important.

The maximum amplitudes of secondary current waves depend on the characteristic impedance and on the length of the antenna. Fig. 17 shows actual secondary current waves for $K=1000$ and $l=\lambda/2$. Of the components in phase (solid curves) with the dominant current $I_0 \sin \beta(l-r)$, only the first is important except at $r=l$; of the quadrature components the first two are sufficient. Both components are inversely proportional to $K$.

In Fig. 18 the solid curve represents the amplitude of the total current, the dash curve shows the amplitude of the component in phase with $I_0$, and the dash-dot curve represents the amplitude of the quadrature component. In this figure the current does not quite vanish at the end of the antenna; this is because near the very end of the antenna that part of the total secondary current which is in phase with the dominant current term $I_0 \sin \beta(l-r)$ is determined by a very large number of secondary-current waves and in computing our curve we have taken into account only two. This situation is closely related to very slow convergence of the series representing $F(L)$ in (18) and it is understandable on physical grounds. The field distortion in the immediate vicinity of a sharp end must be much greater than elsewhere and more terms will be needed to represent the field accurately. If we dissolve both the current and the charge near the end of the antenna into two quadrature components, then it becomes evident that the slope of the current curve depends on the charge at the end and must be quite large. Thus near the ends of the antenna, the current approaches zero very abruptly.

In Fig. 19 the total current in the antenna is compared with the principal current. The difference between the real parts is seen to be quite small; but the difference between the imaginary parts is relatively large, except near the center.

*Minimum Amplitude*

We shall now find the ratio $I_{\min}/I_{\max}$ of the first minimum amplitude to the first maximum amplitude (counting from the generator). The first minimum is relatively close to the generator where the secondary current wave is very small. The first maximum is farther away where the secondary current is greater; but there the principal current is large. Thus we can obtain the desired information fairly accurately from the principal current

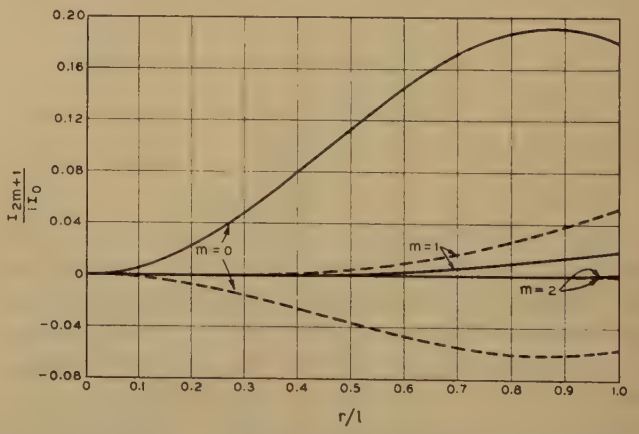


Fig. 17—Secondary current waves for $K=1000$ and $l=\lambda/2$. The solid curves show the components in phase with the dominant current $I_0 \sin \beta(l-r)$, and the dotted curves show the quadrature components.

$$\frac{I_0(r)}{I_0} = \left[\sin \beta(l-r) + \frac{F(L)}{K} \cos \beta(l-r)\right] - i \frac{G(L)}{K} \cos \beta(l-r). \quad (37)$$

[29] More accurately, the amplitude varies as $(2m+1+120/K)$th power of $r$.

[30] The even-order waves are absent when a generator is at the center.

The maximum value of this ratio will occur where $\sin \beta(l-r)$ is nearly unity and where $\cos \beta(l-r)$ is, therefore, nearly zero. Hence, the maximum value of (37) is nearly unity. The minimum value will occur where $\cos \beta(l-r)$ is nearly unity. In the vicinity of this point, we can find a value of $\beta(l-r)$ for which the real part of (37) vanishes; thus, $G/K$ is nearly the minimum of $I_0(r)/I_0$ and

$$\frac{I_{\min}}{I_{\max}} = \frac{G(L)}{K}. \tag{38}$$

There are no measurements of current distribution in antennas with uniform characteristic impedance. However, it is of interest to compare the measurements on nonuniform antennas with values computed for uniform antennas. In the case of the Copenhagen antenna,[9] a vertical antenna directly above the ground, the *average* characteristic impedance is 540 ohms and $L_{\text{eff}}=3.64$. Replacing the ground by the image of the antenna, we take the characteristic impedance of the corresponding free-space antenna[31] as 1080 ohms. The ratio $I_{\min}/I_{\max}$ is computed to be 0.131. As nearly as we can read from Pedersen's picture, enlarged by King,[3] the experimental value is 0.132. The ratio calculated by King is approximately $3/34=0.0882$; this is lower than the experimental value by about 33 per cent, the difference being considerably larger than the experimental error. We can offer no explanation of this discrepancy. King's method is rigorous; and the accuracy of his approximation would seem to be of the same order of magnitude as ours.

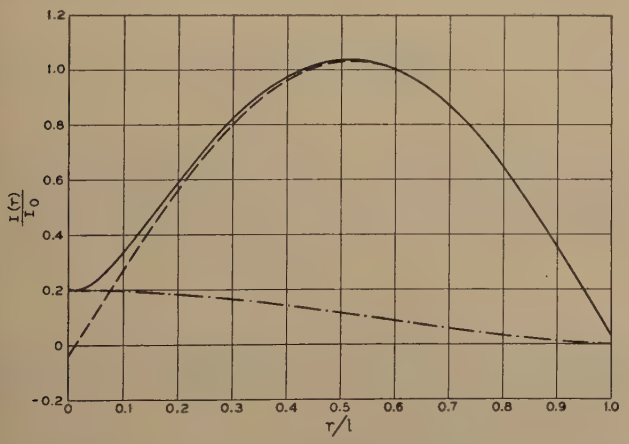


Fig. 18—The total current in the antenna of length $2l=\lambda$; $K=1000$. The solid curve represents the amplitude of the total current; the dash curve represents the amplitude of the component in phase with $I_0$ and the dash-dot curve is the amplitude of the quadrature component.

Morrison and Smith[32] have measured the current distribution in a tower 6 feet and 6 inches square and 400 feet long. The diagonal of the cross section is 9.2 feet and rather arbitrarily we have chosen $2a=8$ feet as the diameter of an equivalent circular tower in our computation of the average characteristic impedance. Thus we have obtained $K=516$ ohms (for free space; 258 ohms for the actual tower above the ground). The phase length of the antenna is $L=3.7$ and $G(L)=134$.

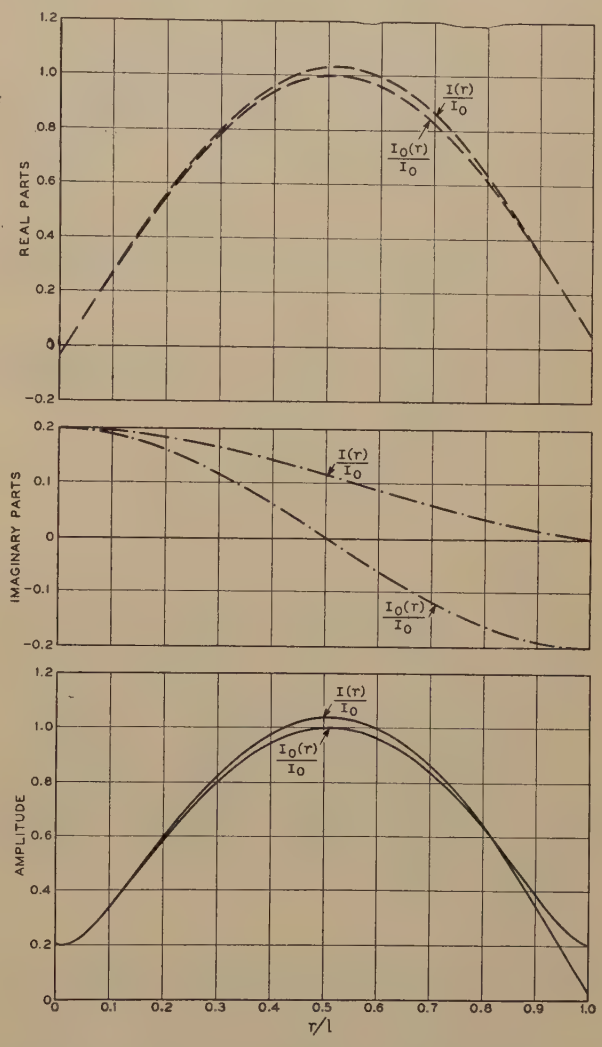


Fig 19—Curves for the total current and the principal current.

The calculated ratio is 0.26 and the measured ratio as read from the picture[32] is $17.5/75=0.233$.

### *Transmitting Antennas Fed at an Arbitrary Point and Receiving Antennas*

Most of the foregoing formulas have been derived specifically for free-space antennas fed at the center (or for vertical antennas directly above ground). The method described in Section V is applicable equally well to other cases. Here we shall limit ours to a few general remarks.

If two equal electromotive forces[33] are applied at two points equidistant from the center, then the current distribution will still be given in the form (10) and (11).

[31] See Section IV for a method of computing average impedances.

[32] J. F. Morrison and P. H. Smith, "The shunt-excited antenna," Proc. I.R.E., vol. 25, pp. 673–696; June 1937.

[33] By "equal" we mean equal amplitudes and equal phases, so that at all times the forces act in the same direction.

However, the ratio $I^0/I_0$ will have to be determined anew as a function of the distance from the center as well as a function of $K$ and $L$.

If two equal but oppositely directed electromotive forces are applied at points equidistant from the center, then none of the current components in (10) and (11) will be present in the new expression for the current. This is because all the terms in (10) and (11) correspond to currents flowing in the same direction in the two halves of the antenna. The new expression will contain its own principal wave, *principal* antisymmetric wave, and a set $I_2(r)$, $I_4(r)$, $\cdots$ of antisymmetric secondary waves.

An electromotive force $V$ applied at some point can always be regarded as the resultant of two pairs of forces $(V/2, V/2)$ and $(V/2, -V/2)$ applied at points equidistant from the center.

The same general method can also be used to develop a theory of "end-fed" wires by considering a single cone, instead of a double cone.

## IV. Antennas with Variable Characteristic Impedances

### *The Problem*

Conical antennas support spherical waves regardless of the magnitude of the cone angle and their theory is relatively simple. Antennas of other shapes are definitely more complicated. However, if their transverse dimensions are small enough, they support approximately spherical waves and approximate solutions are rather simple. We obtain these approximations largely on the basis of the physical picture implied by the theory of conical antennas rather than by a direct mathematical analysis.

### *Principal Waves*

Imagine a set of spheres concentric with the generator. Each small segment of the antenna may be regarded as a section of a cone and we may write the following approximate expressions for the distributed series inductance and shunt capacitance per unit length:

$$L = \frac{\mu}{\pi}\log\frac{2}{\psi} = \frac{\mu}{\pi}\log\frac{2r}{\rho},$$

$$C = \frac{\pi\epsilon}{\log\frac{2}{\psi}} = \frac{\pi\epsilon}{\log\frac{2r}{\rho}}. \tag{39}$$

The transmission equations for the principal waves will be

$$\frac{dV}{dr} = -i\omega LI, \qquad \frac{dI}{dr} = -i\omega CV. \tag{40}$$

If $\rho \to 0$, $L$ and $C$ become increasingly more constant as $r$ varies. We expect, therefore, the following asymptotic solutions of (40)

$$V(r) = \sqrt{K(r,\rho)}\,(Ae^{-i\beta r} + Be^{i\beta r}),$$

$$I(r) = \frac{Ae^{-i\beta r} - Be^{i\beta r}}{\sqrt{K(r,\rho)}}, \tag{41}$$

where the characteristic impedance $K(r, \rho)$ is now a slowly varying function of the distance from the generator

$$K(r,\rho) = \frac{1}{\pi}\sqrt{\frac{\mu}{\epsilon}}\log\frac{2r}{\rho} = 120\log\frac{2r}{\rho}. \tag{42}$$

It is interesting to note that (41) are exactly the approximate expressions obtained by Brillouin[34] directly from the second-order differential equations resulting from elimination of either $V$ or $I$ from (40).

### *Average Characteristic Impedances*

We shall define the average characteristic impedance $K_a$ as follows

$$K_a = \frac{1}{l}\int_0^l K(r,\rho)dr. \tag{43}$$

Applying this formula to a cylindrical wire, we obtain

$$K_a = 120\left(\log\frac{2l}{a} - 1\right); \tag{44}$$

this is substantially equal to the characteristic impedance of a cylindrical antenna as given by Pedersen.[9]

For a spheroidal antenna, the average characteristic impedance is

$$K_a = 120\log\frac{l}{a}, \tag{45}$$

where "$a$" is the radius at the base of the antenna.

For an antenna of the shape (5) among those in Fig. 2, the average characteristic impedance is

$$K_a = 120\log\frac{2l}{a}, \tag{46}$$

where "$a$" is the maximum radius of the antenna. These average characteristic impedances are shown in Fig. 20 as functions of $l/a$.

As $K_a$ approaches infinity, the difference $(K(r,\rho) - K_a)/K_a$ approaches 0 and the transmission line becomes more nearly uniform. Consequently, we may regard the uniform line with the characteristic impedance $K_a$ as a first approximation to the given nonuniform line. The second approximation will contain terms depending on the reciprocal of $K_a$ and these terms are large enough to be of importance in engineering applications. For example, sections of transmission lines with variable $K(r, \rho)$ do not resonate at the same frequencies as uniform sections of equal lengths. The effect is of the same order of magnitude as the effect

[34] J. C. Slater and N. H. Frank, McGraw-Hill Book Company, New York, N. Y., (1933), pp. 147–148.

due to radiation and may either aid or oppose it. We can compute this effect if we find the second approximation to the input impedance of nonuniform lines; but there exists a somewhat simpler method which will be employed in the following section.

*Variable Capacitance and Inductance Affect Resonance Conditions in Finite Sections of Nonuniform Transmission lines*

Multiplying the first equation in (40) by $I^*$ and the conjugate of the second by $V$, adding the results and integrating from 0 to $l$, we have

$$V(l)I^*(l) - V(0)I^*(0) = i\omega \int_0^l [CVV^* - LII^*]dr. \quad (47)$$

If the section of the line is either electrically open or

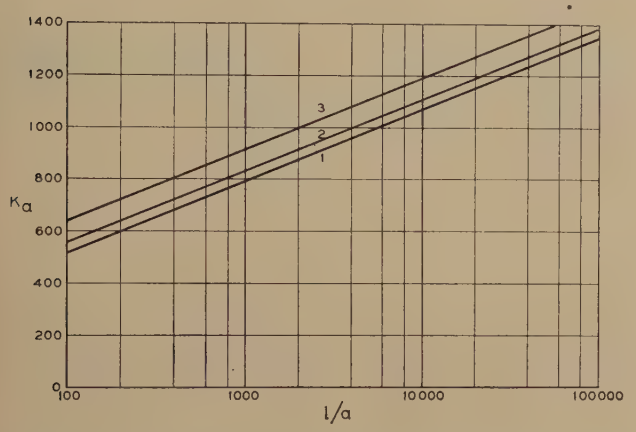


Fig. 20—The average characteristic impedance: (1) cylindrical antenna, (2) spheroidal antenna, (3) antenna shape (5) shown in Fig. 2.

short-circuited at both ends, the left side of this equation vanishes and we have

$$\int_0^l CVV^*dr = \int_0^l LII^*dr. \quad (48)$$

This is merely an expression of the well-known fact that at resonance the average electric energy and the average magnetic energy are equal. Furthermore, Rayleigh has shown that the first-order errors in distribution of $V$ and $I$ result in second-order errors in the resonant frequencies. Thus, (48) can be used for an approximate computation of resonant frequencies.

First of all, however, we shall obtain two special forms of (48), especially adapted to the case when

$$LC = \frac{1}{v^2} = \text{constant}. \quad (49)$$

Taking this relationship into consideration, we rewrite (40) as follows:

$$I = \frac{iv^2C}{\omega}\frac{dV}{dr}, \qquad V = \frac{iv^2L}{\omega}\frac{dI}{dr}. \quad (50)$$

Substituting from (50) in (48), we have

$$\frac{\omega^2}{v^2} = \frac{4\pi^2}{\lambda^2} = \frac{\int_0^l L\left|\frac{dI}{dr}\right|^2 dr}{\int_0^l L|I|^2 dr} = \frac{\int_0^l C\left|\frac{dV}{dr}\right|^2 dr}{\int_0^l C|V|^2 dr}. \quad (51)$$

The foregoing formulas are exact. In order to obtain approximate formulas, we shall assume sinusoidal voltage-current distributions. Thus, for the first resonance with one end short-circuited and the other open (let the end at $r=0$ be short-circuited and the end at $r=l$ open), we have

$$I(r) = I\cos\frac{\pi r}{2l}, \qquad V(r) = V\sin\frac{\pi r}{2l}. \quad (52)$$

Substituting in (51), we obtain

$$\frac{16l^2}{\lambda^2} = \frac{1-\chi}{1+\chi} = \frac{1+\bar{\chi}}{1-\bar{\chi}}, \quad (53)$$

where

$$\chi = \frac{\int_0^l L\cos\frac{\pi r}{l}dr}{\int_0^l Ldr}, \qquad \bar{\chi} = \frac{\int_0^l C\cos\frac{\pi r}{l}dr}{\int_0^l Cdr}. \quad (54)$$

Similarly, for the first resonance with both ends open, $I(r)=I\sin(\pi r/l)$ and

$$\frac{4l^2}{\lambda^2} = \frac{1+\xi}{1-\xi} = \frac{1-\bar{\xi}}{1+\bar{\xi}},$$

$$\xi = \frac{\int_0^l L\cos\frac{2\pi r}{l}dr}{\int_0^l Ldr}, \qquad \bar{\xi} = \frac{\int_0^l C\cos\frac{2\pi r}{l}dr}{\int_0^l Cdr}. \quad (55)$$

For the first resonance with both ends short-circuited, we have

$$\frac{4l^2}{\lambda^2} = \frac{1-\xi}{1+\xi} = \frac{1+\bar{\xi}}{1-\bar{\xi}}. \quad (56)$$

It will be observed from (39) and (42) that $L$ is directly proportional and $C$ inversely proportional to $K(r,\rho)$. Evidently, the approximations corresponding to $\chi$ and $\xi$ on the one hand and to $\bar{\chi}$ and $\bar{\xi}$ on the other are not necessarily the same. In fact, in some extreme cases in which either $L$ or $C$ become infinite at one end too rapidly, one of the above formulas becomes entirely useless. For example, in a cylindrical cavity[35] for cylindrical waves $C$ is directly proportional and $L$ inversely proportional to the distance $r$ from the axis.

[35] A section of a circular cylinder between two parallel planes.

For the principal resonance with voltage maximum at $r=0$ and 0 voltage at $r=l$, we have

$$\frac{16l^2}{\lambda^2}=\frac{1+\chi}{1-\chi}=\frac{1-\bar{\chi}}{1+\bar{\chi}}, \tag{57}$$

where $\chi$ and $\bar{\chi}$ are given by (54). The first formula is useless but the second gives

$$\frac{16l^2}{\lambda^2}=\frac{1+\frac{4}{\pi^2}}{1-\frac{4}{\pi^2}}=2.35,\quad \frac{4l}{\lambda}=1.53,\quad \frac{2\pi l}{\lambda}=2.41. \tag{58}$$

The value of $2\pi l/\lambda$ as given by the exact theory should be the first root of $J_0(x)=0$; this root is $2.40\cdots$.

In connection with antenna problems $L$ becomes infinite in the approximate equations (39) but not rapidly enough to cause any trouble. Using these equations we obtain the following results for wires enclosed within fictitious "reflecting" spheres, with their centers at mid-points of the wires and with their surfaces passing through the ends of the wires.

*For cylindrical wires*

$$\chi=-\frac{\mathrm{Si}\,\pi}{\pi\left(\log\frac{2l}{a}-1\right)}=-\frac{120\,\mathrm{Si}\,\pi}{\pi K_a}=-\frac{70.74}{K_a},$$

$$\xi=-\frac{\mathrm{Si}\,2\pi}{2\pi\left(\log\frac{2l}{a}-1\right)}=-\frac{27.08}{K_a}. \tag{59}$$

*For thin spheroidal wires*

$$\chi=-\frac{\mathrm{Si}\,\pi+0.5\,\mathrm{Si}\,2\pi}{\pi\log\frac{l}{a}}=-\frac{120(\mathrm{Si}\,\pi+0.5\,\mathrm{Si}\,2\pi)}{\pi K_a}=-\frac{97.82}{K_a},$$

$$\xi=-\frac{\mathrm{Si}\,2\pi-0.5\,\mathrm{Si}\,4\pi}{2\pi\log\frac{l}{a}}=-\frac{12.84}{K_a}. \tag{60}$$

*For wires with diamond-shaped longitudinal cross section*

$$\chi=-\frac{\mathrm{Si}\,\pi}{\pi\log\frac{2l}{a}}=-\frac{70.74}{K_a},$$

$$\xi=\frac{\mathrm{Si}\,\pi-0.5\,\mathrm{Si}\,2\pi}{\pi\log\frac{2l}{a}}=\frac{43.66}{K_a}. \tag{61}$$

*Resonance in Very Thin Conical Antennas*

We are now ready to consider the relations between lengths of antennas of various sizes and shapes and resonant wavelengths, under the condition that $K$ is very large. Subsequently, we shall obtain approximate expressions for the input impedance of nonuniform antennas from which resonant lengths can be computed for antennas with moderate characteristic impedances.

In conical antennas $L$ and $C$ are distributed uniformly and the resonant wavelength is affected only by the end reactance. In so far as the first power of $1/K$ is concerned this effect is given by (30) which becomes

$$\frac{4l}{\lambda}=1-\frac{2F\left(\frac{\pi}{2}\right)}{\pi K}=1-\frac{120\,\mathrm{Si}\,\pi+60\,\mathrm{Si}\,2\pi}{\pi K}=1-\frac{97.82}{K}$$

$$\frac{2l}{\lambda}=1-\frac{F(\pi)}{\pi K}=1-\frac{60\,\mathrm{Si}\,2\pi-30\,\mathrm{Si}\,4\pi}{\pi K}=1-\frac{12.84}{K}, \tag{62}$$

for the first and the second resonances, respectively.

*Resonance in Very Thin Spheroidal Antennas*

In spheroidal antennas we have to consider two effects: The end reactance and the nonuniform distribution of $L$ and $C$. Ultimately, as $K$ increases indefinitely, the two effects become additive. Thus for the first resonant wavelength, we have

$$\frac{4l}{\lambda}=1-\frac{2F\left(\frac{\pi}{2}\right)}{\pi K_a}-\chi=1. \tag{63}$$

Hence, in thin spheroidal antennas the deviation of the resonant length $2l$ from $\lambda/2$ is proportional at least to the square of $1/K$. This result agrees with Abraham's formula which, when expressed in terms of $K_a$, is

$$\frac{4l}{\lambda}=1-\frac{5040}{(K_a+83)^2}. \tag{64}$$

For the second resonance we have

$$\frac{2l}{\lambda}=1-\frac{F(\pi)}{\pi K_a}+\xi=1-\frac{2F(\pi)}{\pi K_a}=1-\frac{25.68}{K_a}. \tag{65}$$

*Resonance in Very Thin Cylindrical Antennas*

Similarly at the first resonance in cylindrical antennas, we have

$$\frac{4l}{\lambda}=1-\frac{2F\left(\frac{\pi}{2}\right)}{\pi K_a}-\chi=1-\frac{60\,\mathrm{Si}\,2\pi}{\pi K_a}=1-\frac{27.08}{K_a}. \tag{66}$$

At the second resonance we shall have

$$\frac{2l}{\lambda}=1-\frac{F(\pi)}{\pi K_a}+\xi=1-\frac{120\,\mathrm{Si}\,2\pi-30\,\mathrm{Si}\,4\pi}{\pi K_a}=1-\frac{39.92}{K_a}. \tag{67}$$

*Resonance in Very Thin Antennas with "Diamond-Shaped" Longitudinal Cross Sections*

For these antennas we have

$$\frac{4l}{\lambda}=1-\frac{60\,\mathrm{Si}\,2\pi}{\pi K_a}=1-\frac{27.08}{\pi K_a},$$

$$\frac{2l}{\lambda}=1+\frac{120\,\mathrm{Si}\,\pi-120\,\mathrm{Si}\,2\pi+30\,\mathrm{Si}\,4\pi}{\pi K_a}=1+\frac{30.82}{K_a}, \quad (68)$$

for the first and second resonances, respectively.

*Resonant Conditions Depend on the Shape of the Longitudinal Cross Section of the Antenna as Well as on the Size of the Transverse Cross Section*

In its effect on the resonant length the average characteristic impedance $K_a$ represents the "average size" of the cross section of the antenna. Since $K_a$ depends on the logarithm of some mean radius, the resonant length varies rather slowly with the size of the cross section of the antenna.

The second factor is the *shape* of the longitudinal cross section. Page and Adams have supposed that a cylindrical wire is equivalent to a somewhat fatter and somewhat longer spheroid. On geometric grounds this appears reasonable; but our computations do not support the assumption. For a very thin cylindrical wire the "equivalent spheroid" would have to be very fat in comparison. In fact, if we let the radius of the cylinder approach zero, then the ratio of the base radius of the equivalent spheroid to the radius of the cylindrical wire will approach infinity.

*The Input Impedance of Antennas with Variable Characteristic Impedance*

We have already stated that in the first approximation a nonuniform line may be regarded as a uniform line with a characteristic impedance equal to the average characteristic impedance. The goodness of this approximation depends on the relative deviation of $K(r, \rho)$ from $K_a$. Even when these deviations are small for sections only a few wavelengths long, they will be prohibitively large for really long sections. For example, the average characteristic impedance of an infinitely long cylindrical wire is infinite; but the input impedance of a cylindrical wire extending to infinity on both sides of a generator is certainly not infinite. As a matter of fact (see footnote 20), for thin wires this input impedance is approximately[36]

$$K(0) = 120 \log \frac{\lambda}{2a} - 207. \quad (69)$$

This impedance is represented by curve a in Fig. 21. Curve b is a plot of a more accurate equation (165). Fig. 22 is a plot of $K(0)$ over a wider range of radii.

[36] There is a reactance in shunt with the resistance (69); this reactance depends on the length of the segment over which the electromotive force is applied, and has little effect on the total impedance unless the segment is very short. Theoretically, the terminals of the generator could be brought so close together as to short-circuit it; but, in practice, this is not done.

In practice, however, antennas are never very long and we can treat them as transmission lines with slightly variable characteristic impedances. One solution for such lines, based on Picard's method of integrating differential equations, has been obtained by Carson.[6] Adapting his solution to our problem and retaining only the first order of correction terms, we obtain the following expression for the input impedance:

$$Z_i = K_a \frac{G \sin L + i[(F-N)\sin L - (K_a - M)\cos L]}{[(K_a+M)\sin L + (F+N)\cos L] - iG\cos L}; \quad (70)$$

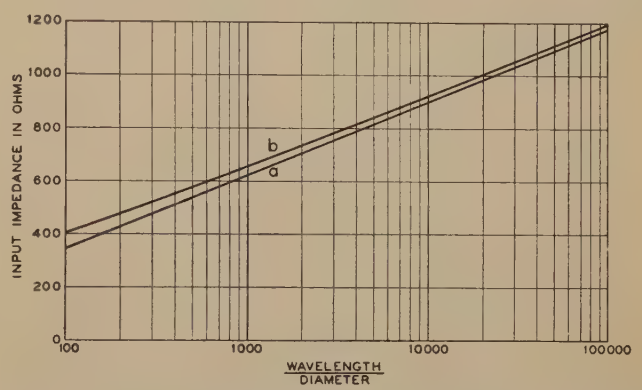


Fig. 21—The input impedance of an infinitely long cylindrical wire. Curve (a) is a plot of equation (69); curve (b) is a plot of the more accurate equation (165).

where $M$ and $N$ functions are defined by

$$M(L) = \beta \int_0^l [K_a - K(r, \rho)] \sin 2\beta r \, dr,$$

$$N(L) = \beta \int_0^l [K_a - K(r, \rho)] \cos 2\beta r \, dr. \quad (71)$$

The real and imaginary parts of the input impedance are

$$R_i = \frac{K_a G(K_a + N \sin 2L - M \cos 2L)}{G^2 \cos^2 L + [(K_a + M)\sin L + (F + N)\cos L]^2}$$

$$X_i = \frac{K_a[\tfrac{1}{2}(G^2 + F^2 + M^2 - N^2 - K_a^2)\sin 2L + (MN - K_aF)\cos 2L + (MF - K_aN)]}{G^2 \cos^2 L + [(K_a + M)\sin L + (F + N)\cos L]^2}. \quad (72)$$

For *cylindrical antennas* $M$ and $N$ functions become

$$M(L) = 60(\log 2L - \mathrm{Ci}\,2L + C - 1 + \cos 2L),$$
$$N(L) = 60(\mathrm{Si}\,2L - \sin 2L). \quad (73)$$

For antennas in free space, with a *rhombic* longitudinal cross section, or for vertical antennas of triangular shape[37] of base radius $a$, above a perfectly conducting ground, we have

$$M(L) = 60(C + \log 2L - \mathrm{Ci}\,2L)(1 - \cos 2L) - 60\,\mathrm{Si}\,2L \sin 2L,$$
$$N(L) = 60\,\mathrm{Si}\,2L - 60(C + \log 2L - \mathrm{Ci}\,2L)\sin 2L,$$
$$K_a = 120 \log \frac{2l}{a}. \quad (74)$$

[37] Inverted conical antennas.

For spheroidal antennas we obtain

$$M(L)=60(C+\log L-\mathrm{Ci}\,2L)+30(\mathrm{Si}\,4L-2\,\mathrm{Si}\,2L)\sin 2L$$
$$+30(C+\log 2L-2\,\mathrm{Ci}\,2L+\mathrm{Ci}\,4L-1)\cos 2L,$$
$$N(L)=60\,\mathrm{Si}\,2L+30(\mathrm{Ci}\,4L-\log L-C-2\log 2)\sin 2L$$
$$-30\,\mathrm{Si}\,4L\cos 2L;$$
$$M(L)=G(L)-60\log 2-30(1-\log 2)\cos 2L,$$
$$N(L)=F(L)-60\log 2\sin 2L. \qquad (75)$$

Diamond-shaped antennas can be treated more accurately if we take cognizance of the fact that the first

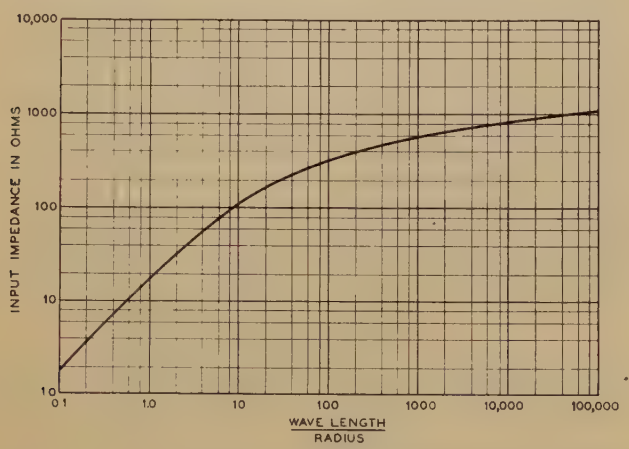


Fig. 22—The input impedance of the infinitely long cylindrical wire. For $0.1<\lambda/2a\leqq 3$, this curve has been computed by numerical integration from (164); for $\lambda/2a\geqq 500$, the curve has been computed from the approximate equation (165); then, the two curves have been freely joined together.

half of the antenna has a uniform characteristic impedance and the second half, nonuniform. Thus we may obtain the input impedance into the second half from

$$Z_i = K_a\frac{G\sin\frac{L}{2}+i\left[(F-N)\sin\frac{L}{2}-(K_a-M)\cos\frac{L}{2}\right]}{\left[(K_a+M)\sin\frac{L}{2}+(F+N)\cos\frac{L}{2}\right]-iG\cos\frac{L}{2}} \qquad (76)$$

and, then, compute the input impedance into the first half using (76) as its terminating impedance. The functions $M$ and $N$ to be used in (76) are[38]

$$M(L) = 60\log 2+60(C+\log L-\mathrm{Ci}\,2L)\cos L$$
$$-60\,\mathrm{Si}\,2L\sin L,$$
$$N(L) = 60(\mathrm{Si}\,2L-2\,\mathrm{Si}\,L)\cos L$$
$$-60(C+\log L+\mathrm{Ci}\,2L-2\,\mathrm{Ci}\,L)\sin L,$$
$$K_a = 120\log\frac{2l}{a}\cdot \qquad (77)$$

*Input Impedance Curves for Cylindrical Antennas*

In Figs. 23 and 24 the input resistance and the reactance of cylindrical antennas in free space are shown as functions of $l/\lambda$ for different values of $K$. In Fig. 25 we have the input resistance at resonance ($X_i=0$) in the vicinity of $l=\lambda/4$. Fig. 26 shows the resonant impedance in the vicinity of $l=\lambda/2$. The points (except the first) are values obtained experimentally by Feldman[39] for $\lambda=9$ meters. The first point is the value obtained by Morrison and Smith[32] for the square tower.

Resonant lengths of cylindrical antennas are short of $\lambda/2$ and $\lambda$ by the percentages shown in Fig. 27;

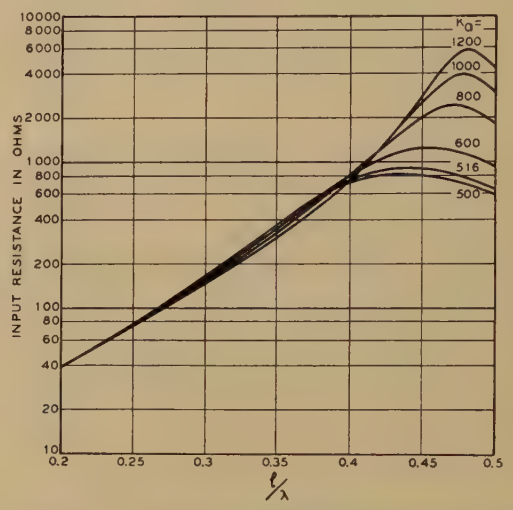


Fig. 23—The input resistance of cylindrical antennas in free space. For vertical antennas over a perfectly conducting ground divide the ordinates and $K_a$ by 2.

curve 1 is for the principal resonance and curve 2 for the second resonance. The points above curve 1 have been taken from Englund,[16] those above curve 2 have been supplied by Feldman with one exception, the first point comes from the paper by Morrison and Smith.

In this latter case, it is known that the base insulator is responsible for about 30 micromicrofarads in shunt with the antenna; this capacitance is more than sufficient to account for the difference of $2\frac{1}{2}$ per cent between the measured and computed values. On the other hand, the tower is tapered near the base and consequently has less capacitance than it would have had if it were not tapered; we feel confident that if all these factors are taken into consideration the discrepancy between the theory and experiment would be quite

[38] In (76) $G$, $F$, $M$, and $N$ are functions of $L$, as indicated by the first term in the numerator, while the argument of the sines and cosines is $L/2$.

[39] Feldman's measurements were made for vertical wires of different sizes; we have doubled his results to obtain the values corresponding to the free-space condition.

small. Hence, it is unnecessary to postulate the existence of a lumped series inductance of 6.8 microhenrys and a lumped shunt capacitance of 200 micromicrofarads at the base of the antenna in order to explain the measurements. These values were assumed, but not accounted for, by Morrison and Smith in order to bring their measurements into agreement with formulas from Siegel and Labus.

We now believe that the antenna theory is in such a state that accurate results can be calculated if all "visible" factors, such as base capacitances and antenna shapes are taken into consideration. The imperfect conductivity of the ground does not appear to affect the results.

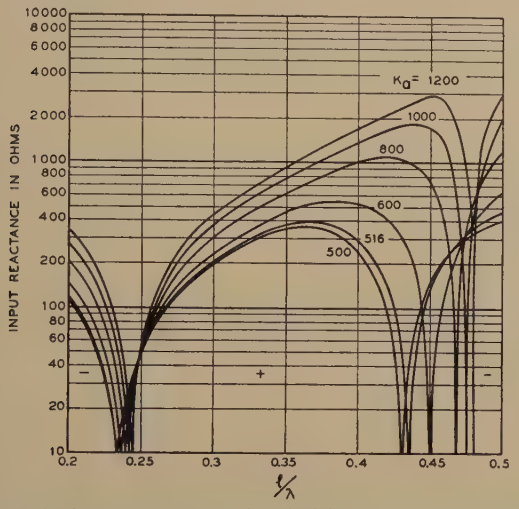


Fig. 24—The input reactance of cylindrical antennas in free space. For vertical antennas over a perfectly conducting ground divide the ordinates $K_a$ by 2.

For some unexplained reason the impedance curves for cylindrical antennas published by King are considerably in error in some regions. Thus, when $\log 2l/a=10.58$ so that $K_a=1150$, King obtains[40] $R_{max}=16{,}000$ and $X_{max}=9000$; our values are $R_{max}=5500$ and $X_{max}=3000$. Available measurements of $R_{max}$ support our results (Fig. 26).

*The Input Impedance for $l=\lambda/4$ and $l=\lambda/2$*

When $l=\lambda/4$ and $=\lambda/2$, we have, respectively,

$$Z_i=\frac{K_a}{K_a+M\left(\frac{\pi}{2}\right)}\left[G\left(\frac{\pi}{2}\right)+iF\left(\frac{\pi}{2}\right)-iN\left(\frac{\pi}{2}\right)\right]$$

$$Z_i=\frac{K_a[K_a-M(\pi)]}{G^2+(F+N)^2}\,[G(\pi)-iF(\pi)-iN(\pi)]. \qquad (78)$$

The quantity $G(\pi/2)=73.13$ is the input resistance of a half-wave antenna for $K_a=\infty$, that is, for an infinitely thin wire. For any finite value of $K_a$, the input resistance depends also on $M(\pi/2)$, that is, on the shape of the longitudinal cross section of the antenna.

[40] King's values have been doubled to obtain the free-space figures.

For example, for cylindrical and spheroidal antennas $M(\pi/2)$ is equal, respectively, to $-21$ and 41. Hence, when $l=\lambda/4$, the input resistance of cylindrical antennas is somewhat higher than 73.13 and the input resistance of spheroidal antennas is somewhat lower than 73.13.

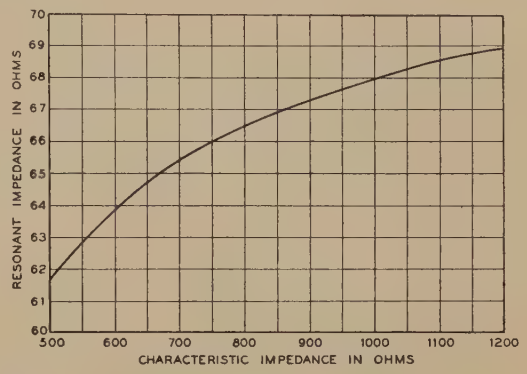


Fig. 25—The resonant impedance of cylindrical antennas as a function of $K$, when $l$ is in the vicinity of $\lambda/4$.

When $l=\lambda/4$ and $K_a=\infty$, the input reactance of cylindrical antennas is $30\,\mathrm{Si}\,2\pi=42.5$ and that of spheroidal antennas is 0. For cylindrical antennas with finite characteristic impedances the input reactance is somewhat higher than 42.5 and for spheroidal antennas it is still zero. These results do not include terms depending on $1/K_a$. From Abraham's expression for the resonant frequencies and from (70), we find that the approximate value of the input reactance of thin spheroidal antennas, when $l=\lambda/4$, is $7900(K_a-41)/(K_a+83)^2$.

*Bent Antennas*

Our method of antenna analysis is applicable to bent antennas (Fig. 28). From the theory of principal waves guided by thin diverging conical wires[21] we observe

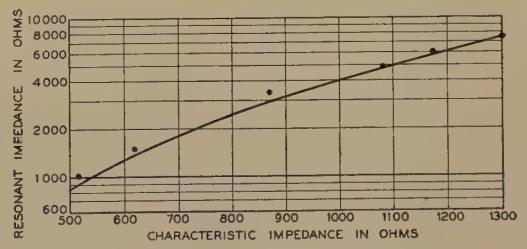


Fig. 26—The resonant impedance of cylindrical antennas is a function of $K$, when $l$ is in the vicinity of $\lambda/2$.

that the capacitance between two elements at $A$ and $A'$ depends only on the distance between them and on their radii. For equal radii, we shall have then

$$K(x,\,a)=120\log\frac{d(x)}{a}\,. \qquad (79)$$

For unequal radii, $a$ is the geometric mean of the actual radii.

From (79) we can obtain the average characteristic impedance; then from (71) we compute $M$ and $N$ functions which are needed to correct transmission equations

of the principal waves for the nonuniform distribution of the inductance and capacitance. The function $G(L)$ is obtained from (25): First we compute the radiated power on the assumption that $a=0$ and that the current distribution is sinusoidal with current nodes at the open ends of the antenna; then, we divide this power by $\frac{1}{2}$ of the square of the current amplitude. This calculation can be carried out by either of two methods: (1) The Poynting flux method and (2) the produced-electromotive-force method. Only the second of these methods can be used for calculating $F(L)$; moreover, in this calculation $a$ must be assumed not

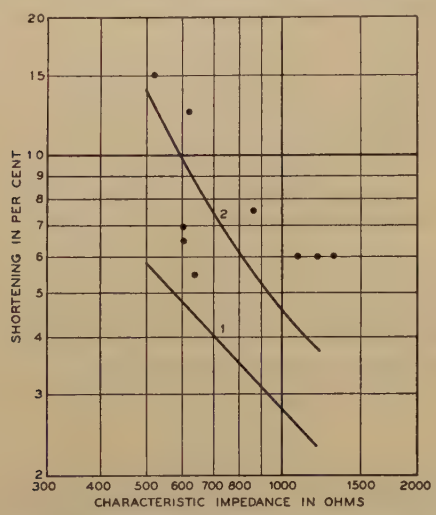


Fig. 27—The resonant length of cylindrical antennas in free space. Curve 1 is for the principal resonance. Curve 2 is for the second resonance. The ordinates represent the required shortening in per cent.

merely infinitely small but also varying with $x$ in such a way that $d(x)/a$ remains constant.

When these functions have been computed, the input impedance is obtained from (70).

*Loop Antennas*

If an antenna is bent into a complete loop and the ends are joined together, the procedure for calculating $G$ and $F$ functions is the same as that outlined above except that the sinusoidal current distribution must be chosen to have an antinode instead of a node at the far end of the antenna. Naturally, $M$ and $N$ functions are not affected by the conditions at the far end.

*Current Distribution*

In order to find the current distribution in nonuniform antennas we should calculate the principal current distribution from Carson's equations,[6] assuming that the transmission line is terminated by the output radiation impedance as given in this paper, and superimpose on it the secondary current distribution. The latter can be obtained from (11) and (36).

Knowledge of current distribution is needed largely in computing radiation patterns, and these are affected by the ground conditions to a much greater extent than by the changes in the current distribution. It is doubtful, therefore, that the labor expended in calculating current distributions, light as it is, would be commensurate with the practical value of the results. However, the current distribution can be measured and, hence, used for checking the theory.

## V. Antennas with Uniform Characteristic Impedances: Mathematical Analysis

A set of equations for transverse magnetic spherical waves and its general discussion may be found in previous papers.[21,41] This set will now be developed to suit the needs of our particular problem. In the first place we shall assume that $\partial/\partial\phi=0$. It may appear that this assumption will restrict the analysis to coaxial cones; in reality, however, the solutions of the restricted equations can be used for the more general case of two conical wires inclined to each other.

Thus, if $\partial/\partial\phi=0$ our fundamental equations become

$$rE_\theta = -\frac{\partial V}{\partial\theta}, \qquad i\omega\epsilon r^2 E_r = n(n+1)A,$$

$$rH_\phi = -\frac{\partial A}{\partial\theta}, \qquad V = -\frac{1}{i\omega\epsilon}\frac{\partial A}{\partial r} \tag{80}$$

where $n$ is a constant depending upon the boundary conditions at the surface of the antenna and the "flux function" $A$ is

$$A^+ = \sqrt{\beta r}\,[J_{n+1/2}(\beta r) - iN_{n+1/2}(\beta r)]T(\theta),$$
$$A^- = \sqrt{\beta r}\,J_{n+1/2}(\beta r)T(\theta). \tag{81}$$

The function $A^+$ defines the outward-bound progressive wave while $A^-$ the standing wave finite at the

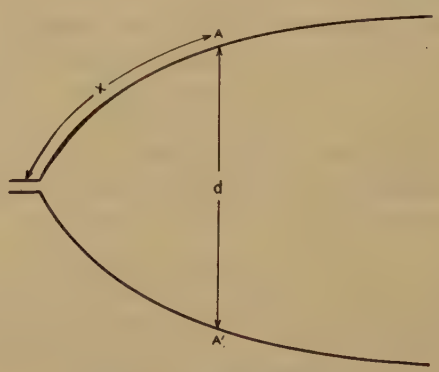


Fig. 28—A bent antenna.

origin $r=0$. The function $V(r,\theta)$ is the "potential" defined as the line integral of $E_\theta$ along any path beginning on some fixed radius $\theta=\theta'$ and contained entirely in the co-ordinate sphere of radius $r$. The function $T(\theta)$ is a solution of Legendre's equation

$$T(\theta) = pP_n(-\cos\theta) + qP_n(\cos\theta), \quad \text{if} \quad n \neq 0,$$
$$= p\log\cot\frac{\theta}{2}, \quad \text{if} \quad n=0. \tag{82}$$

[41] W. L. Barrow, L. W. Chu, and J. J. Jansen, "Biconical electromagnetic horns," Proc. I.R.E., vol. 27, pp. 769–779; December, 1939.

The function $P_n(x)$ is so defined that

$$P_n(1) = 1. \tag{83}$$

If $n$ is not an integer, $P_n(x)$ has a logarithmic singularity at $x=-1$. If $n$ is an integer, $P_n(-x)=(-)^nP_n(x)$ and (82) is not the most general solution of Legendre's equation. There is a second solution $Q_n(x)$ which is singular at two points $x=\pm 1$.

The boundary conditions are: the electric intensity $E_r$ must vanish at the surface of the antenna and the field must be finite. If the conical conductors are of finite length, the entire space must be divided by co-ordinate spheres into regions: (1) free from conductors, (2) containing only one conductor, and (3) containing two conductors.

In the region free from conductors $n$ must necessarily be an integer because for nonintegral values of $n$ Legendre's equation possesses no solutions finite for all values of $\theta$. The function $Q_n(\cos\theta)$ being singular at $\theta=0, \pi$ is also out of the picture. Thus in such regions the complete solution is a series of functions $P_n(\cos\theta)$ corresponding to different integral values of $n$.

In the region containing only one cone with its axis along $\theta=0$, the coefficient $q$ in (82) must vanish because $P_n(\cos\theta)$ is infinite where $\theta=\pi$. Thus (82) becomes

$$T(\theta) = pP_n(-\cos\theta). \tag{84}$$

The singularity of this function at $\theta=0$ is, of course, excluded by the conductor. If $\psi$ is the angle made by the generators of the conical conductor with the axis, then $E_r$ will vanish on the conductor if

$$P_n(-\cos\psi) = 0. \tag{85}$$

This is the equation for the constant $n$.

In the region containing two conductors, one with its axis along $\theta=0$ and the other along $\theta=\pi$, we must have $T(\psi_1)=T(\pi-\psi_2)=0$ and therefore

$$\begin{aligned} pP_n(-\cos\psi_1) + qP_n(\cos\psi_1) &= 0, \\ pP_n(\cos\psi_2) + qP_n(-\cos\psi_2) &= 0. \end{aligned} \tag{86}$$

Eliminating $p$ and $q$, we have the equation for $n$,

$$\frac{P_n(-\cos\psi_1)}{P_n(\cos\psi_2)} = \frac{P_n(\cos\psi_1)}{P_n(-\cos\psi_2)}. \tag{87}$$

If the cone angles $\psi_1$ and $\psi_2$ are small their cosines are nearly equal to unity, $P_n(\cos\psi_1)\doteq P_n(\cos\psi_2)\doteq 1$ and (87) becomes approximately

$$P_n(-\cos\psi_1)P_n(-\cos\psi_2) = 1. \tag{88}$$

If the cones are equal $\psi_1=\psi_2=\psi$ then

$$P_n(-\cos\psi) = \pm P_n(\cos\psi), \quad \text{and} \quad p = \mp q. \tag{89}$$

For small values of $\psi$, this becomes

$$P_n(-\cos\psi) = \pm 1. \tag{90}$$

If the two cones are inclined toward each other and if their angles $\psi_1$ and $\psi_2$ are so small that the "proximity effect" is negligible, we can express the total field as the resultant of two fields, associated with the individual cones, and the function that must vanish on the boundaries becomes

$$T(\theta_1,\theta_2) = pP_n(-\cos\theta_1) + qP_n(-\cos\theta_2), \tag{91}$$

where $\theta_1$ and $\theta_2$ are the angles made by typical radius with the axes of the conductors. If the angle between the axes is $\zeta$, we have approximately

$$\begin{aligned} pP_n(-\cos\psi_1) + qP_n(-\cos\zeta) &= 0, \\ pP_n(-\cos\zeta) + qP_n(-\cos\psi_2) &= 0. \end{aligned} \tag{92}$$

The equation for $n$ will then become

$$P_n(-\cos\psi_1)P_n(-\cos\psi_2) = [P_n(-\cos\zeta)]^2. \tag{93}$$

For equal cones, we have

$$P_n(-\cos\psi) = \pm P_n(-\cos\zeta), \quad p = \mp q. \tag{94}$$

Inasmuch as with reference to a single co-ordinate system $T(\theta_1,\theta_2)$ is a function of two spherical co-ordinates $\theta$ and $\phi$ the field, if wanted, must be computed from the general equations[21] and not from (80).

The boundary condition $E_r=0$ on the surface of the antenna will also be satisfied (see (80)) if $E_r$ vanishes *everywhere;* this happens when $n=0$. In this case the nontrivial solution is singular for two values of $\theta$ so that the wave can exist only in the presence of two conductors excluding the corresponding radii from the field. This is the so-called "principal" wave and its properties have already been discussed in detail.[21]

In the region containing two conductors, the transverse voltage $V_n(r)$ between the conductors, corresponding to any transmission mode except the principal, vanishes,

$$V(r) = 0. \tag{95}$$

This is true because $V(r)$ is the difference between the values of $V(r,\theta)$ on the two conductors and these values, being proportional to $T(\theta)$, vanish with $T(\theta)$; and it is only for the principal wave that $T(\theta)$ does not vanish on the conductors. Hence, the total transverse voltage $V(r)$ between two conductors depends entirely on the principal wave.

Let $I'_n(r)$ be the electric current in the upper cone of the double cone and $I''_n(r)$ the corresponding current in the lower cone (Fig. 5). Assuming that the upward direction is positive, we have

$$\begin{aligned} I_n'(r) &= 2\pi r\sin\psi H_\phi(r,\psi) = -2\pi\sin\psi\frac{\partial A}{\partial\psi}, \\ I_n''(r) &= 2\pi r\sin\psi H_\phi(r,\pi-\psi) = 2\pi\sin\psi\left.\frac{\partial A}{\partial\theta}\right|_{\theta=\pi-\psi}. \end{aligned} \tag{96}$$

For all values of $n>0$ the function $\sqrt{x}N_{n+\frac{1}{2}}(x)$ is

infinite at $x=0$; therefore, the proper expression for $A$ is $A^-$ (see (81)) and

$$I_n'(r) = -2\pi\sqrt{\beta r}\,J_{n+1/2}(\beta r)\sin\psi\frac{\partial}{\partial\psi}T(\psi),$$

$$I_n''(r) = 2\pi\sqrt{\beta r}\,J_{n+1/2}(\beta r)\sin\psi\frac{\partial}{\partial\psi}T(\pi-\psi). \quad (97)$$

Since for $n>0$, the function $\sqrt{x}J_{n+\frac{1}{2}}(x)$ vanishes at $x=0$, we have

$$I_n'(0) = I_n''(0) = 0. \quad (98)$$

At the apex the electric current is determined solely by the principal wave.

Thus, we have justified equations (10) and the equivalent circuit for double cones of equal length that follows from these equations. It was shown there that the first approximation for the output impedance (19) can be obtained in the form (26) by a method quite different from the present and yielding the results in their simplest form. On the other hand, the present method permits the use of successive approximations and is quite general. For this reason, we are justified in developing it still further.

In the case of a double cone (Fig. 5) different transmission modes are determined by the roots of (89) or, for small cone angles $\psi$, by (90). The latter equation is a very good approximation even if $\psi$ is as large as 0.1 since $\cos\psi=1-\frac{1}{2}\psi^2$ will differ from unity by less than 1 per cent and $P_n(1)=1$. From the theory of Legendre's functions, we have

$$P_n(-\cos\theta)=\frac{\sin n\pi}{\pi}\sum_{\alpha=0}^{\infty}\frac{(-)^\alpha\Gamma(n+\alpha+1)}{\Gamma(n-\alpha+1)}\left[2\log\sin\frac{\theta}{2}+\psi(n+\alpha)+\psi(-n+\alpha-1)-2\psi(\alpha)\right]\frac{\sin^{2\alpha}\frac{\theta}{2}}{\alpha!\alpha!}, \quad (99)$$

where

$$\psi(x)=\frac{\Gamma'(x+1)}{\Gamma(x+1)},\ \psi(-x-1)=\psi(x)+\pi\cot\pi x. \quad (100)$$

For small values of $\psi$ the term corresponding to $\alpha=0$ is dominant and we have approximately

$$P_n(-\cos\theta)=\frac{2}{\pi}\sin n\pi\left[\log\frac{\theta}{2}+\psi(n)-\psi(0)\right]+\cos n\pi. \quad (101)$$

Hence, the equation

$$P_n(-\cos\psi)=1 \quad (102)$$

becomes

$$\tan\frac{n\pi}{2}=-\frac{2}{\pi}\left[\log\frac{2}{\psi}+\psi(0)-\psi(n)\right]=-\frac{2}{\pi}\left[\frac{K}{120}+\psi(0)-\psi(n)\right], \quad (103)$$

where $K$ is the characteristic impedance to the principal waves.[21]

Similarly, the equation

$$P_n(-\cos\psi)=-1 \quad (104)$$

becomes

$$\cos\frac{n\pi}{2}=\frac{2}{\pi}\left[\frac{K}{120}+\psi(0)-\psi(n)\right]. \quad (105)$$

As the characteristic impedance $K$ increases indefinitely, the roots of (103) approach

$$n=2m+1+\frac{120}{K},\quad m=0,1,2,\cdots. \quad (106)$$

Likewise, the roots of (105) approach

$$n=2m+\frac{120}{K},\quad m=0,1,2,\cdots. \quad (107)$$

The roots of the characteristic equation (85) for a single cone approach

$$n=m+\frac{60}{K},\quad m=0,1,2,\cdots. \quad (108)$$

When $n$ is a root of (102) then by virtue of (89) the corresponding field function $T(\theta)$ is proportional to

$$L_{2m+1}(\theta)=\tfrac{1}{2}[P_{2m+1+\Delta}(\cos\theta)-P_{2m+1+\Delta}(-\cos\theta)], \quad (109)$$

where

$$\Delta=\frac{120}{K}. \quad (110)$$

The derivatives of the $L$ functions at $\theta=\psi$ and $\theta=\pi-\psi$ are approximately

$$\frac{dL(\psi)}{d\psi}=-\frac{dL(\pi-\psi)}{d\psi}=\frac{\sin\pi\Delta}{\pi\psi}=\frac{\Delta}{\psi}=\frac{120}{K\psi}. \quad (111)$$

Hence, the electric currents in the antenna, associated with these waves are nearly inversely proportional to the characteristic impedance and they flow in the same direction at points equidistant from 0.

When $n$ is a root of (104), the field function $T(\theta)$ is proportional to

$$L_{2m}(\theta)=\tfrac{1}{2}[P_{2m+\Delta}(\cos\theta)+P_{2m+\Delta}(-\cos\theta)]. \quad (112)$$

In this case

$$\frac{dL_{2m}(\psi)}{d\psi}=\frac{dL(\pi-\psi)}{d\psi}=\frac{\sin\pi\Delta}{\pi\psi}=\frac{120}{K\psi}, \quad (113)$$

and the electric currents at points equidistant from 0 are in opposite directions

For small values of $\Delta$, we have approximately

$$P_{n+\Delta}(\cos\theta)=P_n(\cos\theta)+2\Delta\left[P_n(\cos\theta)\log\cos\frac{\theta}{2}+S_n'\right]$$

$$P_{n+\Delta}(-\cos\theta)=(-)^nP_n(\cos\theta)$$
$$+2\Delta\left[(-)^nP_n(\cos\theta)\log\sin\frac{\theta}{2}+S_n''\right],$$
$$S_n'=\sum_{\alpha=1}^{n}\frac{(-)^\alpha(n+\alpha)!}{\alpha!\alpha!(n-\alpha)!}\left(\frac{1}{n+\alpha}+\frac{1}{n+\alpha-1}+\cdots+\frac{1}{n+1}\right)\sin^{2\alpha}\frac{\theta}{2},$$
$$S_n''=\sum_{\alpha=1}^{n}\frac{(-)^\alpha(n+\alpha)!}{\alpha!\alpha!(n-\alpha)!}\left(\frac{1}{n+\alpha}+\frac{1}{n+\alpha-1}+\cdots+\frac{1}{n+1}\right)\cos^{2\alpha}\frac{\theta}{2}. \quad (114)$$

Also, $\Delta\to 0$, we have

$$L_n(\theta)\to P_n(\cos\theta). \quad (115)$$

Thus, the characteristic functions for the region containing two cones approach the characteristic functions for free space except that free space cannot support the principal wave.

This property may be used for obtaining the second approximation to the solution of the antenna problem. We shall write general solutions appropriate to the free space, and to the "antenna region" within the sphere of radius $l$ (Fig. 5). The two solutions must satisfy certain continuity conditions at the boundary sphere and it is in this matching operation that (115) is useful.

In the antenna region we can write

$$2\pi i\omega\epsilon r^2E_r=\sum_n a_n\frac{\sqrt{\beta r}\,J_{n+1/2}(\beta r)}{\sqrt{\beta l}\,J_{n+1/2}(\beta l)}L_n(\theta),$$

$$\bar{I}(r)=2\pi r\sin\psi H_\phi$$
$$=-\sum_n\frac{a_n\sqrt{\beta r}\,J_{n+1/2}(\beta r)}{n(n+1)\sqrt{\beta l}\,J_{n+1/2}(\beta l)}\sin\psi\frac{d}{d\psi}L_n(\psi), \quad (116)$$

where $\bar{I}(r)$ is the total current in the upper cone, associated with all waves except the principal. We shall call this current *complementary*. The summation in (116) is extended over the roots of (89), excepting $n=0$.

In the free space we write

$$2\pi i\omega\epsilon r^2E_r$$
$$=\sum_{k=1}^{\infty}b_k\frac{\sqrt{\beta r}\,[J_{k+1/2}(\beta r)-iN_{k+1/2}(\beta r)]}{\sqrt{\beta l}\,[J_{k+1/2}(\beta l)-iN_{k+1/2}(\beta l)]}P_k(\cos\theta). \quad (117)$$

At $r=l$, $C$ must be continuous

$$\sum_n a_nL_n(\theta)=\sum_{k=1}^{\infty}b_kP_k(\cos\theta). \quad (118)$$

But as $K\to\infty$ and $\psi\to 0$, we have (115) and, therefore, in the limit the coefficients $a_n$ and $b_k$ must be correspondingly equal.

The coefficients $b_k$ can be easily determined for the limiting case $K=\infty$. In the first place $\bar{I}(r)\to 0$ as $K\to\infty$. This can be shown by substituting from (111) into (116) and obtaining

$$I(r)=-\frac{120}{K}\sum_n\frac{a_n\sqrt{\beta r}\,J_{n+1/2}(\beta r)}{n(n+1)\sqrt{\beta l}\,J_{n+1/2}(\beta l)}. \quad (119)$$

The only term which would not approach zero is the term corresponding to $m=0$ in (107). This term is entirely absent, however, in the symmetric case of Fig. 5. In the case of cones of unequal length this term would be present and we would exclude it from $\bar{I}(r)$ and consider it separately as the "*principal antisymmetric current wave.*" In either case, the conclusion is that *as* $K\to\infty$, *the current distribution in the antenna tends to become strictly sinusoidal.*

If the current distribution is known, the field can be determined by the retarded-potential method. For a sinusoidal distribution of amplitude $I_0$, with current nodes at the ends of the antenna, we have

$$C=2\pi r\sin\theta H_\phi$$
$$=-iI_0(e^{-i\beta r}\cos\beta l-\tfrac{1}{2}e^{-i\beta r_1}-\tfrac{1}{2}e^{-i\beta r_2}), \quad (120)$$

where $r_1$ and $r_2$ are distances from the upper and the lower ends of the antenna. At great distances from the antenna this becomes

$$C=iI_0[\cos(\beta l\cos\theta)-\cos\beta l]e^{-i\beta r}. \quad (121)$$

From Maxwell's equations we have

$$2\pi i\omega\epsilon r^2E_r=\frac{1}{\sin\theta}\frac{\partial C}{\partial\theta}=i\beta l\sin(\beta l\cos\theta)e^{-i\beta r}. \quad (122)$$

On the other hand, at great distances from the antenna (117) becomes

$$2\pi i\omega\epsilon r^2E_r=\sum_{k=1}^{\infty}\sqrt{\frac{2}{\pi}}\,i^{k+1}b_k(\beta l)^{-1/2}[J_{k+1/2}(\beta l)-iN_{k+1/2}(\beta l)]^{-1}P_k(\cos\theta)e^{-i\beta r}. \quad (123)$$

Hence, in order to find $b_k$ we only have to expand $\sin(\beta l\cos\theta)$ into a series of Legendre's functions. This expansion is known to be

$$\sin(\beta l\cos\theta)$$
$$=\sum_{m=0}^{\infty}(-)^m(4m+3)\sqrt{\frac{\pi}{2\beta l}}\,J_{2m+3/2}(\beta l)P_{2m+1}(\cos\theta). \quad (124)$$

Substituting in (122) and comparing the result with (123) we obtain

$$b_{2m+1}=-i(2M+\tfrac{3}{2})\pi LJ_{2m+3/2}(L)[J_{2m+3/2}(L)-iN_{2m+3/2}(L)]$$
$$b_{2m}=0, \qquad L=\beta l=\frac{2\pi l}{\lambda}. \quad (125)$$

Letting in (119) $a_n=b_{2m+1}$, we obtain the asymptotic value for the complementary current as given by (16) and (18).

The above matching of radial electric fields in the

two regions can be regarded as the second step in a sequence of successive approximations. If we were to compute $E_\theta$, we would discover that it is discontinuous at the boundary sphere $r=l$. By adding a proper expression to the external field, we can make $E_\theta$ continuous again and after matching $E_r$ for the second time we shall have a more accurate expression for the complementary current. In all these higher approximations we no longer can make the coefficients $a_n$ and $b_k$ equal but have to expand the functions to be matched in series of Legendre's functions, $L_n(\theta)$ or $P_n(\cos\theta)$ as the case may be.

These functions are orthogonal[42] and, therefore, the coefficients of expansions are expressed by definite integrals.

## VI. The "Induced-Electromotive-Force" Method of Computing Radiation and the Radiation Paradox

The "induced-electromotive-force" method[43] of computing radiation consists in obtaining the work done (and thus the energy contributed to the field) in driving given electric currents against the electric forces produced by them. This method furnishes not only the power lost by the source in radiation but also the average reactive power, that is, the average interchange of energy between the field and the generator.

For a linear current filament situated along the $z$ axis and extended from $z=-l$ to $z=l$, the complex power $\Psi$ is

$$\Psi = -\frac{1}{2}\int_{-l}^{l} E_z(z)I^*(z)dz, \tag{126}$$

where $E_z$ is the electric intensity parallel to the filament at the surface of the latter. If the filament consists of two perfectly conducting wires, one extending from $z=-l$ to $z=-s$ and the other from $z=s$ to $z=l$, and if the "generator" between $z=-s$ and $z=s$ consists of some means for transferring an electric charge from one wire to the other, then (126) becomes

$$\Psi = -\frac{1}{2}\int_{-s}^{s} E_z(z)I^*(z)dz \tag{127}$$

since $E_z=0$ on the surface of a perfect conductor.

Furthermore, if we assume that in the short interval $(-s, s)$ occupied by the source of energy the current $I(z)$ is equal to a constant $I$, (127) becomes

$$\Psi = -\frac{1}{2}I^*\int_{-s}^{s} E_z(z)dz. \tag{128}$$

Since "action equals reaction," we have

$$V + \int_{-s}^{s} E_z(z)dz = 0, \tag{129}$$

where $V$ is the "applied" electromotive force, that is, the force transferring the charge from one wire to the other, while the integral is the counterelectromotive force of the field. Hence, (128) may be rewritten as

$$\Psi = \tfrac{1}{2}VI^*. \tag{130}$$

In order to find $\Psi$, it is necessary to compute the current $I$ flowing through the generator in response to the electromotive force $V$—a major problem in itself.

The approximate method of computing $\Psi$ is based on the following facts: (1) In thin wires the current $I(z)$ is nearly sinusoidal, (2) the field and, in particular, $E_z(z)$ can be calculated from $I(z)$ by the retarded-potential method, and (3) the error in the field becomes smaller as the error in $I(z)$ becomes smaller. This method has already been applied successfully to find the approximate power radiated from thin cylindrical antennas.

In the case of conical antennas we have

$$\Psi = -\frac{1}{2}\int_{-l}^{l} E_r(r)I^*(r)dr, \tag{131}$$

for the average work done in order to maintain electric current in the lateral conical surface. To this we must add another integral if the top and bottom surfaces of the cone are large enough to make a noticeable contribution to $\Psi$. It is from this integral that we have computed $F(L)$ as given by (26). For thin antennas $G(L)$ is independent of the shape of the antennas and can be obtained equally well from (126). In order to carry out the necessary computations, the following expressions for the field produced by an infinitely thin filament supporting sinusoidal current have been used

$$\begin{aligned}
I(z) &= I\sin\beta(l-z), \qquad z>0;\\
&= I\sin\beta(l+z), \qquad z<0;\\
E_z &= 30iI\left(2\frac{e^{-i\beta r}}{r}\cos\beta l - \frac{e^{-i\beta r_1}}{r_1} - \frac{e^{-i\beta r_2}}{r_2}\right),\\
\rho E_\rho &= 30iI\left[\frac{(z-l)e^{-i\beta r_1}}{r_1} + \frac{(z+l)e^{-i\beta r_2}}{r_2} - \frac{2ze^{-i\beta r}}{r}\cos\beta l\right]\\
2\pi\rho H_\phi &= -iI(e^{-i\beta r}\cos\beta l - \tfrac{1}{2}e^{-i\beta r_1} - \tfrac{1}{2}e^{-i\beta r_2}).
\end{aligned} \tag{132}$$

In these equations $r_1$, $r$, and $r_2$ are, respectively, the distances from the lower end, the center, and the upper end of the antenna; $\rho$ is the distance from the $z$ axis.

In view of (23) and (25), $G(L)$ and $F(L)$ can be obtained correctly in this manner.

In (126) the quantity $-E_z(z)$ is the applied electromotive force per unit length and, therefore, $-E_z(z)/I(z)$ is the radiation impedance per unit length. If the antenna is perfectly conducting, this impedance is 0 along the entire antenna except in the region from $z=-s$ to $z=s$, occupied by the source of energy. The

[42] It should be noted, however, that $L_0(\theta)$ is not a member of the orthogonal set $[L_n(\theta)]$ but $dL_0(\theta)/d(\theta)$ *is* a member of the orthogonal set $[dL_n(\theta)/d\theta]$.

[43] For a brief history of this method see S. A. Schelkunoff, "A general radiation formula," Proc. I.R.E., vol. 27, pp. 660–666; October, 1939.

conclusion is not startling, since after all energy does come out of its source.

What we have just said does not vitiate our previous assertion to the effect that an approximate value of $\Psi$ can be obtained from an approximate value of $I(z)$. It is true that if $I(z)$ is taken to be a sinusoidal function of $z$, then $E_z$ is different from zero and it would appear that there exists a nonvanishing distributed radiation impedance; but this means merely that the power given out by the "point generator" is approximately equal to the power given out by a certain continuous distribution of generators along the entire antenna. If the sinusoidal function for $I(z)$ is replaced by a more accurate function, then $E_z$ will become smaller along the greatest part of the antenna but it will become larger in the interval from $z=-s$ to $z=s$. What the discussion in connection with (7) tells us is that if $K$ is large, the more accurate expression for $\Psi$ will not differ very much from the one obtained on the basis of sinusoidal distribution of current.

On the other hand, it is perfectly obvious that in the case of an antenna fed from a point generator the distributed radiation resistance $-E_z(z)/I(z)$, obtained from sinusoidal distribution, should not possess any significance since it is bound to approach zero as $I(z)$ is made to approach its exact value.

Feldman has communicated to the author that by taking the real part of $-E_z(z)/I(z)$, computed on the assumption that $I(z)$ is sinuscidal, and regarding this real part as a distributed series resistance added by radiation to the ohmic resistance, he computed the current and charge distributions along a long wire. Then he measured the shape of the minima of the current and of the charge. The measured values agreed well with the computed values.

Now, there is no question that there exists a distribution of series impedance that will represent correctly the effect of radiation on the *total current* and the *total charge* in the antenna (Section VII). What is surprising is that this resistance has been obtained fairly accurately as the real part of $-E_z(z)/I(z)$. After all, if this were a correct method of finding the equivalent distributed resistance, we should expect that its exact value will be found when the exact value of $I(z)$ is used. And yet if the exact value of $I(z)$ is used, then $-E_z(z)/I(z)$ must be equal to zero because this is precisely the boundary condition from which the exact current must be obtained!

## VII. Current-Charge Equations

The customary form of transmission equations for a line with distributed series resistance $R$, series inductance $L$, and shunt capacitance $C$ is

$$\frac{dV}{dx} = -(R + i\omega L)I, \quad \frac{dI}{dx} = -i\omega CV. \tag{133}$$

Since the electric charge per unit length is $q=CV$, the above equations can be written also in the current-charge form

$$\frac{dq}{dx} = -(RC + i\omega LC)I, \quad \frac{dI}{dx} = -i\omega q. \tag{134}$$

provided, however, that $C$ is independent of $x$. The second equation of this set expresses the law of conservation of electric charge.

For a conical antenna (for any antenna for that matter) the second equation is satisfied automatically

$$\frac{dI}{dr} = -i\omega q. \tag{135}$$

Differentiating this with respect to $r$, we have

$$\frac{dq}{dr} = \frac{i}{\omega}\frac{d^2I}{dr^2}. \tag{136}$$

It has been shown in Section V that the total current $I(r)$ is the sum of the principal current $I_0(r)$ and an infinite number of complementary currents corresponding to characteristic values of $n$

$$I(r) = I_0(r) + \sum_n I_n(r). \tag{137}$$

Each component of the current satisfies the following equation[21]

$$\frac{d^2I_n}{dr^2} + \left[\beta^2 - \frac{n(n+1)}{r^2}\right]I_n = 0, \beta = \frac{2\pi}{\lambda} = \frac{\omega}{v}. \tag{138}$$

Substituting the second derivative from this equation into (136), we obtain

$$\frac{dq}{dr} = -\frac{i\omega}{v^2}I(r) + \frac{i\omega}{v^2}\sum_n \frac{n(n+1)}{(\beta r)^2}I_n(r). \tag{139}$$

We have seen that as $K$ increases indefinitely, all the complementary current waves approach zero; consequently the current-charge equations for the antenna become substantially the equations of a uniform transmission line. *If $I(r)$ is known*, we can determine $RC$ and $LC$ so that (139) would become identical with (134). *Assuming* that $C$ is independent of $r$ and is equal to the capacitance for the principal wave[44]

$$C = \frac{\pi\epsilon}{\log\cot\frac{\psi}{2}} = \frac{1}{vK}, \tag{140}$$

and comparing (134) and (139) we obtain

$$R + i\omega L = i\beta K - i\beta K\frac{\sum_n \frac{n(n+1)}{(\beta r)^2}I_n(r)}{I(r)}. \tag{141}$$

Taking $I(r)$ and $I_n(r)$ from the equations contained in the main section of the paper we can replace (141) by the following approximate expression:

[44] We must bear in mind that nothing can be deduced from (139) concerning the nature of $C$. In this respect the total-current—total-charge equations are unlike the principal-current—principal-charge equations.

$$R + i\omega L = i\beta K + \frac{60\pi \sum_{m=0}^{m} (4m+3)\left[J_{2m+3/2}(\beta l) - iN_{2m+3/2}(\beta l)\right]\sqrt{rl}\, J_{2m+3/2}(\beta r)}{r^2\left[\sin\beta(l-r) + \frac{F-iG}{K}\cos\beta(l-r) + \frac{\bar{I}(r)}{I_0}\right]} + \text{remainder.} \quad (142)$$

In order to obtain an expression for $R$ when $l=\lambda/4$, we need only one term in the numerator and we may retain only the principal term in the denominator. Thus we shall have

$$R = \frac{360\left[\frac{\sin\beta r}{\beta r} - \cos\beta r\right]}{l(\beta r)^2\cos\beta r}. \quad (143)$$

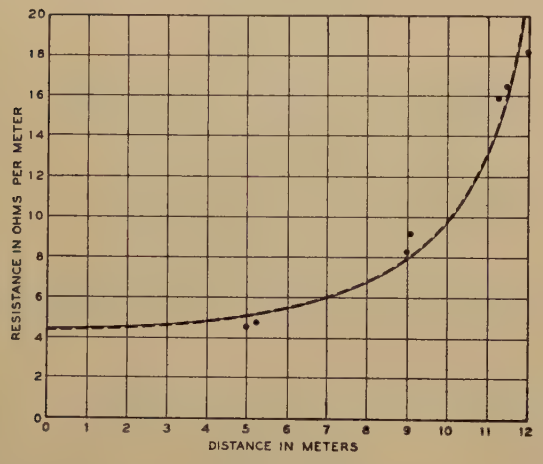


Fig. 29—Distribution of radiation resistance in the current-charge transmission equations. The calculated curve is for $2l=\lambda/2$; the experimental points, obtained from Feldman, are for $2l\doteq 2.5\lambda$.

In the neighborhood of the generator this becomes approximately

$$R = \frac{120}{l} = \frac{480}{\lambda}; \quad (144)$$

and, near the ends,

$$R = \frac{5760}{\pi^4(l-r)} = \frac{59}{l-r}. \quad (145)$$

The approximate expression for $R$ obtained from $-E_z(z)/I(z)$, on the assumption that $I(z)$ is sinusoidal, is

$$R = \frac{120l}{(l^2-r^2)}. \quad (146)$$

This expression agrees quite well with ours (Fig. 29). However, there are no theoretical objections to (143) as there are to (146).

If the antenna is so short that $\beta l$ is substantially smaller than unity and if we neglect those components of the total current which depend on $K$, then approximately

$$R = \frac{160\pi^2 l^2}{(l-r)\lambda^2}. \quad (147)$$

The total radiated power calculated from (147) is found to agree with the well-known expression for the power radiated by a short doublet.

Besides introducing a distributed resistance into the current-charge equations of the antenna, radiation modifies the distributed inductance. Thus for $\beta l=\pi/2$ we find approximately (retaining only the first term in the summation)

$$\omega L = \beta K + 360\beta\frac{\frac{\sin\beta r}{\beta r} - \cos\beta r}{(\beta r)^2\cos\beta r}. \quad (148)$$

The first term of this expression represents the series reactance per unit length of an infinitely long conical antenna while the second term is the end effect. Near the center of the antenna (148) becomes

$$\omega L = \beta K + 120\beta. \quad (149)$$

In the neighborhood of the ends of the antenna, the added reactance depends appreciably on other terms in (141); there the series converges slowly and even the approximation for the reactive part used by us in (142) is not good.

It is worth observing that if the series inductance is obtained from the imaginary part of $-E_z(z)/I(z)$ assuming $I(z)$ to be sinusoidal, the result

$$\omega L = \frac{120r}{l^2-r^2}\tan\beta r \quad (150)$$

is very disappointing and may be regarded as an additional reminder that the comparative success with the resistance must have been purely coincidental.

Thus from a theory in which antennas are regarded as multiple transmission lines, we have obtained two restricted theories. In the first of these radiation appears as a terminal impedance and in the second it appears as a distributed series impedance. There is no inconsistency between these two views and both are valid provided they are suitably qualified. Thus in the second theory, we think in terms of electric charge and electric current and must not assume the usual transmission-line relations between the voltage and the charge. In the first theory, on the other hand, all the usual transmission-line relations hold but the voltage, the charge, and the current in the transmission line representing the antenna correspond respectively to the voltage, the "principal" charge, and the principal current in the antenna.

## VIII. Wave Propagation along Perfectly Conducting Parallel Wires

Consider a pair of parallel perfectly conducting wires (Fig. 30), energized by any number of "point generators." The electromagnetic field on or outside the wires can be expressed in the following general form

$$E = -i\omega\mu A - \text{grad } V, \quad H = \text{curl } A, \quad V = -\frac{\text{div } A}{i\omega\epsilon}, \tag{151}$$

where $A$ is the retarded magnetic vector potential and $V$ the retarded electric scalar potential.

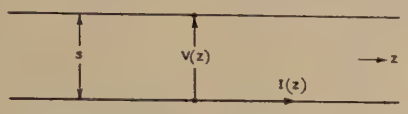


Fig. 30—A diagram showing two perfectly conducting parallel wires.

If the wires are so energized that the electric conduction current is strictly longitudinal, and if the wires are thin, the current is always at least approximately longitudinal; the only nonvanishing component of $A$ is the one parallel to the wires

$$A_x = A_y = 0, \qquad A_z = \Pi. \tag{152}$$

In this case we obtain from (151)

$$E_z = -i\omega\mu\Pi - \frac{\partial V}{\partial z}, \quad V = -\frac{1}{i\omega\epsilon}\frac{\partial \Pi}{\partial z}. \tag{153}$$

Since the wires are perfectly conducting, $E_z$ must vanish on the surface of each wire except at points of application of electromotive forces. Thus, we have

$$\frac{dV_1}{dz} = -i\omega\mu\Pi_1, \qquad \frac{d\Pi_1}{dz} = -i\omega\epsilon V_1,$$
$$\frac{dV_2}{dz} = -i\omega\mu\Pi_2, \qquad \frac{d\Pi_2}{dz} = -i\omega\epsilon V_2, \tag{154}$$

where the subscripts designate the values of the corresponding functions on the wires. Subtracting, we have

$$\frac{d(V_1 - V_2)}{dz} = -i\omega\mu(\Pi_1 - \Pi_2),$$
$$\frac{d(\Pi_1 - \Pi_2)}{dz} = -i\omega\epsilon(V_1 - V_2). \tag{155}$$

Thus, *the voltage across parallel perfectly conducting wires and the difference of vector potentials satisfy the equations of a uniform nondissipative transmission line. The phase velocity is the velocity of light.*

On the other hand, the electric current $I(z)$ does not satisfy the transmission-line equations. The vector potential $\Pi$ is determined by the complete current distribution

$$\Pi(z) = \frac{1}{4\pi}\int \frac{I(z_1)e^{-i\beta r}}{r}\,dz_1, \tag{156}$$

where $r$ is the distance between the points $z$ and $z_1$ and the integration is extended over both wires. If the distance between the wires is small compared with the wavelength and with the length of the wires and if the wires are energized in "push-pull" so that the currents in the wires are equal and oppositely directed, then $\Pi_1 - \Pi_2$ is substantially proportional to the electric current at the corresponding point and (155) turns into the usual engineering equations governing transmission of waves on parallel wires.

The current in two thin infinitely long perfectly conducting parallel wires, energized in push-pull can be expressed in the following form[45]

$$I(z) = -\frac{i\beta a V_0}{2\eta\tau}\int_{(C)} \frac{\sinh \gamma\tau K_1(-ia\sqrt{\gamma^2+\beta^2})e^{\gamma z}d\gamma}{\gamma\sqrt{\gamma^2+\beta^2}[K_0(-is\sqrt{\gamma^2+\beta^2} - K_0(-ia\sqrt{\gamma^2+\beta^2})]}, \tag{157}$$

where $V_0$ = an electromotive force distributed in push-pull in two short segments of length $2\tau$, one on each wire,
$a$ = the radius of the wires,
$s$ = the interaxial separation between the wires,
$z$ = the distance from the mid-points of the "generators," and
$C$ = the imaginary axis in the $\gamma$-plane indented around $\gamma = \pm i\beta$ (Fig. 31(A)).

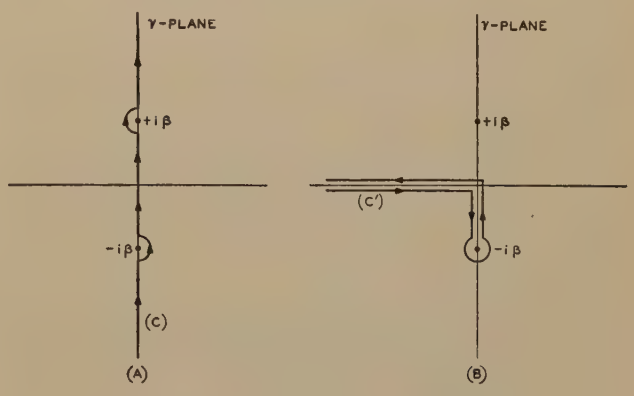


Fig. 31—Contours of integration.

The phase of $\sqrt{\gamma^2+\beta^2}$ at $\gamma = \pm i\infty$ is $\pi/2$. The only approximation involved in (157) is that the radius of the wires be small compared with their interaxial separation; consequently, the "proximity effect" is not included in (157).

If $z$ is positive, the contour $(C)$ can be deformed into $(C')$ as shown in Fig. 31(B). The integration around the point $\gamma = -i\beta$ which happens to be a pole as well as a branch point of the integrand, yields the following term

$$I_0(z) = \frac{V_0}{2K}\cdot\frac{\sin \beta\tau}{\beta\tau}e^{-i\beta z}, \quad K = \frac{\eta}{\pi}\log\frac{s}{a}, \quad z > 0. \tag{158}$$

This "principal" current wave is unattenuated and is substantially independent of $\tau$ if $2\pi\tau/\lambda$ is small

[45] In order to obtain this equation as well as equation (163) we express the "pulse function," representing the applied electromotive intensity $-E_z$, as a contour integral; then, we obtain the magnetic intensity $H_\phi$ as the quotient of $-E_z$ and the radial impedance; and finally we compute the current from $I(z) = 2\pi a H_\phi(a, z)$.

compared with unity. The remainder

$$I(z) = I(z) - I_0(z) \tag{159}$$

is a purely local wave in the neighborhood of the generator and it represents the effect of radiation as well as the local reactance depending on $\tau$.

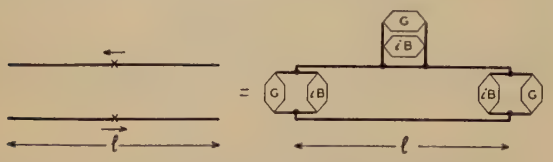


Fig. 32—The equivalent circuit for two parallel wires, open at both ends and energized in push-pull.

Radiation introduces a resistance in parallel with the applied electromotive force. If the interaxial separation is small compared with the wavelength, this resistance is approximately

$$R = \frac{K^2\lambda^2}{60\pi^2 s^2}. \tag{160}$$

If the wires are of finite length, the expression for the current becomes vastly more complex. The result, however, will consist of two parts, one of which will represent the principal current wave and the other local waves in the neighborhood of the discontinuities, that is, ends of the wires or generators. It is fortunate, however, that the impedances introduced by radiation *at the points of discontinuity* can be calculated with good engineering accuracy without setting up exact equations but using in the proper manner the field produced by the principal current wave. The accuracy of such expressions increases with increasing characteristic impedance $K$.

Let a pair of parallel wires of radius $a$, whose interaxial separation is $s$, be open at both ends and be energized in "push-pull"; then, in free space, the radiation can be represented by parallel combinations of conductance $G$ and susceptance $B=\omega C$ as shown in Fig. 32, where

$$G = \frac{60\pi^2(s^2 - a^2)}{\lambda^2}, \qquad C = \frac{60(s - a)}{vK^2},$$

$$B = \omega C = \frac{120\pi(s - a)}{K^2\lambda}. \tag{161}$$

We omit the details of calculation.

If the wires are imperfect conductors, the first equation of the set (155) becomes

$$\frac{d(V_1 - V_2)}{dz} = -i\omega\mu(\Pi_1 - \Pi_2) - Z_1 I_1 - Z_2 I_2, \tag{162}$$

where $Z_1$ and $Z_2$ are the surface impedances of the wires. The added terms affect the voltage across the pair continuously. The principal effect is due to dissipation of energy in the wires; but since the current distribution is affected by radiation, the latter also will produce a continuously distributed effect on the voltage. The latter is, however, a second-order effect; besides, it is concentrated largely in the immediate vicinity of the ends, even though mathematically speaking it extends over the entire length.

## IX. On the Impedance of an Infinitely Long Perfectly Conducting Cylindrical Wire

It is readily shown[46] that the current in an infinitely long perfectly conducting cylindrical wire of radius $a$ is

$$I(z) = \frac{i\beta a V_0}{\eta\tau} \int_{(C)} \frac{\sinh \gamma\tau\, K_1(-ia\sqrt{\gamma^2+\beta^2})}{\gamma\sqrt{\gamma^2+\beta^2}\, K_0(-ia\sqrt{\gamma^2+\beta^2})} e^{\gamma z} d\gamma, \tag{163}$$

where $V_0$ is the applied electromotive force uniformly distributed over a section of length $\tau$ and $C$ is the contour shown in Fig. 31(A).

Deforming $(C)$ into $(C')$, we can show that the real component of the input admittance is substantially independent of $\tau$ and for $\tau = 0$ is

$$\frac{1}{K(0)} = \frac{4\beta}{\eta\pi} \int_0^\beta \frac{d\xi}{(\beta^2 - \xi^2)\left[J_0^2(a\sqrt{\beta^2 - \xi^2}) + N_0^2(a\sqrt{\beta^2 - \xi^2})\right]}. \tag{164}$$

After some tedious transformations we have obtained the following approximate expression (when $\eta = 120\pi$) for thin wires

$$K(0) = \frac{120M}{1 + \dfrac{\log 2}{2M} - \dfrac{\frac{2}{3}\pi^2 - (\log 2)^2}{4M^2}}$$

$$M = \log\frac{\lambda}{2\pi a} + \tfrac{1}{2}\log 2 - C, \tag{165}$$

where $C = 0.577\cdots$ is Euler's constant. As $a \to 0$, (165) approaches

$$K(0) = 120\left(\log\frac{\lambda}{2\pi a} - C\right) = 120\log\frac{\lambda}{2a} - 207. \tag{166}$$

## X. An Approximation of a Dissipative Transmission Line by a Nondissipative Line with an Effective Load at the Last Current Node or Antinode

The input impedance of a dissipative line of length $l$, electrically open at the far end, is

$$Z_i = K \coth(\alpha + i\beta)l, \tag{167}$$

where $\alpha + i\beta$ is the propagation constant. If $\alpha l$ is small compared with unity, then we have approximately

$$Z_i = K\frac{\cos\beta l + i\alpha l \sin\beta l}{\alpha l\cos\beta l + i\sin\beta l}. \tag{168}$$

For a nondissipative line with a terminal impedance $Z_t$ at the far end, we have

[46] See footnote 45.

$$Z_i = K \frac{Z_t \cos \beta l + iK \sin \beta l}{K \cos \beta l + iZ_t \sin \beta l}. \qquad (169)$$

Multiplying the numerator and the denominator of (168) by $K/\alpha l$ and comparing with (169) we obtain

$$Z_t = \frac{K}{\alpha l} = \frac{K^2}{\frac{1}{2}Rl}, \qquad (170)$$

where $R$ is the resistance per unit length of the dissipative line.

The same input impedance will be obtained, of course, if the nondissipative line is electrically open and at the point $\frac{1}{4}$ wavelength from the open end there is an impedance $Z$, in series with the line, defined by

$$Z = \frac{K^2}{Z_t} = \frac{\alpha l}{K} = \tfrac{1}{2}Rl. \qquad (171)$$

It is to be expected, therefore, that the electric currents in these three different cases will be approximately the same in the neighborhood of the generator. If the line is about $\frac{1}{2}$ wavelength long, the minimum current will occur close to the generator and its measured value will not enable us to decide which, if any, of the three above-discussed distributions of loss happens to be the true distribution. At the current antinode, the electric currents in the three cases differ by larger absolute amounts; these differences are, however, small compared with the total current.

# High-Frequency Radio Transmission Conditions, August, 1941, with Predictions for November, 1941*

NATIONAL BUREAU OF STANDARDS, WASHINGTON, D. C.

*Note:* In order to make these monthly reports of maximum service, changes are made from time to time. The Bureau welcomes suggestions for improvement of both form and substance. Address any communications to the National Bureau of Standards, Washington, D. C.

THE radio transmission data herein are based on observations at Washington, D. C., of long-distance reception and of the ionosphere. Fig. 1 gives the August average values of maximum usable frequencies, for undisturbed days, for radio transmission by way of the regular layers of the ionosphere. The regular-layer maximum usable frequencies were determined by the F layer at night and by the E, $F_1$, and $F_2$ layers during the day. Fig. 2 gives the expected values of the maximum usable frequencies for radio transmission by way of the regular layers, average for

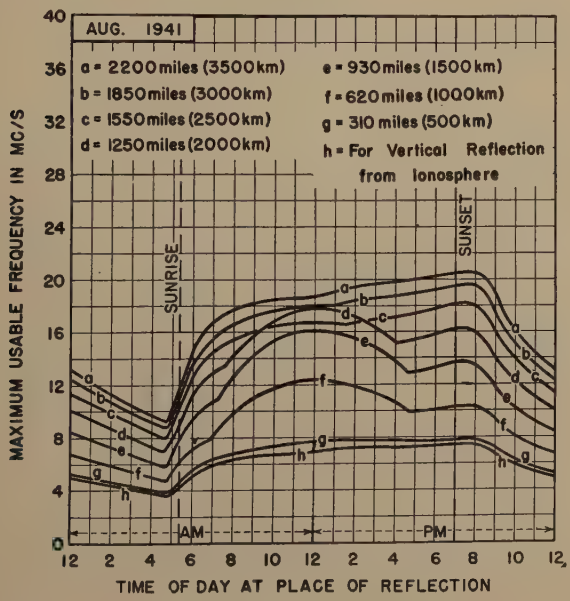
AUG. 1941
a = 2200 miles (3500 km)
b = 1850 miles (3000 km)
c = 1550 miles (2500 km)
d = 1250 miles (2000 km)
e = 930 miles (1500 km)
f = 620 miles (1000 km)
g = 310 miles (500 km)
h = For Vertical Reflection from Ionosphere
SUNRISE
SUNSET
AM
PM
MAXIMUM USABLE FREQUENCY IN MC/S
TIME OF DAY AT PLACE OF REFLECTION

Fig. 1—Maximum usable frequencies for dependable radio transmission via the regular layers, average for undisturbed days, for August, 1941. The values shown were considerably exceeded during frequent irregular periods by reflections from clouds of sporadic E layer. (See Table II.) These curves and those of Fig. 2 also give skip distances, since the maximum usable frequency for a given distance is the frequency for which that distance is the skip distance.

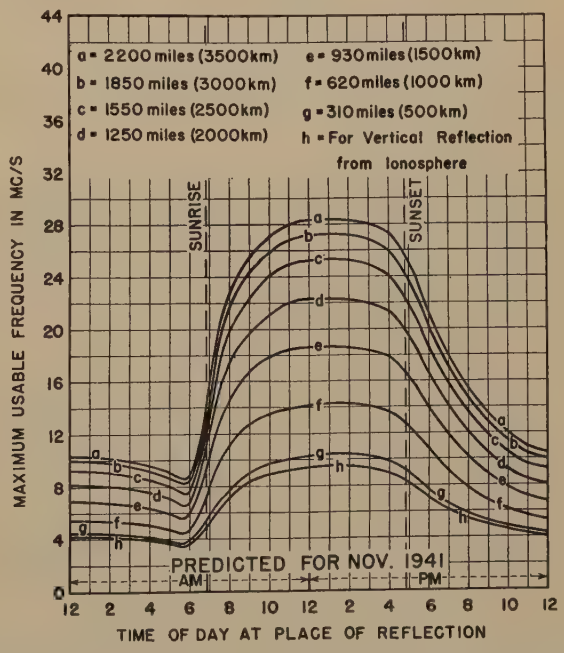
a = 2200 miles (3500 km)
b = 1850 miles (3000 km)
c = 1550 miles (2500 km)
d = 1250 miles (2000 km)
e = 930 miles (1500 km)
f = 620 miles (1000 km)
g = 310 miles (500 km)
h = For Vertical Reflection from Ionosphere
SUNRISE
SUNSET
PREDICTED FOR NOV. 1941
AM
PM
MAXIMUM USABLE FREQUENCY IN MC/S
TIME OF DAY AT PLACE OF REFLECTION

Fig. 2—Predicted maximum usable frequencies for dependable radio transmission via the regular layers average for undisturbed days, for November, 1941. For information on use in practical radio transmission problems, see the pamphlets "Radio transmission and the ionosphere" and "Distance ranges of radio waves," obtainable from The National Bureau of Standards, Washington, D. C., on request.

* Decimal classification: R113.61. Original manuscript received by the Institute, September 12, 1941.

undisturbed days, for November, 1941. These frequencies are exceeded at times because of sporadic-E propagation which sometimes lasts for hours. The times of occurrence are unpredictable.

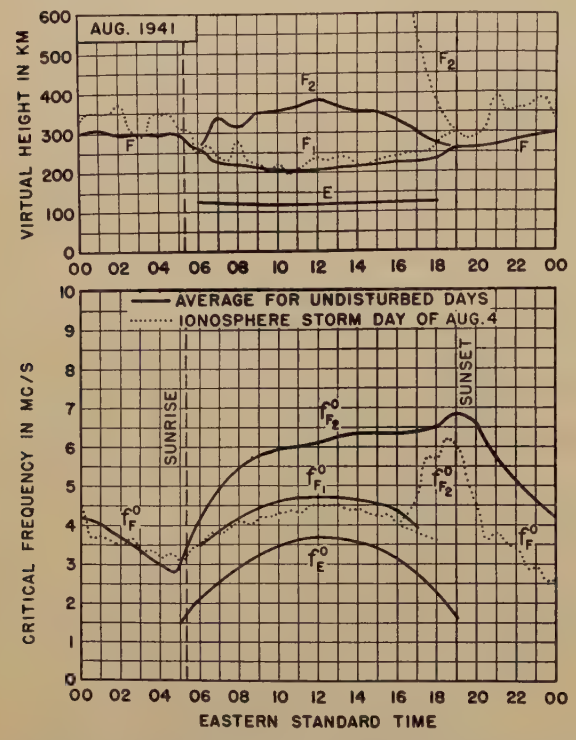


Fig. 3—Virtual heights and critical frequencies of the ionospheric layers, observed at Washington, D. C., August, 1941.

Average critical frequencies and virtual heights of the ionospheric layers as observed at Washington, D. C., during August are given in Fig. 3. Critical frequencies for each day of the month are given in Fig. 4.

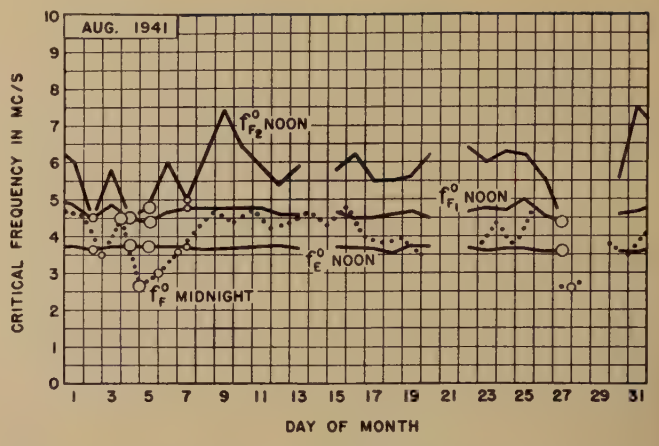


Fig. 4—Midnight and noon critical frequencies for each day of August. Open circles indicate critical frequencies observed during ionospheric storms. Sizes of circles represent approximately the severity of the storms.

TABLE I

IONOSPHERIC STORMS

| Day and hour E.S.T. | $h_F$ before sunrise (km) | Minimum $f_F$ before sunrise (Mc) | Noon $f_{F_2}$ (Mc) | Magnetic character[1] 00–12 G.M.T. | Magnetic character[1] 12–24 G.M.T. | Ionospheric character[2] |
|---|---|---|---|---|---|---|
| August | | | | | | |
| 2 (from 0200) | 324 | 3.0 | <4.5 | 3.9 | 3.6 | 4 |
| 3 (through 0500) | 310 | 2.8 | — | 2.8 | 2.0 | 3 |
| 4 | 338 | 3.3 | <4.5 | 5.2 | 5.9 | 5 |
| 5 | 393 | 0.9 | 4.8 | 2.9 | 2.6 | 5 |
| 6 (through 0900) | 365 | 1.7 | — | 2.6 | 3.1 | 4 |
| 7 (through 1300) | 325 | 2.2 | 5.0 | 3.0 | 2.4 | 3 |
| 26[3] | — | — | — | 3.8 | 3.0 | —[4] |
| 27 | —[4] | —[4] | <4.5 | 5.8 | 3.8 | 5 |
| 28[3] | 317 | 0.9 | —[4] | 4.2 | 2.5 | 4 |
| For comparison: Average for undisturbed days | 296 | 2.86 | 6.06 | 1.7 | 1.8 | 1.5 |

[1] Average for 12 hours of American magnetic K figure determined by seven observatories, on an arbitrary scale of 0 to 9, 9 representing the most severe disturbance.
[2] An estimate of the ionospheric storminess at Washington, on an arbitrary scale of 0 to 9, 9 representing the greatest disturbance.
[3] Times of beginning and end of storm not known because of recorder failure.
[4] Recorder not in operation.

TABLE II

APPROXIMATE MAXIMUM USABLE FREQUENCIES IN MEGACYCLES, FOR RADIO TRANSMISSION BY MEANS OF STRONG SPORADIC-E REFLECTIONS, AT WASHINGTON[1]

| Day | Hour, E.S.T. 00 | 01 | 02 | 03 | 04 | 05 | 06 | 07 | 08 | 09 | 10 | 11 | 12 | 13 | 14 | 15 | 16 | 17 | 18 | 19 | 20 | 21 | 22 | 23 |
|---|---|---|---|---|---|---|---|---|---|---|---|---|---|---|---|---|---|---|---|---|---|---|---|---|
| August | | | | | | | | | | | | | | | | | | | | | | | | |
| 1 | | | 14 | 15 | 14 | 15 | 17 | 25 | 44 | | | | | | | | | | | | | | | |
| 2 | | | | | | | | | | | | | | | | | 34 | 28 | 45 | 23 | | | | |
| 3 | | | | | | | 23 | 34 | 50 | 34 | | | | | | | | | | | | | | |
| 5 | | | | | | | | | NR | 23 | 23 | | 23 | | | | 34 | 21 | | | | | | |
| 6 | | | | | | | 19 | 22 | 23 | | | | | | | | | | | | | | | |
| 7 | | | | | | | | | | 38 | 27 | | 21 | | | | | | 17 | 17 | 27 | 19 | | |
| 8 | 14 | | | | | | 18 | 25 | 24 | 24 | ← | NR | → | | | | | 20 | 23 | 20 | 19 | 20 | 23 | 19 |
| 9 | 18 | 15 | 19 | 15 | 15 | 18 | 16 | 22 | 19 | | | 22 | 21 | | | | | 20 | 16 | | | 19 | 18 | 23 |
| 10 | 24 | 23 | 18 | 17 | 18 | | 18 | 28 | 33 | 45 | 25 | 27 | | | | | | | 19 | 16 | 20 | 38 | 19 | 19 |
| 11 | | | | 15 | | | 16 | 22 | 19 | NR | 25 | 25 | 42 | | | 22 | 20 | 50 | 33 | 50 | 40 | 18 | 18 | 50 |
| 12 | 23 | | | | 17 | 16 | 18 | 18 | 17 | 22 | 22 | 32 | 22 | | | | | | | 25 | 17 | 24 | 18 | |
| 13 | 16 | | | | 17 | 15 | 16 | 16 | 22 | 33 | 21 | | | | 39 | 33 | 35 | 34 | 21 | | 16 | | | NR |
| 14 | ← | | | | | | No Record | | | | | | → | | | | | | | | | | | 15 |
| 15 | 15 | 16 | 18 | 28 | | | | | 28 | | 35 | ← | No Record | → | | | | 24 | 21 | 18 | | NR | | 16 |
| 16 | | | | 15 | 15 | 16 | 21 | 22 | 34 | 43 | 29 | 23 | 24 | | | | | | 17 | 14 | | | | |
| 17 | | | | | 18 | | | | | | | | | | | | | | | | 23 | 36 | 21 | 18 |
| 18 | 17 | 18 | 18 | 18 | 16 | | | | | | | | | | | | 39 | 24 | 39 | 25 | 18 | 29 | 16 | 16 |
| 19 | | | | | | | | | | | ← | No Record | → | | | | | | 21 | 21 | 21 | 18 | | |
| 20 | | | | | | 21 | 21 | 21 | | | | | | | ← | | | | No Record | | | | | → |
| 21 | ← | | | | | | | | | | No Record | | | | | | | | | | | | | → |
| 22 | ← | | | | | | No Record | | | | | | → | | | | | | | | | | | |
| 23 | 16 | | | | | | 17 | 18 | 18 | 18 | 33 | | | | | | | | 16 | 16 | 20 | | | |
| 24 | | | | | | | | | | | | | | | | | | | 18 | 18 | 17 | 34 | | |
| 25 | | | | | | | | | | | | | | | | | | | | | 18 | | 18 | |
| 26 | | | | 16 | 23 | 17 | | | | | NR | | | NR | | | | ← | | No Record | | | | → |
| 27 | ← | | No Record | | → | | | | | | | | | | | | | | | | | | | |
| 28 | | | | | | | ← | | | | | | No Record | | | | | | | | | | | → |
| 29 | ← | | | | | | | No Record | | | | | → | | | | | | | | | | | |
| 30 | | | | | | | | | | | | | | | | | | | | | 17 | 18 | 15 | 15 |
| 31 | 15 | 14 | 18 | 16 | 15 | | | | | | | | | | | | | | | | | 16 | 26 | 22 |

[1] "NR" or "No Record" in table indicates recorder not operating.

Ionospheric storms are listed in Table I. Beginning in last month's report the storms are given in chronological order rather than in order of severity as formerly. The details of the ionospheric storm day of August 4 are shown in Fig. 3. Noon and midnight critical frequencies observed during the ionospheric storms listed in Table 1 are indicated by circles in Fig. 4.

No sudden ionospheric disturbances were observed during August. Table II gives the approximate maximum usable frequencies for good radio transmission by means of sporadic-E reflections (as observed at Washington; sporadic-E conditions are patchy, not uniform over wide areas).

## Discussion on "Radiation from Rhombic Antennas"*

DONALD FOSTER

**Leonard Lewin:**[1] The expressions obtained by the author of this paper for the radiation resistance and gain of the inverted-V and rhombic aerials raise a point of considerable interest with regard to the radiating efficiency of antennas.

In general, the far-field electric field strength produced by a radiator depends on two quantities, the inverse distance $1/r$, and a directivity factor $K$, depending on the current in the aerial and the orientation of the field point with respect to the system. Since the far-field magnetic field strength differs from the electric field strength only by a constant factor, the power radiated per second by the aerial is proportional to $K^2/r^2$ per unit area. In this expression, $K$ in the optimum direction is a function of the amplitude of the antenna current $I_0$ and the aerial dimensions and wavelength. If we are to compare the gains of different systems, they must be referred to a common base; i.e., the input power must be the same for each. Therefore the expression $K^2_{max}$/input power is a measure of the gain of the aerial.

Generally, the power dissipated as heat in the resistance of the conductors is negligible compared to the radiation, so we may set the input power equal to the radiated power $\frac{1}{2}I_0^2R$, where $R$, the radiation resistance of the system is equal to

$$\frac{30\pi}{I_0^2\lambda^2}\int K^2 d\Omega.$$

This leads to the equation (p. 1353)

$$\text{gain} = \frac{4\pi K^2_{\max}}{\int K^2 d\Omega}. \qquad (1)$$

However, in the case of the rhombic aerial, the conductors are terminated by an ohmic resistance equal in magnitude to the wave impedance $Z_0$ between the aerial wires; and a considerable portion of the input power will be lost in this termination. Moreover, on account of the spatial damping of the current amplitude, the value of $K^2_{max}$ will be diminished. For these reasons, it does not appear correct to identify the input power with the radiated power, and (1) cannot be considered applicable to the rhombic aerial.

If we assume,[2] for the purpose of calculation, that the rhombic aerial may be treated as a transmission line with the effect of the radiation simulated by an ohmic resistance, equal in magnitude to the radiation resistance, distributed uniformly over the wires (the same method has been used with success in the determination of the characteristics of other types of antenna), then it is readily shown that the current distribution takes the form of an attenuated wave running from the fed to the terminated end of the aerial. The input impedance differs inappreciably from $Z_0$ (the value for the unattenuated system) and so the input power is $\frac{1}{2}Z_0I_0^2$.

The value of the directivity factor $K$ must be recalculated as it has been altered by the new form of current distribution. But in the neighborhood of the maximum of the field-strength pattern, it is equal, to a very good approximation, to the product of the average current amplitude and the directivity factor of the unattenuated system. We then have for the antenna gain, the following expression:

$$\frac{4\pi K^2_{\max}}{\int K^2 d\Omega}\left[\frac{4(1-e^{-1/2(R/Z_0)})^2}{R/Z_0}\right]. \qquad (2)$$

The correction factor

$$\frac{4(1-e^{-1/2(R/Z_0)})^2}{R/Z_0}$$

is by no means negligible. For example, with $R=600\Omega$ and $Z_0=800\Omega$, its value is 0.52, thus contributing $-3$ decibels to the gain.

Equation (2) may be written in the alternative form

$$\frac{4\pi K^2_{\max}\cdot 30\pi}{Z_0I_0^2\lambda^2}\left[\frac{1-e^{-1/2(R/Z_0)}}{\frac{1}{2}R/Z_0}\right]^2 \qquad (3)$$

which shows how the antenna gain varies with the radiation resistance. The statement (p. 1349) that "a design which effects a reduction of the radiation resistance permits the use of a larger antenna current without increasing the power expenditure" should now be taken to mean that "a design which effects a reduction of radiation resistance will produce an increase in the antenna gain." This increase, however, is due entirely to the increase in average current amplitude involved in the expression for the gain, and not to a decrease of input impedance. For example, if it is assumed that by suppressing certain side lobes of the radiation pattern, that the radiation resistance can be decreased from say $600\,\Omega$ to $550\,\Omega$, then (3) indicates that the gain should be increased by about 2 per cent. This increase, however, is likely to be offset by the fact that $K^2_{max}$ will have been reduced owing to the slight departure from the optimum designing conditions entailed by the suppression of the side lobes. Equation (1) would have indicated an increase of about 9 per cent.

The expressions for the radiation resistance of the inverted-V and the rhombic aerial in free space are not so cumbersome as might at first have been expected from the rather complicated form of the integrals involved. For the rhombic aerial in free space it may be shown that

$$\begin{aligned} R = 120\{&S_1[2\beta a(1+\cos A)] + S_1[2\beta a(1-\cos A)] \\ &- 2S_1(2\beta a) + 2S_1[(2\beta a \sin A)] \\ &- \cos(2\beta a\cdot\sin^2 A)\{S_1[2\beta a\cdot\sin A(1+\sin A)] \\ &\quad + S_1[2\beta a\cdot\sin A(1-\sin A)] \\ &\quad - 2S_1[2\beta a\cdot\sin^2 A] \\ &\quad + S_1[2\beta a\cdot\cos A(1+\cos A)] \\ &\quad + S_1[2\beta a\cdot\cos A(1-\cos A)] \\ &\quad - 2S_1[2\beta a\cdot\cos^2 A]\} \\ &+ \sin(2\beta a\cdot\sin^2 A)\{\mathrm{Si}[2\beta a\cdot\sin A(1+\sin A)] \\ &\quad - \mathrm{Si}[2\beta a\cdot\sin A(1-\sin A)] \\ &\quad - 2\mathrm{Si}[2\beta a\cdot\sin^2 A] \\ &\quad - \mathrm{Si}[2\beta a\cdot\cos A(1+\cos A)] \\ &\quad + \mathrm{Si}[2\beta a\cdot\cos A(1-\cos A)] \\ &\quad + 2\mathrm{Si}[2\beta a\cdot\cos^2 A]\}\}. \end{aligned}$$

while for the inverted-V the value is halved. ($A$ = semivertical angle of the rhombus, $a$ = length of one limb, and $\beta = 2\pi/\lambda$. $S_1(x)$ and Si(x) are the tabulated integrals

$$\int_0^x \frac{1-\cos x}{x}dx \text{ and } \int_0^x \frac{\sin x}{x}dx,$$

respectively.) In most practical applications, the various arguments will be greater than $\pi$, so that the approximations $S_1(x) = 0.577 + \log_e x$ and $\mathrm{Si}(x) = \pi/2$ may be used. In this case the above formula simplifies considerably, and we have, approximately

$$R = 240[\log_e(2\beta a\cdot\sin^2 A) + 0.577] \text{ ohms}.$$

**Donald Foster:**[3] Mr. Lewin is to be congratulated on his announcement that he has obtained the radiation resistance of isolated rhombic antennas in a form which allows computation by the use of tabulated functions. I hope that the details of his calculations will soon be published.

While his assumed distribution of current probably is not exact, it is justifiable practically on the ground that it appears to have provided a convenient expression for the power radiated from an antenna in empty space.

I do not agree with Mr. Lewin's views concerning the definition of gain. It seems to me that this term should be reserved for a compendious description of the radiation or receiving *pattern* of the antenna, and that energy converted into heat in the terminal resistance of the antenna is no more appropriately considered here than that which is dissipated locally elsewhere in the transmitter.

* PROC. I.R.E., vol. 25, pp. 1327–1353; October, 1937.

[1] 8 Wilson Road, Southend-on-Sea, Essex, England.

[2] In his treatment, Mr. Foster expressly refrains from a detailed consideration of the current distribution, in order not to lengthen the analysis unduly. It would appear, however, that it is necessary to take into account the attenuation of the current amplitude if we are to obtain an accurate expression for the antenna gain.

[3] Stevens Institute of Technology, Hoboken, N. J.

# Institute News and Radio Notes

## Board of Directors

A regular meeting of the Board of Directors was held in the Institute office on Wednesday, September 3, 1941. Those present were F. E. Terman, president; Haradan Pratt, treasurer; Austin Bailey, A. B. Chamberlain, I. S. Coggeshall, Alfred N. Goldsmith, Virgil M. Graham, O. B. Hanson, R. A. Heising, L. C. F. Horle, C. M. Jansky, Jr., F. B. Llewellyn, H. M. Turner, A. F. Van Dyck, H. A. Wheeler, L. P. Wheeler, and H. P. Westman, secretary.

Several additions were made to the list of Institute Representatives. It was agreed that Institute Representatives would serve for a period starting July 1 and ending June 30, thus being concurrent with the school year.

The payment of an entrance fee was waived in the case of college professors applying before September 1, 1942, for Institute membership.

The Public Relations Committee was instructed to prepare preliminary plans for a celebration next year of the 100th anniversary of Joseph Henry's discovery of the oscillatory nature of a condenser discharge.

Attention was drawn to notifications already given to the Board of Directors of petitions which were received naming Edwin H. Armstrong and Virgil M. Graham as candidates for the presidency for 1942. Professor Armstrong declined and Mr. Graham accepted the nomination. Ballots were mailed to the voting membership under date of August 25.

Ballots have been mailed to the membership concerning proposed revisions of the Constitution.

## Executive Committee

The Executive Committee met on June 14 and those present were F. E. Terman, president; J. M. Clayton, guest; Alfred N. Goldsmith, Haraden Pratt, B. J. Thompson, J. D. Crawford, advertising manager, and H. P. Westman, secretary.

It was agreed that in the future publication of Institute standards, the present general format of the PROCEEDINGS will be followed.

It was reported that the Twin Cities section petition was in good order and the section established.

A meeting of the Executive Committee was held on July 29, 1941. Those present were Haraden Pratt, chairman; Melville Eastham, Alfred N. Goldsmith, R. A. Heising, B. J. Thompson, and H. P. Westman, secretary.

A report was presented on the annual meeting of the Sections Committee by Mr. Heising, its chairman. He stated that unless the meetings are held at a time that permits those in attendance to stay until the conclusion of the meeting, this method of providing contact between the membership and the Board of Directors may not be very effective. For the conditions under which this meeting was held, the regional-Director plan or tours by the President would be more useful in supplying this contact.

It was agreed that the summer convention for 1942 would be held in Cleveland, Ohio, on June 29, 30, and July 1, with headquarters at the Hotel Statler. Carl E. Smith was named chairman of the convention committee.

It was agreed that we would reprint "Standards on Radio Receivers, 1938" as our supply is exhausted.

Approval was granted for the publication of several new standards reports entitled "Definitions for Facsimile Systems, 1941," "Definitions on Radio Wave Propagation, 1941," and "Measuring Methods in Radio Wave Propagation, 1941." Copies of these standards will be distributed to the membership when available.

Haraden Pratt, chairman; R. A. Heising, B. J. Thompson, and H. P. Westman, secretary attended a meeting of the Executive Committee on August 7, 1941.

The following admissions and transfers to Member grade were approved. Admissions: H. W. Bode, J. A. Boyajian, J. M. Brumbaugh, D. E. Chambers, J. C. Franklin, P. J. Herbst, G. L. Hoard, F. O. McMillan, E. D. Phinney, F. Rieber, J. J. Rogan, L. J. A. Van Lieshout, E. Weber, and R. O. Williams. Transfers: R. C. Ayres, H. G. Doll, I. H. Gerks, H. E. Hartig, M. Hobbs, P. M. Honnell, F. V. Hunt, G. A. O'Reilly, J. S. Starrett, P. H. Thomsen, and J. V. Wilcox.

The Executive Committee met on September 2, 1941, and those present were F. E. Terman, president; Haraden Pratt, Melville Eastham, Alfred N. Goldsmith, R. A. Heising, B. J. Thompson, and H. P. Westman, secretary.

Approval was granted of sixty-nine applications for Associate, two for Junior, and five for Student memberships.

President Terman reported that there were 122 men and 21 women at the Pacific Coast Convention which was held in Seattle, Washington, on August 20, 21, and 22. The program for the meeting was published in the June issue of the PROCEEDINGS.

## Sections

### Baltimore

This was the annual meeting of the Baltimore section and V. D. Hauck of the Bendix Radio Corporation was elected chairman; J. E. Allen of the Pennsylvania Water and Power Company was named vice chairman; and G. J. Gross of the same organization was re-elected secretary-treasurer.

A paper on "The Radio System of a Modern Air Transport" by A. E. Abel, J. Moore, and J. Hammond, engineers of the Bendix Radio Corporation, was presented.

The essential features of many equipments used by the air lines are 100 watts output, fan-cooling, crystal control, frequency range from 1.6 to 16 megacycles, remotely controlled motor-driven selector for any of 8 channels with a separate antenna-tuning unit, and an engine-driven 1000-volt 400-watt generator. The weight of an installation is about 140 pounds and is divided almost uniformly among the transmitter, power-supply unit, and receiver.

A description was given of an equipment to provide a 10-channel service within the range from 2.5 to 15 megacycles. The transmitter output is 50 watts and it may be modulated to 100 per cent. It will operate into antennas of 1 to 100 ohms and reactances of $+j100$ to $-j300$ ohms.

The receiver requires an input of 2 microvolts to produce its full output of 50 milliwatts. A 6-decibel signal-to-noise ratio is obtained. Automatic volume control will hold the output within a 6-decibel range when the input is varied from 2 microvolts to 100 millivolts

The same crystals are used for both the transmitter and the receiver. The equipment without shock mounting weights 74½ pounds.

The radio compass was pointed out to be essentially a homing device indicating whether the plane is to the right or left of a course to the homing station. By using an electronic coupling device with a rotating loop and remote indicator, tuning to the desired station is the only adjustment required. Compensation may be provided to correct for errors caused by the proximity of the ship. Instrument point-to-point flying is possible using two radio-compass receivers tuned to takeoff and destination stations and indicating two bearings on one azimuth scale. Deviation in bearings indicates off-course.

Itinerant ships not in transport service are required to carry radio equipment capable of making contact with the control tower at airports. Such equipment generally includes a 15- to 25-watt 3105-kilocycle transmitter with a range of about 15 miles and a superheterodyne receiver having a range from 200 to 400 kilocycles. This permits listening to the 278-kilocycle airport-control channels and also to radio ranges.

May 16, 1941, Ferdinand Hamburger, chairman, presiding.

### Boston

B. W. St. Clair of the Mico Instrument Company presented a paper entitled "Tricks of the Trade—Properties of Some Materials Used in Electrical Manufacturing."

A discussion was first presented of the so-called Mohs' scale of hardness used to evaluate materials in 10 steps between a very soft material such as talc and the hardest, a diamond. The grades are approximately logarithmically spaced. Only those near the highest, 9 and 10, are suitable for abrasives or jewels.

A description was given of a method of producing artificial rubies and sapphires to be used as jewels for electric meters and kindred applications.

A general description was given of the range of plastics available as engineering materials. It was pointed out that in the case of the thermosetting plastics, the coefficient of linear expansion could be used as a good index of the extent of the cure in the mold.

The next subject covered was that of oils and lubricants. Explanations were given of the phenomenon of surface wetting. There followed a discussion of the question of the stability of lubricating materials, particularly oils, and the reasons for the exceptional stability of certain nondrying oils, such as whale and blackfish.

In connection with lubrication, attention was called to the materials known as hydrofils. These are substances used to coat over a surface prior to applying a lubricant to prevent the lubricant from wetting the surface and thus spreading over a large area and dissipating itself. They are usually fatty acids having long molecules—the longer the better. One end is inert, and the other is terminated in a radical such as COOH. This radical is attracted to water, and it is relatively easy to apply a monomolecular film in which the molecules stand up on end like the pile of a carpet. The radical end is next to the water and the inert ends are presented to the lubricant which is next applied and is unattracted to this layer. The lubricant, therefore, does not wet nor spread but stays where needed.

These same materials can be applied to a metallic surface by heating them just above their melting points and flowing them on the surface. The bond between the hydrofil and the metal is very good, being quasi chemical in nature. It is not readily broken under the influence of high bearing pressures or the sliding and scraping actions encountered in some equipment.

April 26, 1940, W. L. Barrow, chairman, presiding.

This was the annual meeting and in the election which was held J. M. Henry of the New England Telephone and Telegraph Company was elected chairman; R. W. P. King of Harvard University was named vice chairman; and R. O. Oberg of Northeastern University was designated secretary-treasurer. P. K. McElroy of the General Radio Company was named representative to the Engineering Societies of New England.

"Practical Engineering Aspects of Frequency-Modulation Broadcasting" was the subject of a paper by P. A. de Mars, vice president and chief engineer of the Yankee Network.

Such factors as radiated power, terrain, and meteorology which affect the propagation of frequency-modulated waves were first discussed. The variation in field strength from the transmitter at Paxton to Boston was compared with a plot of the elevations above sea level along the same path. The propagation is not strictly line of sight for there is an appreciable signal even in the shadow of a hill and the signal is stronger on the face of a hill. The changes brought about by a hill are of the order of 10 to 20 decibels.

A general description was given of what had been achieved in the way of quality and strength of signals from both the commercial station at Paxton and the experimental station on Mount Washington. A description was given of these two installations. The extreme weather conditions on the top of Mount Washington were indicated and the problem of obtaining power supply during the winter was also discussed.

A demonstration was given by means of a special program from the Paxton station. Vocal and intrumental music as well as special sound effects to illustrate the extended audio-frequency range obtained with frequency modulation were included in the demonstration.

June 6, 1941, P. K. McElroy, secretary-treasurer, presiding.

## Buenos Aires

"The Selection of Transmitting Tubes" was the subject of a paper presented by P. J. Arnaud of Transradio Internacional.

To obtain the lowest possible cost both in manufacture and merchandising of air-cooled tubes for use in transmitters having output powers up to 4 kilowatts, a simplification in the existing large number of tube types is desired.

The desirable characteristics of tubes used as oscillators were first considered. These tubes should have a high value of the product of amplification constant by transconductance, low excitation voltage for normal output, low excitation power, low grid-to-plate capacitance, and relatively high output. It was concluded that the ideal oscillator would be a beam power tube or a pentode. The characteristics of various types of small tubes were examined and it was considered that the 802 and the RK-29 types best satisfy the above conditions.

The 813 and RK-48A were selected as best suited for amplifier stages of the order of 150 watts. They require little driving power and need no neutralization. For cases where the cost factor is of greater importance than the elimination of neutralizing equipment, the 811 was included.

Amplifier stages providing between 1 and 4 kilowatts were next considered. Relatively low plate voltage permits the use of economical components. Although it is desirable that all tubes be of types not requiring neutralization, for this particular purpose, no such tubes are available at reasonable cost. Therefore, the 833 and 357 triodes were selected.

As a test of the soundness of these selections, by various combinations of the four types of tubes presented, it was shown to be possible to design efficient and economical transmitters having power ratings between 25 and 4000 watts output.

June 27, 1941, P. J. Noizeux, chairman, presiding.

"The Selection of Modulator Tubes" was discussed by P. J. Arnaud at this meeting.

Using the four tube types presented in his paper on "The Selection of Transmitting Tubes" the author presented about twenty different arrangements of these tubes in transmitters having output powers of 25 to 4000 watts.

The general requirements for modulator tubes were then discussed. These tubes require low internal capacitance, high output per volt of excitation, and a high product of amplification constant by transconductance.

The modulating power required for each of the various transmitters under discussion was calculated. Provision was made for modulation-transformer losses. It was shown that nearly all of the transmitters could be adequately and economically modulated with tubes in the selected group. It was found desirable to add to that list only one tube, the 810, thus bringing to five the number of tubes now on the selected list.

July 4, 1941, P. J. Noizeux, chairman, presiding.

"Aviation Radio in the United States" was the subject of a paper by P. J. Noizeux, assistant general manager of Transradio Internacional.

The various ways in which radio is used to aid and protect flyers were pointed out. A description was given of the "*A-N*" beam transmitters and the manner in which the beams are made to coincide with the air routes was covered. The number, location, and technical features of these radio beacon stations in the United States were shown.

By means of recordings, there was reproduced for the audience the radio signals heard by a pilot flying over an air route. As the speaker indicated on a map the position of the aircraft, the audience heard the type and intensity of signal produced in the pilot's earphones as the aircraft moved to the left or right of the airway, approached the airport, or passed over the cone of silence. Similarly, the transmitters marking junction points of two beams and those indicating the position of an aircraft with respect to an airport were demonstrated. The effects of static and its relation to the distance between an aircraft and the transmitter were included and the nature of the improvement obtained by the use of ultra-high-frequency beam transmitters demonstrated.

July 11, 1941, Rodolfo Roth, president of the Asociacion Argentina de Electrotécnicos, presiding.

"Frequency Standards for High Frequencies" was the subject of a paper by R. P. McLoughlin of the faculty of Ciencias Fisicomat.

The design and construction of a tuning-fork oscillator, starting with the derivation of the important formulas and continuing on to the practical results, was described. The effect of the temperature on the frequency of the fork was demonstrated and methods of reducing this effect to a minimum were considered.

The feedback amplifier used to maintain oscillation was described. Means used to maintain constant the amplitude and phase of the feedback voltage were discussed.

A high degree of frequency stability

may be obtained, even when all possible sources of variation act simultaneously. The use of frequency-dividing devices for comparing the generated frequency with astronomical movements and of frequency multipliers for applying the generated frequency to radio uses were considered briefly.

July 24, 1941, P. J. Noizeux, chairman, presiding.

## Chicago

In the preliminary session, "Electronic Musical Instruments" was the subject discussed by P. A. Kransz, a student at RCA Institutes.

An electronic musical instrument was defined as a device which produces and reproduces musical tones electrically. Various methods of producing musical tones electrically were then discussed and included commutators, alternators operated at suitable speeds, phonic wheels or many-sided rotating disks with electric or magnetic coupling to the pickup, the light chopper which is a disk with spaced holes at several radii to interrupt a light beam falling on a phototube, film with sound recording and phototube pickup, film with duplex recording for pitch and stops, vaccum-tube oscillators of the beat-frequency, glow-discharge, or regenerative types, and pickups on strings using conventional musical instruments. Several applications were then described.

The Emereef organ utilizes the light-chopper effect. Twelve phototubes and 75 lights on each chopper are used. Twelve stops are available. A description was then given of the Emereef Universal Recorder which uses film on which records have been made. Separate films running at various speeds are exposed to produce octaves. The Theremin uses 2 radio-frequency oscillators in a beat-frequency arrangement and is played by variation in "hand" capacitance. The Emicon uses 1 gaseous oscillator with controlled resistances for pitch.

A description was then given of the Hammond organ and the Hammond Novacord. The former has 96 phonic wheels with magnetic pickups. The range is from approximately 30 to 6000 cycles. Amplifiers and speakers are provided to develop sufficient acoustic output. Various stops are available.

The Novacord and the Solovox use audio-frequency oscillators of the sawtooth type and frequency "halvers" to produce octaves. The instrument has 72 keys with 2 tubes for each key. The total tube complement is 163. The frequency range is approximately 40 to 2700 cycles. Methods of providing various effects such as percussion, soft, and harsh were then discussed.

At the regular session, B. F. Fredendall, engineer of the audio and video facilities group of the National Broadcasting Company, presented a paper on "High-Fidelity Lateral Recording and Reproduction."

The recording system was divided into two parts, electrical and mechanical. The amplifier, which comprises the electrical part, should have an amplitude response over a frequency range from 30 to 10,000 cycles that is within $\pm 1$ decibel. Its output power should be at least 20 watts and, preferably, 50 watts. It should be of the volume-limiting type to prevent overmodulation, "echoes," or complete cut through of the groove on the record.

Constant energy, constant amplitude, and constant velocity recordings were described and their merits and limitations pointed out. The use of constant amplitude for the low frequencies and constant velocity for the higher frequencies was discussed with stress placed on the lack of standardization of the crossover frequency at which the change takes place. Methods of compensating the various types of cutters to obtain these desirable characteristics were outlined.

The basic recording characteristics to be used for electrical and optical test comparisons were then discussed.

Two of the most important adjustments in recording are the placement of the stylus and the depth of the cut. The stylus is a sapphire set into a duralumin shank with its leading face approximately at right angles to the surface of the record. The exact angle is indicated by minimum noise. The depth of the cut is determined with a microscope and 60 per cent groove and 40 per cent adjacent "land" is considered optimum. The width of the cut is determined by the tension of a spring.

The thickness of a good recording blank should be uniform to within 0.001 inch. The surface should be homogeneous and free from dust, bubbles, or foreign particles.

Orthacoustic recording was then discussed. Special equalization is employed to improve the signal-to-noise ratio, reduce distortion, and provide better over-all performance.

For only a few copies, simultaneous recording or re-recording from an original disk is most economical. When more than ten copies are to be made, processing is employed. This involves gold sputtering over which copper is plated to form a negative. The negative is plated to form a nickel "mother" which, in turn, is plated to provide a "chrome stamper" from which the final copies are pressed. A demonstration was given to show the slight difference between an original and a pressing.

In reproduction, accurate and constant speed is required. Rapid variations in speed are called "wows" and should be rated in terms of the rate of change of speed rather than in the maximum deviation from the average speed.

Tracking is very important and the most common causes of groove jumping are low-frequency amplitudes in the record exciting the tone arm at its low-frequency resonance and the lateral component of friction on the needle tending to rotate the pickup arm. By using a playback with a needle of low stiffness and an arm with a large moment of inertia and equipped with a properly positioned "straight head" rather than an "offset head," much jumping can be eliminated.

May 23, 1941, Karl Hassel, vice chairman, presiding.

## Detroit

This meeting was devoted to a visit to Lawrence Institute of Technology.

C. E. Quinn of the Institute and of the Philco Radio Laboratories (Detroit) described the television transmitter and receiver which are under construction.

Eric Rohl, instructor in glass blowing, gave a very interesting glass-blowing demonstration and showed some of the glass laboratory equipment which he had constructed.

H. L. Byerlay of the electrical engineering department conducted a tour through the electrical and electronics laboratories and through the glider department.

May 9, 1941, R. J. Schaefer, vice chairman, presiding.

Carl Wesser, chief engineer of W45D, presented a paper on the "W45D Frequency-Modulation Station."

This transmitter, which was built by Radio Engineering Laboratories, is of 50 kilowatts rating and is located on the 45th and 46th floors of the Penobscot Building in Detroit. Many of the problems encountered in its installation and unusual difficulties which were encountered in obtaining power from the basement of the building were discussed.

After the paper, the transmitter and studios of W45D were inspected.

June 20, 1941, M. Cottrell, chairman, presiding.

# Membership

The following indicated admissions and transfers of memberships have been approved by the Admissions Committee. Objections to any of these should reach the Institute office by not later than October 31, 1941.

## Transfer to Member

Baldwin, C. F., 254 Bradley Blvd., Schenectady, N. Y.
Cochran, L. B., University of Washington, Seattle, Wash.
Flynn, R. M., 2915 Lovers Lane, Dallas, Texas
Gluyas, T. M., Jr., 6727 Montgall Ave., Kansas City, Mo.
Hauck, V. D., 427 Alabama Rd., Towson, Md.
Hunt, C. M., Radio Station WJSV, Earle Bldg., Washington, D. C.
Kallmann, H., 417 Riverside Dr., New York, N. Y.
Keen, A. W., Hygrade Sylvania Corp., Emporium, Pa.
Moody, R. C., 9023 Lloyd Pl., West Hollywood, Calif.
Nelson, W. H., 910 Spencer Ave., Marion, Ind.
Novy, J. F., 153 E. Quincy Rd., Riverside, Ill.
Plotts, E. L., 2509 E. 76th St., Chicago, Ill.
Reich, H. J., University of Illinois, Urbana, Ill.
Taylor, G. L., 2900 Power & Light Bldg., Kansas City, Mo.
Taylor, P. B., Aircraft Radio Laboratory, Wright Field, Dayton, Ohio
Thompson, S. T., 1033 Ontario St., Oak Park, Ill.
Troxler, L. J., 38-25 218th St., Bayside, N. Y.

## Admission to Member

Beatty, W. A., 12 Sidcup Hill Gardens, Sidcup, Kent, England
Bull, V. G., 5551 Queen Mary Rd., Montreal, Que., Canada
Cage, J. M., Colorado University, Boulder, Col.
Caldwell, C. W., Purdue University, Lafayette, Ind.
Dunn, W. L., 865 Thornwood Lane, Glenview, Ill.
Edson, W. A., 3300 Federal St., Chicago, Ill.
MacLeod, H. J., The University of British Columbia, Vancouver, B. C., Canada
Quarles, D. A., Bell Telephone Laboratories, 463 West St., New York, N. Y.
Sarbacher, R. I., 5555 Sheridan Rd., Chicago, Ill.
Sashoff, S. P., University of Florida, Gainesville, Fla.
Skene, A. A., Bell Telephone Laboratories, Whippany, N. J.
Smith, N. R., 9 Barnett St., Bloomfield, N. J.
Tillyer, E. D., American Optical Co., Southbridge, Mass.
Tratt, F. H., 86 Morningside Rd., Verona, N. J.

---

The following admissions to Associate grade were approved by the Board of Directors on September 3, 1941.

Allen, H. E., Headquarters Battery, 120 Field Artillery, 32 Division, Camp Livingston, La.
Ames, D., Main St., North Easton, Mass.
Anderson, L. T., 3520 Wilcox St., Bellwood, Ill.
Anderson, W. A., 184 Edison St., New Dorp, S. I., N. Y.
Aronson, C. A., 23 N. Ferry S., Schenectady, N. Y.
Bagg, T. C., 3220 Oliver St., Chevy Chase, D. C.
Barnes, T., 4350 Copeland Ave., San Diego, Calif.
Beren, H. E., 456 Post St., San Francisco, Calif.
Blackburn, R. K., 1739 Main St., Newington, Conn.
Bliss, W. H., 6 N. Main St., Orono, Maine
Braun, V. J., 81 N. Dearborne St., Indianapolis, Ind.
Breiding, E. J., Bell Telephone Laboratories, Whippany, N. J.
Briggs, R. S., 13 Clark Ave., Beverly, Mass.
Cahoon, B. B., Bell Telephone Laboratories, 463 West St., New York, N. Y.
Connolly, J. K., Jr., Holy Cross College, Worcester, Mass.
Cooney, J. R., Box 5, Emporium, Pa.
Cooper, J. D., 1817 Nebraska St., Sioux City, Iowa
Crawford, A. L., Jr., 424 Montgomery Ave., Haverford, Pa.
Crose, G. G., 901 W. Touhy Ave., Park Ridge, Ill.
DeHart, R. N., 20 Chestnut St., Malden, Mass.
Ducore, H., 1740 Grand Ave., New York, N. Y.
Duffy, M. P., Hazeltine Service Corp., 58-25 Little Neck Pkwy., Little Neck, L. I., N. Y.
Estes, R. A., Panagra, Santiago, Chile
Fendrich, L., 1600 Maple Ave., Hillside, N. J.
Fleming, C. C., 173-08 82nd Ave., Jamaica, N. Y.
Freeman, J. E., 63 Fisher St., Fullerton, South Australia
Frutchey, M. P., Jr., 14 Marshall St., Caldwell, N. J.
Girdner, W. I., 584 Vista Ave., Palo Alto, Calif.
Gittelman, A., 300 W. Pennsylvania Ave., Towson, Md.
Ginsberg, A. J., 6 W. 74th St., New York, N. Y.
Goswamy, P. B., Aerodrome Bhuj, Bhuj, Kutch State, India.
Hamilton, R. H., 7A Kircher Pl., Belleville, Ill.
Hansen, W. H., Box 14, Oceanport, N. J.
Hanson, K. W., 156 Westervelt Ave., Baldwin, N. Y.
Heck, A. C., Box 541, Sharon, Pa.
Hulse, B. T., 7 Dodd St., East Orange, N. J.
Hyrne, E. E., Liberty St., Matawan, N. J.
Ivers, J. H., 50 Fulton Spring Rd. Ext., Medford, Mass.
Jacobs, G. W., 50 E. Reid Pl., Verona, N. J.
Keister, J. E., 821 Sanders Ave., Scotia, N. Y.
Keith, W. S., 47-45 43rd St., Woodside, N. Y.
Kennedy, J. R., 18 Wyckwood Ave., Toronto, Ont., Canada.
King, E. F., 94 Glendale Ave., Bridgeport, Conn.
Laeser, P. B., 9410 Harding Blvd., Milwaukee, Wis.
Lattin, W. J., 2808 First Rd. N., Arlington, Va.
Lautzenheiser, R. W., 2506 Virginia St., Sioux City, Iowa.
Lawry, H. M., 605 S. 21st St., Belleville, Ill.
Lyons, L. E., Jr., Aircraft Radio Laboratory, Wright Field, Dayton, Ohio.
Mannheimer, D., c/o Sperry Gyroscope Co., Garden City, L. I., N. Y.
McCoppin, E. R., 321 W. Fifth St., Chillicothe, Ohio
McPherson, 3009 N. W. Quimby St., Portland, Ore.
Miller, C. F., 314 E. Third St., Frederick, Md.
Newbeck, J. J., 406 W. 47th St., New York, N. Y.
Nuebling, C. A., Sperry Gyroscope Co., Garden City, L. I., N. Y.
Ogg, R. D., 670 Creston Rd., Berkeley, Calif.
Pan, W. Y., Universal Trading Corp., 630 Fifth Ave., New York, N. Y.
Peck, R. C., R.F.D. 1, Herndon, Va.
Pramann, H. J., 531 Walnut St. S. E., Minneapolis, Minn.
Rae, J. R., 171 Riverview Ave., Tarrytown, N. Y.
Renne, H. S., 14745 Main St., Harvey, Ill.
Reque, S. G., Jr., 13 State St., Schenectady, N. Y.
Rubin, J. H., 115 S. High St., Belleville, Ill.
Runge, J. N., 514 Moore St., Middletown, Ohio.
Shrotri, B. M., Jitekar's Chawl, Thakurdwar, Bombay 2, India.
Shuey, L. S., 8 Wellington Rd., Hempstead, L. I., N. Y.
Skipper, L. C., 142 E. 33rd St., New York, N. Y.
Spindler, J. C., c/o Federal Telegraph Co., 200 Mount Pleasant Ave., Newark, N. J.
Swanson, C. W., 5020 Warwick Ave., Irving Park, Chicago, Ill.
Talmage, F. E., 1004 Green St., Haddon Heights, N. J.
Todd, T. H., 318-10th St., Tuscaloosa, Ala.
Walker, O. F., 229 Cherry St., Schenectady, N. Y.
Weiss, W. A., Hickok Electrical Instrument Co., 10514 Dupont Ave., Cleveland, Ohio.
Wetherell, J. E., 6429 S. Lavergne Ave., Chicago, Ill.
Whatman, A. B., Brockenhurst, Hants., England.
Wimpy, E. K., 31 Parkway East Halcyon Park, Bloomfield, N. J.
Young, P. G., 4609 College Ave., College Park, Md.
Yungwirth, G. J., 1314 Helderberg Ave., Schenectady, N. Y.

# Contributors

S. Frankel (A'37) was born in New York City, on October 6, 1910. He received the B.A. degree in electrical engineering at the Rensselaer Polytechnic Institute in 1931, the M.A. degree in mathematics in 1934, and the Ph.D. degree in mathematics in 1936. He was an instructor in mathematics at Rensselaer Polytechnic Institute from 1931 to 1933.

During 1936–1937 Dr. Frankel was a sound-recording engineer with the Brook-

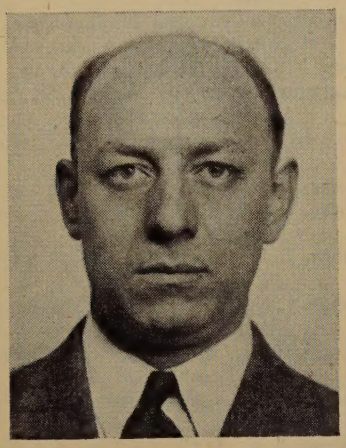

S. Frankel

lyn Vitaphone Corporation, and in 1937–1938 an assistant engineer in design and development of electronic flight instruments with the Eclipse Aviation Corporation, at Bendix, New Jersey.

Since 1938, he has been an engineer in the design and development of radio transmitters with the Federal Telegraph Company, Newark, New Jersey.

He is a member of Sigma Xi.

❖

Joseph Charles Frommer was born at Budapest in 1904. He received the degree of mechanical engineering from the Hungarian Technical University in 1925 and did research work there the following year. From 1926 to 1927 Mr. Frommer worked in the Liancourt (France) plant of agricultural tractors of the Austin auto-

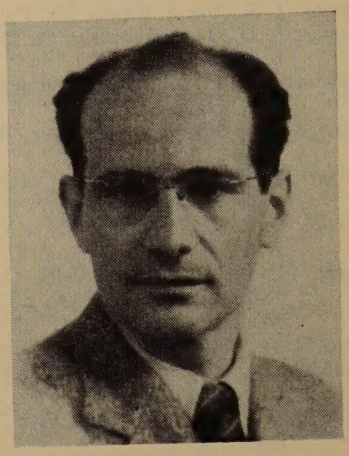

J. C. Frommer

mobile works, and from 1928 to 1929 in a textile mill in Budapest. From 1929 to 1939 he was a member of the research laboratory of the United Incandescent Lamp and Electric Co. (TUNGSRAM works), Ujpest, Hungary, doing research work in connection with the production of photocells, vacuum tubes, incandescent lamps, design of valve circuits, and the setting of operating ratings. During 1940–1941 he was employed at the McKay-Massey-Harris Harvester works, Sunshine, Australia,

R. E. Spencer

and is now at the Beck-Lee Corporation in Chicago, working on the development of new apparatus.

❖

S. A. Schelkunoff (A'40) received the B.A. and M.A. degrees in mathematics from the State College of Washington in 1923, and the Ph.D. degree in mathematics from Columbia University in 1928. He was

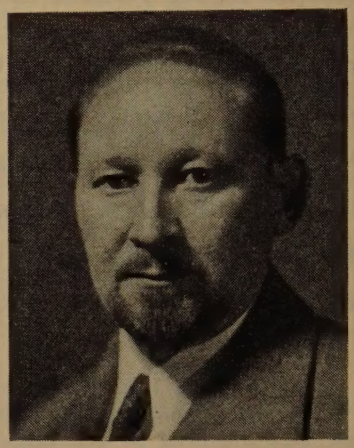

S. A. Schelkunoff

in the engineering department of the Western Electric Company from 1923 to 1925; the Bell Telephone Laboratories from 1925 to 1926; the department of mathematics of the State College of Washington, 1926 to 1929; and Bell Telephone Laboratories, 1929 to date. Dr. Schelkunoff has been engaged in mathematical research, especially in the field of electromagnetic theory.

❖

Rolf Edmund Spencer* was born at Sutton, Surrey, England, on April 19, 1908. He received the B.A. degree in mathematics from Oxford University in 1929, and since that date Mr. Spencer has been a member of the designs department of the Electric and Musical Industries, Ltd., at Hayes-Middlesex, England.

* Paper appeared in the December, 1940, issue of the Proceedings.